P. I. D. CONTROLLER FOR LOAD FREQUENCY CONTROL OF SINGLE AND INTER - CONNECTED POWER SYSTEMS

A Thesis Submitted
in Partial Fulfilment of the Requirements
for the Degree of
MASTER OF TECHNOLOGY

by

SQN LDR SURESH CHAND

to the

DEPARTMENT OF ELECTRICAL ENGINEERING
INDIAN INSTITUTE OF TECHNOLOGY KANPUR

APRIL 1990

EE-1990-M-CHA-P.I.D

4 JAN 1991

CERTIFICATE

This is to certify that the work entitled, 'P.I.D. CONTROLLER FOR LOAD FREQUENCY CONTROL OF SINGLE AND INTER-CONNECTED POWER SYSTEMS', by Sqn.Ldr Suresh Chand has been carried out under ~~my~~ our supervision and has not been submitted elsewhere for award of a degree.

Prem Kumar Kalra.

Dr. P.K.KALRA
Assistant Professor
Department of
Electrical Engineering
I.I.T.Kanpur
April 1990

B Sarkar

Dr.B.SARKAR
Assistant Professor
Department of
Electrical Engineering
I.I.T.Kanpur
April 1990

ABSTRACT

This report presents an approach for improving the stability of load-frequency for single area and multi-area interconnected power systems using P.I.D. controller i.e. proportional, integral and derivative controls. These three components of the P.I.D. controller have been used in various combination in forward and feedback paths. Only some of the combinations were found to give improved transient and steady state responses. The proposed technique is applied to single area power system as well as two-area interconnected power systems like thermal-thermal and hydro-thermal systems. The P.I.D. controller can be applied to multi-area-interconnected power systems.

A comparison of the Load Frequency Control (LFC) response with Conventional and Variable-Structure System (VSS) control and proposed P.I.D. control strategies shows that, with the application of the proposed algorithm, the system performance is improved significantly.

CONTENT

LIST OF SYMBOLS

ΔP_{ref}	=	Change in Reference Signal
ΔP_D	=	Step Disturbance
K_G	=	Gain of Governor
K_T	=	Gain of Turbine
K_P	=	Gain of Generator
R	=	Self Regulation Factor
Δf_1	=	Frequency Deviation Area 1
Δf_2	=	Frequency Deviation Area 2
β	=	Area Frequency Response Characteristics (AFRC)
T_g	=	Governor Time Control
T_t	=	Turbine Time Constant
T_P	=	Generator Time Constant
K_p	=	Proportional Gain
K_i	=	Integral Gain
K_d	=	Derivative Gain
B	=	Damping Coefficient

LIST OF TABLES

CHAPTER - 1

INTRODUCTION

1.1 GENERAL

It is important to maintain the frequency constant in the power systems. Variation of the frequency in the power system may cause problems. Some of these problems are listed below:

(i) Most AC motors run at speeds that are directly related to the frequency. The speed and induced electromotive force (EMF) may vary because of the change of frequency of the power circuit.

(ii) When operating at frequencies below 49.5Hz, some types of steam turbine, certain rotor state undergo excessive vibrations which results in metal fatigue and blade failures.

(iii) The turbine regulating devices fully open when the frequency falls below 49Hz. This situation causes extra loading on the generators. A decrease in frequency may cause reduction in the equipment efficiency, e.g., feed pumps.

(iv) A large number of electrically operated clocks are used for certain purposes. If frequency changes, it can influence the operation of these clocks.

(v) The change in frequency can cause maloperation of power convertors by producing harmonics.

The load-frequecy control is installed for better exchange of Mega-Watt Hour (M.W.H),stability and minimize above mentioned problems. For reasons of economy and system reliability, neighbouring power systems are interconnected, forming an augmented system refered to as 'power pool'. The net power flow on the tie-lines connecting a system to the external system is frequently scheduled by apriori contact basis. System disturbances caused by load fluctuations result in changes in tie-line power and system frequency which gives rise to a "load frequency control" (LFC) problem.

To study the load frequency control, the excitation control influence on the system performance can be ignored because of the following reasons:

(i) For small changes, it can safely be assumed that change in real power only causes change in load angle. Hence, the variations in load angle causes momentry change in generation speed. This means generator has been supplied with sufficient reactive power to maintain the voltage constant at the terminals.

(ii) The major time constant involved in the excitation system is generator's field time constant. The time constants involved in load frequency control are those of the turbine and

inertia of generator. The Latter time constants are much longer compared to the excitation system time constant. Hence it is fair to assume that the transients of the excitation system will vanish much faster then the transients of the load frequency control system and does not affect the response of the load frequency control system.

The load frequency control is based on an error signal called Area Control Error (ACE) which is a linear comnbination of net interchange and frequency errors. The conventional control strategy used in industries is to take the integral of ACE as the control signal [4-6]. It has been found that the use of ACE as the control signal reduces the frequency and tie-line power errors to zero in the steady state, but the transient response is not satisfactory[6].

To improve the transient response, linear dcentralised Load Frequency Control using Pole-Placement [15] and linear optimal control theory [6] has been investigated. The realisation of such controllers is difficult, cumbersome and expensive because the feedback portion of the above controller is a function of the complete state vector of the system. Generally, all the state variables are not accessible. Even if state estimation techniques are used to estimate the inaccessible state variables, the data need to be transfered over long distance. This

involves additional cost of telemetering.

The third type of controller called "variable structure-system"(VSS) controller has been used by some of the investigators [14 & 16]. This controller algorithm requires only two measurable variables, i.e., frequency deviation and tie-line power deviation. This controller is practically as simple as that of the conventional controller and can be implemented with very little additional cost. However, the VSS controller needs the switching strategy which may not be simple for large and complex system. To select the best control algorithms the requirement must be known. This requirements have been discussed in the next section.

1.2 REQUIREMENTS FOR SELECTING CONTROL STRATEGY

The following requirements should be satisfied by the control scheme:

(i) Control loop must be characterized by a sufficient degree of stability.

(ii) Following a step load change, the frequency error should return to zero. This is referred to as isochronous control. The magnitude of the transient frequency deviation should be minimized, i.e., frequency swing should not exceed ±0.02Hz.

(iii) The static change in the tie-line power flow following a step load change in either area must be zero.

(iv) The integral of the frequency error should be minimized so that accuracy of "synchronous clocks" are maintained. The time error should not exceed ± 3 seconds.

It has been felt that the modelling of each component evolved in the control system should be discussed. The modelling presented here in brief and is to fimiliarize the reader with basic functions involved in the control system. It is given in App. A & B.

1.3 OBJECTIVE

The need of a fast, effective and economical controller for load frequency control has been established in the foregoing discussions. The main objective of this is to investigate the effectiveness of P.I.D. controller applied to load-frequency control of interconnected power system. Also, to compare and establish that the P.I.D. controlled power system yields relatively much better response than variable structure controlled system and approximately similar to responses of pole placement technique. However, the implementation of P.I.D. controller is much simpler than the above two techniques.

1.4 ORGANISATION

To meet the objective of investigating the P.I.D. controller performance for Load Frequency Control of power systems The thesis has been organized in the following manner:

Chapter Two covers Mathematical analysis of steady state and Dynamic Response.

Chapter three covers the effect of individual control elements on single area as well as two area reheat thermal plant.

Chapter four covers the effet of proportional, integral and derivative control when applied two at a time. The load frequency control response has been obtained for two area reheat thermal plant.

Chapter five covers the load frequency control response of two area reheat and nonreheat thermal plant and Hydro-thermal plant with P.I.D. controller. The load frequency control response with VSS controller has been compared.

Chapter six covers conclusions and future scope of this work.

CHAPTER - 2

MATHEMATICAL ANALYSIS OF STEADY STATE AND DYNAMIC RESPONSE OF SINGLE AND TWO AREA POWER SYSTEMS

2.1 INTRODUCTION

Before proceeding into P.I.D. controller system, it is felt that the load frequency control of power system with and without controller should be analysed for its steady state and dynamic response behaviour. In this chapter the mathematical analysis of load frequency control of single and two area power systems has been studied.

2.2 RESPONSE OF LOAD FREQUENCY CONTROL OF AN ISOLATED (SINGLE AREA) POWER SYSTEM

Now we shall present the analysis of load frequency control of a simple power system. The complete system to be considered for the design of the controller may be obtained using equation (A.9), (A.16) and (A.26) of App. A. It is shown in figure (2.1). The system response has been obtained for uncontrolled and controlled cases in the following sections:

2.2(a) UNCONTROLLED

Steady State Response: In uncontrolled case, speed changer has fixed setting, i.e., $\Delta P_{ref} = 0$

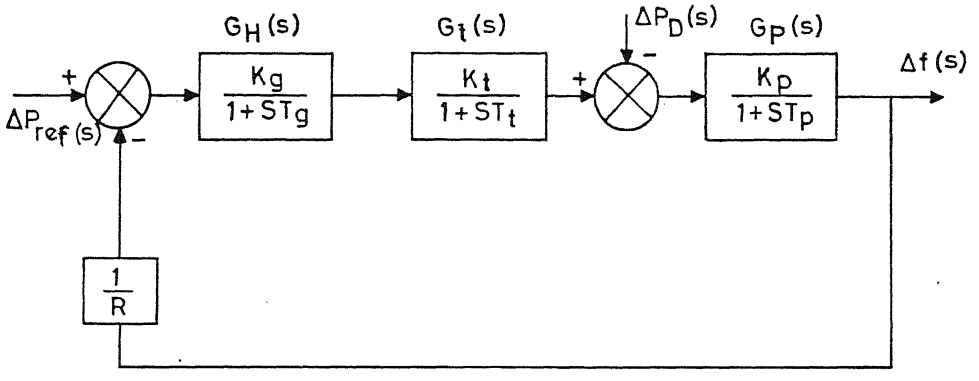

Figure (2-1) Block diagram representation of single area thermal plant (UNCONTROLLED)

For step load change $\Delta P_D = M$

Laplace transform of it is $P_D(s) = \frac{M}{S}$

Now from the block diagram (fig. 2.1) we obtain by inspection

$$\{[\Delta P_{ref} - \frac{1}{R}\Delta f] G_H G_T - \Delta P_D\} G_P = \Delta f \qquad (2.1)$$

In Laplace transform form

$$\Delta f(s) = - \frac{G_P}{1+(\frac{1}{R})G_P G_H G_T} \Delta P_D(s) \qquad (2.2)$$

Using the Final value theorem

$$\Delta f_{SS} = \lim_{s \to o} [S\ \Delta f(S)] = \frac{S\ G_P}{1+(\frac{1}{R})G_P G_H G_T} \times \frac{M}{S} \qquad (2.3)$$

$$= - \frac{K_P M}{1+K_P/R} = - \frac{M}{D+1/R} H_z$$

if $\beta \triangleq D + \frac{1}{R}$ P.U. MWHz

then $\Delta f_{SS} = - \frac{M}{\beta} H_z$ is constant error (2.4)

where β is called area Frequency. Response Characteristics (AFRC). Thus in uncontrolled case we find that the steady state response has constant error.

Dynamic Response

Finding the dynamic response is quite straightforward. By taking inverse laplace transform of equation (2.1), gives an expression for $\Delta f(t)$. However, as G_H, G_T, and G_P contain at least one time constant each, the denominator will be of third order, resulting in unwieldly algebra.

We can simplify the analysis considerably by making the reasonable assumption that the action of the speed governor plus the turbine generation is instantaneous compared with the rest of the power system, ($T_g < T_t << T_p$) where T_p is generally 20 sec.and T_g, $T_t \leq 1$ sec. Thus we can assume $T_g = T_t = 0$ and gains equal to 1.

$$\Delta f(s) \approx - \frac{\frac{K_P}{1+ST_P}}{1+ \frac{1}{R} \frac{K_P}{1+ST_P}} \times \frac{M}{S} \qquad (2.5)$$

Equation (2.5) can also be written as

$$\Delta f(S) = - M \frac{RK_P}{R+K_P} \left(\frac{1}{S} - \frac{1}{S+ \frac{R+K_P}{RT_P}} \right) \qquad (2.6)$$

Taking inverse Laplace transform of (2.6) we get

$$\Delta f(t) = -\Delta P_D \frac{RK_P}{R+KP} \left[1-e^{-t} \left(\frac{K_P+R}{RT_P} \right) \right] \qquad (2.7$$

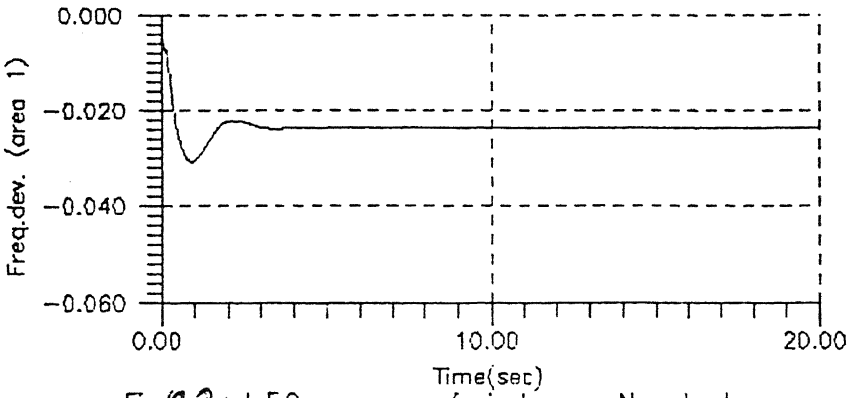

Fig.(2-2) L.F.C. responce of single area Nonreheat
Thermal Plant UNCONTROLLED tg=0.08 sec,Tt=0.3 sec
Kp=120.0/p.u.MW ,Tp=20.0sec & R=2.4 hz/p.u.MW

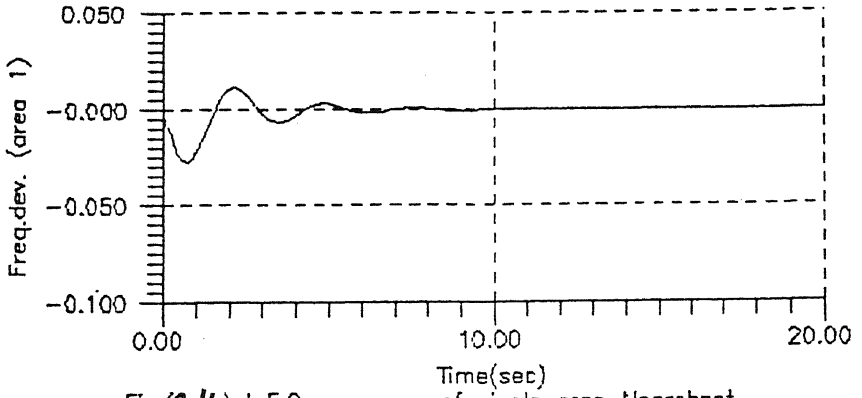

Fig.(2.4) L.F.C. responce of single area Nonreheat
Thermal Plant CONTROLLED tg=0.08 sec,Tt=0.3 sec
Kp=120.0/p.u.MW ,Tp=20.0sec & R=2.4 hz/p.u.MW ,Ki=0.5

Thus the error $= -e^{-t}\left(\frac{K_P+R}{RT_P}\right)$ persists in uncontrolled case

A simulated response of uncontrolled single area nonreheat is shown in fig. (2.2). The system parameter values are also given.

2.2(b) CONTROLLED CASE: Before analyzing the controlled case of a single area power system, we shall define "Control Area".

CONTROL AREA: The power pools in which all the generators are assumed to be tightly coupled, i.e. they swing in "unison" with change in load or due to speed changer settings. Such an area, where all the generators are running coherently, is termed as "control area".

INTEGRAL CONTROL: By using the control strategy shown in fig. [2.3], we can control the intolerable dynamic frequency changes with changes in load and also the synchronous clocks but not without error during transient period. We have added to the uncontrolled system in fig. [2.1] an integral controller which actuates the speed changer by the real power commond signal ΔP_c

$$\Delta P_C = -K_t \int \Delta f dt \qquad (2.8)$$

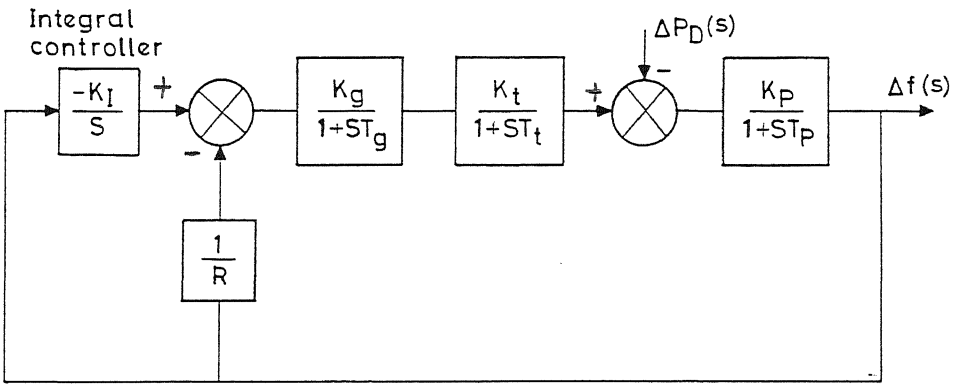

Figure (2-3) Block diagram representation of single area (CONTROLLED) power plant

The negative polarity must be chosen so as to cause a positive frequency error to give rise to a negative, or "decrease" command.

Here K_g and K_t are such that $K_g K_t \triangleq 1$

In central load frequency control of a given area, the signal fed into the integrator is refered to as area control error (ACE), i.e.

$$ACE \triangleq \Delta f \tag{2.9}$$

Taking Laplace transform of equation (2.9). We get

$$\Delta P_C(S) = \frac{K_i}{S} \Delta f(S)$$

and for step input load:

$$\Delta P_D(S) = \frac{M}{S}$$

Thus from the block diagram, of fig. (2.3) we get

$$\Delta f(S) = - \frac{K_P}{(1+ST_P)+(\frac{1}{R} + \frac{K_i}{S}) \times \frac{K_P}{(1+ST_g)(1+ST_t)}} \times \frac{M}{S}$$

$$= - \frac{RK_P S(1+ST_g)(1+ST_t)}{S(1+ST_g)(1+ST_t)(1+ST_P)R+K_P(RK_i+S)} \times \frac{M}{S} \qquad (2.10)$$

By using Final value theorem, we readily obtain from the above equation the static frequency drop as:

$$\Delta f_{steady} = \lim_{S \to 0} [S\Delta f(S)] = 0 \text{ i.e. no error.}$$

Simulated frequency response of single area non-reheat thermal plant is given in fig. (2.4). Integral gain value has been taken from [6].

$\Delta P_D = 0.01$ $\qquad$ $K_i = 0.6$

$T_g = .08$ sec $\qquad$ $K_P = 120$ (Generator Gain)

$T_t = 0.38$ sec. $\qquad$ $K_g * K_t = 1$

$T_P = 20$ sec. $\qquad$ $R = 2.4$

2.3 LIMITATIONS OF INTEGRAL CONTROL

It has been found [6] that the use of ACE as the control signal reduces the frequency and tie-line power errors to zero in the steady state, but the transient response is not satisfactory.

It can be seen in fig. (2.4) that overshoot is more than 0.02Hz and setlling time is also more compared to VSS controller and proposed controller applied to thesame system, which will be illustrated in chapter 6.

2.4 RESPONSE OF LOAD FREQUENCY CONTROL OF TWO AREA INTERCONNECTED POWER SYSTEM.

In this section, analysis of load frequency control of a two area power system is presented. The complete system to be considered for the design of the controller may be obtained using equation (A.9), (A.16), (A.26) of appendix (A) and equation (B.8), of appendix (B).

The system response has been obtained for uncontrolled and controlled cases in the following sections. Figure (2.5) represents the block diagram of two area uncontrolled inter-connected power system.

UNCONTROLLED CASE: Steady State Response:

We consider first the uncontrolled case with $\Delta P_{C1} = \Delta P_{C2} = 0$. Suppose that the load in each area is suddenly increased by incremental steps ΔP_{01} & ΔP_{02}. Due to the incremental loads, we shall have frequency drops in the steady state and these drops will be equal to

$$\Delta f1_{stat} = \Delta f2_{stat} = \Delta f_{stat}$$

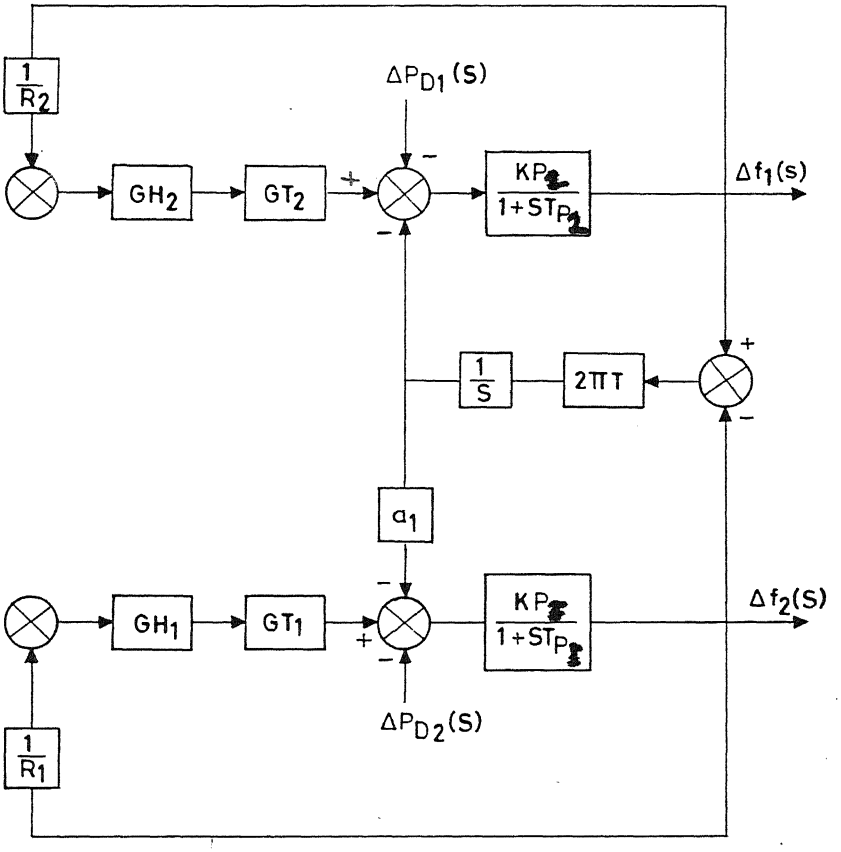

Figure (2-5) Block diagram representation of two inter-connected power plants (UNCONTROLLED)

and we will have incremental tie-line power in steady-state, i.e.

$$\Delta P_{12stat}.$$

also $$\Delta P_{G1stat} = -\frac{1}{R_1}\Delta f_{stat} \qquad (2.11)$$

$$\Delta P_{G2stat} = \frac{1}{R_2}\Delta f_{stat} \qquad (2.12)$$

Refering equation (A.7) for area 1 and setting $\frac{d(\Delta f1)}{dt} = 0$, we write for static conditions

$$\Delta P_{G1stat} - \Delta P_{D1} = B_1 \Delta f_{1stat} + \Delta P_{12stat} \qquad (2.13)$$

Similarly, for area 2 we can write

$$\Delta P_{G2stat} - \Delta P_{D2} = B_2 \Delta f_{2stat} + \Delta P_{21stat}$$

or $$\Delta P_{G2stat} - \Delta P_{D2} = B_2 \Delta f_{2stat} - \Delta P_{12stat} \qquad (2.14)$$

since $\Delta P_{12} = -\Delta P_{21}$

or $\Delta P_{12} = a_{12}\Delta P_{21}$ where $a_{12} = -1$

Making use of Eqs. (2.10), (2.11) and (2.12) we get the following

$$\Delta f_{stat} = -\frac{(\Delta P_{D2} + a_{12}\Delta P_{D1})}{(B_2 + \frac{1}{R_2}) + a_{12}(B_1 + \frac{1}{R_1})}$$

$$\Delta P_{12stat} = \frac{(B_1 + \frac{1}{R_1})\Delta P_{D2} - (\frac{1}{B_2} + \frac{1}{R_2})\Delta P_{D1}}{(B_2 + \frac{1}{R_2}) + a_{12}(B_1 + \frac{1}{R_1})}$$

Let $\beta_1 = B_1 + \frac{1}{R_1}$ or $\beta_2 = B_2 + \frac{1}{R_2}$

Thus we can write

$$\Delta f_{stat} = -\frac{(\Delta P_{D2} + a_{12}\Delta P_{D1}}{(\beta_2 + a_{12}\beta_1)} H_z \qquad (2.15)$$

$$\Delta P_{12stat} = \frac{(\beta_1 \Delta P_{D2} - \beta_2 \Delta P_{D2})}{\beta_2 + a_{12}\beta} \quad P.U.M.W. \qquad (2.16)$$

In case we have $B_1 = B_2 = B$

$$R_1 = R_2 = R$$

$$\beta_1 = \beta_2 = \beta$$

Then (2.15) becomes $\Delta f_{stat} = \frac{\Delta P_{D2} + \Delta P_{D1}}{2\beta} H_Z$

and (2.16) becomes $\Delta P_{12stat} = \frac{\Delta P_{D2} - \Delta P_{D1}}{2}$ P.U. MW

Suppose a step load change occurs in area 1 only, then we get

$$\Delta f_{stat} = -\frac{\Delta P_{D1}}{2\beta} H_Z$$

$$\Delta P_{12stat} = -\frac{\Delta P_{D1}}{2} \text{ P.U. MW}$$

Thus we conclude from above that for a load change in area 1, in a two area system, the steady state error reduced to 50% and tie-line flow by 50%.

2.5 Dynamic Response

Uncontrolled Case

Let us consider the transient period. For the sake of simplicity we shall assume the two areas to be identical. Further, we shall be neglecting the time constants of governors and turbines as these are negligible compared to the time constants of generators.

$$T_{P1} >> T_{t1} \text{ or } T_{g1}$$
$$T_{P2} >> T_{t2} \text{ or } T_{g2}$$

For the uncontrolled case $\Delta P_{C1} = \Delta P_{C2} = 0$, we can write the following equation by refering to fig. (2.5)

$$\Delta f_1(S) = -\frac{K_{P1}}{1+ST}\left[\frac{\Delta f_1(S)}{R} + \Delta P_{D1}(S) + \Delta P_{12}(S)\right] \quad (2.17)$$

$$\Delta f_2(S) = -\frac{K_{P2}}{1+STP}\left[\frac{\Delta f_2(S)}{R} + \Delta P_{D2}(S) - \Delta P_{12}(S)\right] \quad (2.18)$$

also we know $\Delta P_{12}(S) = \frac{2\pi T^{o}}{S} [\Delta f_1(S) - \Delta f_2(S)]$

After substitution we get

$$\Delta P_{12}(S) = \frac{\Delta P_{D2}(S) - \Delta P_{D1(S)}}{S^2 + S(\frac{1}{T_P} + \frac{K_P}{RT_P}) + \frac{4\pi T^{o} K_P}{T_P}} \times \frac{2\pi T\ K_P}{T_P}$$

Since $K_P = \frac{1}{B}$ HB/P.U.MW $T_P = \frac{2H}{Bf^{o}}$ sec.

we get:

$$\Delta P_{12}(S) = \frac{\Delta P_{D2}(S) - \Delta PD_1(S)}{S^2 + (\frac{Bf^{o}}{2n} + \frac{f^{o}}{2HR})S + \frac{2\pi T^{o} f^{o}}{H}} \times \frac{\pi f^{o} T^{o}}{H}$$

We see that the denominator is of second order and has the form $S^2 + 2\alpha S + \omega n^2$

where $\alpha = \frac{f^{o}}{4H} (B + \frac{1}{R})$

$$\omega_n^2 = \frac{2\pi T\ f}{H}$$

If α and ω_n^2 both are +ve then system is stable damped. The roots of the characteristice equation are

$$S_{1,2} = -\alpha \pm \sqrt{\alpha^2-(\omega_n^2)}$$

Now we have three conditions:

(1) If $\alpha = \omega_n$ the system is critically dampled.

(2) If $\alpha > \omega_n$ the system becomes overdamped.

(3) If $\alpha < \omega_n$, underdamped.

A typical example of two area power system with parameter given as shown in fig. (2.6)

CONTROLLED CASE:

Here also we will use integral control in each area.

Here in this case there are two control signal variables, in each area, namely frequency deviation and tie-line power deviation, thus we redefine area control error ACE for the two-areas as follows:

$$ACE_1 = P_{12} + B_1\Delta f_1 \qquad (2.18)$$

$$ACE_2 = P_{21} + B_2\Delta f_2 \qquad (2.19)$$

The block diagram representation of two area interconnectedd power system is shown in fig. (2.7).

The speed changer of governor will get the following command signals:

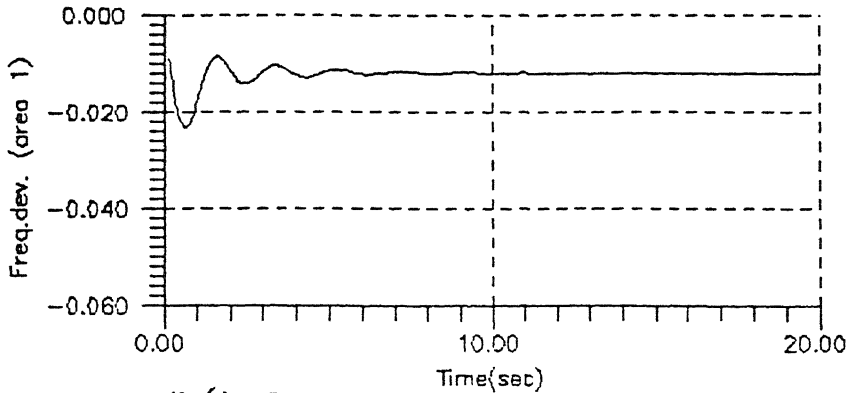

Fig.(2·6) L.F.C. responce of TWO area Nonreheat Thermal Plant UNCONTROLLED tg=0.08 sec,Tt=0.3 sec Kp=120.0/p.u.MW ,Tp=20.0sec & R=2.4 hz/p.u.MW,Kg=Kt=1

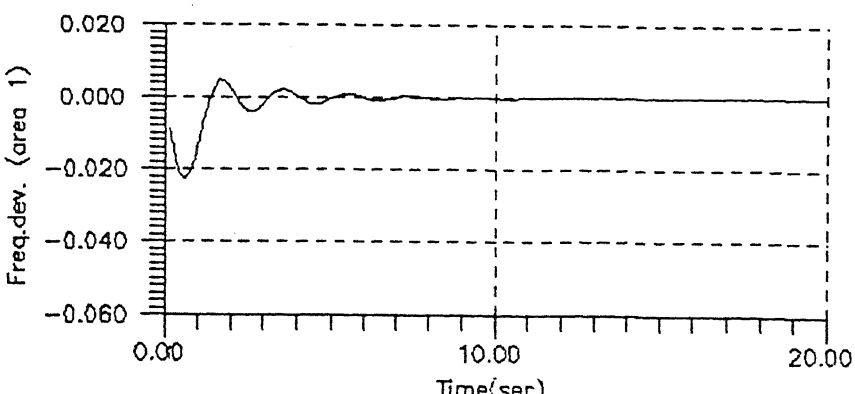

Fig.(2·8) L.F.C. responce of TWO area Nonreheat Thermal Plant CONTROLLED , tg=0.08 sec,Tt=0.3 sec Kp=120.0/p.u.MW ,Tp=20.0sec & R=2.4 hz/p.u.MW, Ki=0.67

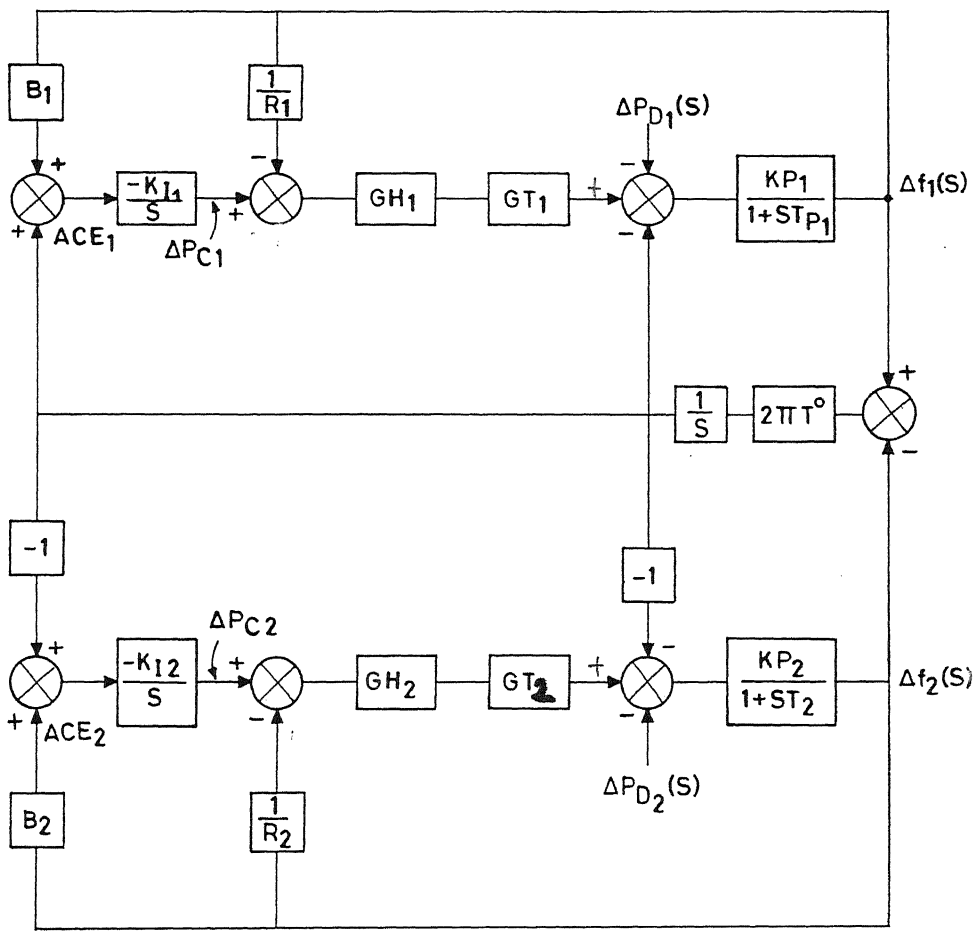

Figure (2-7) Block diagram representation of two area (CONTROLLED) power plant

$$\Delta P_{C1} = - K_{i1}\int(\Delta P_{12}+B_1\Delta f_1)dt \qquad (2.20)$$

$$\Delta P_{C2} = - K_{i2}\int(\Delta P_{21}+B_2\Delta f_2)dt \qquad (2.21)$$

2.6 STATIC RESPONSE

The choosen strategy will eliminate the steady state frequency and tie-line deviations for the following reasons. Following a step load change in either area, a new static equilibrium, if such an equilibrium exists, can be achieved only after the speed changer commands have reached constant values. But this evidently requires that both integrands in equation (2.20) & (2.21) be zero.

$$\Delta P_{12,o} + B_1\Delta f_o = 0$$
$$\Delta P_{21,o} + B_2\Delta f_o = 0$$

But as we know $\Delta P_{12} = - \Delta P_{21}$

Therefore $\Delta f_o = \Delta P_{21,o} = 0$.

We conclude that for the above equations to be satisfied, both the steady state frequency and tie-line deviations should vanish. When this aim is achieved the system frequency equals the desired value and the interchange schedule is met which is the guiding principle in pool operation. Each area in steady state absorbs

its own load. Simulated result of previous example with integral control is shown in fig. (2.8).

2.7 CONCLUSIONS

In this chapter we have tried to give a balanced presentation for the analysis of load-frequency control of the power system using the methods of modern control theory.

Under normal operation the controllers keep the generator operating around a pre-selected "normal" state with minimal excursions. The dynamic models of all controllers that have been discussed have therefore been linear.

CHAPTER - 3

STUDY OF PROPORTIONAL INTEGRAL (CONVENTIONAL) AND DERIVATIVE CONTROL ON POWER SYSTEMS, AS USED INDIVIDUALLY

3.1. INTRODUCTION

In this chapter, the load frequency control response of single and double area thermal plant will be studied with controller used as proportional or integral or derivative controller alone. Simulated results have been shown for study.

3.2. PROPORTIONAL CONTROLLER

This controller has been evaluated for the specific example of load frequency control problem. It has been already established that only proportional controller when used alone as controller, is not good. It gives steady state error if value of gain K_p is increased, the steady state error reduces but transient oscillations increase. In fig. [3.1a] the frequency response of single area reheat thermal plant is shown for K_p= 0.5 when controller is in forward path.

The value of system parameters have been taken from [14]. For ready reference it is given in table (3.1)

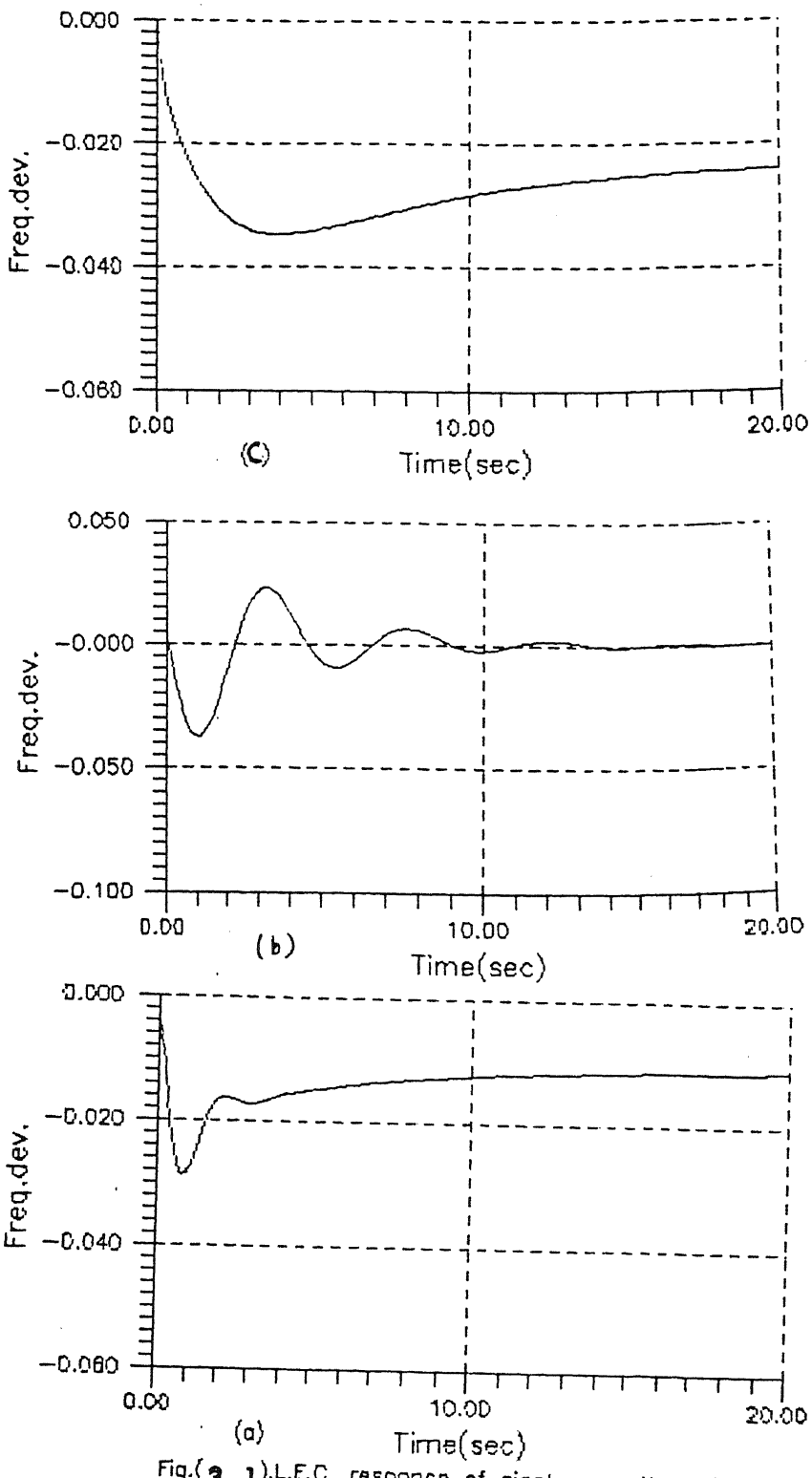

Fig.(3.1).L.F.C. responce of single area thermal plant . (a) is with only proportional controller (b) is with only conventional controller (c) is with only derivative controller kp=.5 ki=.5 kd=.5

Table 3.1

T_g = 0.08	K_P = 120H_z/P.U.MW
T_t = 0.3 sec	K_r = 0.5
T_r = 10 sec	R = 2.4H_z/P.U.MW
T_P = 20 sec	ΔP_t = 0.01

3.3. CONVENTIONAL(INTEGRAL) CONTROLLER

This is the only controller which brings the steady state error to zero. It integrates the error and gives control action to speed changer mechanism in governor system so as to bring output error to zero. This controller have been in use in Load frequency control of power plants for quite long time [1,3,4,5]. The simulated results of load frequency control of single reheat thermal plant with integral controller is shown in figure (3.1-b).

3.4 DERIVATIVE CONTROLLER:

This controller alone is not suitable for control action. As it can be seen in fig. (3.1c) it gives constant error. This controller action can be explained as follow:

When the rate of change of error is higher, the controller is more active and as the rate of change goes lower, the

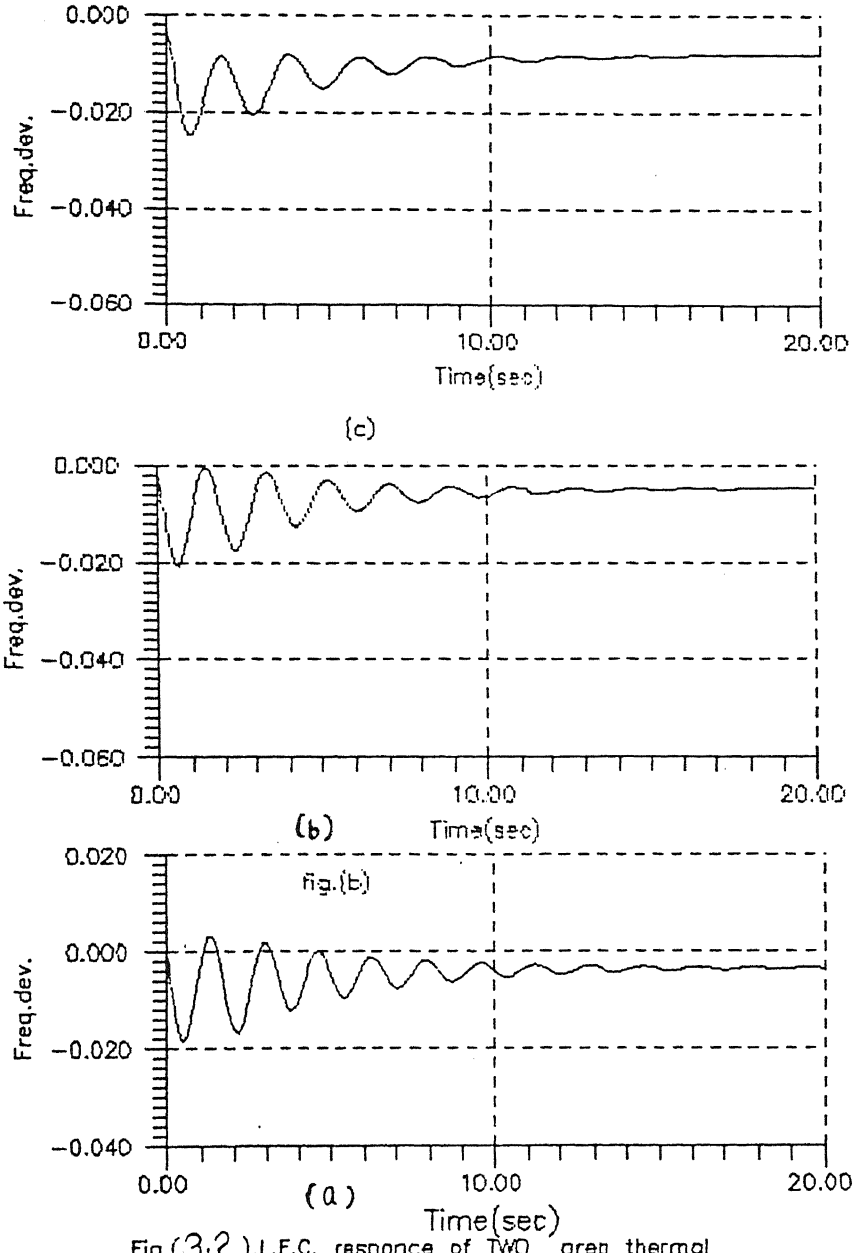

fig.(b)

Fig.(3.2).L.F.C. responce of TWO area thermal plant. with only proportional controller
(a) is with kp=2.5 ,(b) is with kp=1.5 (c) kp=0.5

controller action reduces. If error remains constant (i.e. no change in error) then the controller output will be zero. Therefore, the Load Frequency control developes a constant error response.

3.5 EFFECT ON TWO AREA INTERCONNECTED POWER SYSTEM

3.5.1 Proportional Controller: The effect of proportional controller for different values of K_p = 2.5, 1.5 & 0.5 on two area reheat thermal plant is studied. The frequency response, when controller is in forward path, is shown in fig. (3.2). The frequency response with proportional controller in feed back path is shown in fig. (3.5c). The value of parameters of interconnected thermal plant is given in table (3.2).

Table (3.2)

$T_{P1}=T_{P2}=20$	$K_{P1}=K_{P2}=120H_Z/P.U.MW$
$T_{r1}=T_{r2}=10sec$	$K_{r1}=K_{r2}=0.5$
$T_{t1}=T_{t2}=0.3sec$	$T_{g1}=T_{g2}=0.08sec$
$R_1=R_2=2.4H_Z/P.U.MW$	$a_{12}=-1$
$B_1=B_2=0.545$	$\Delta P_{t1}=0.01$
	$\Delta P_{t2}=0.0$

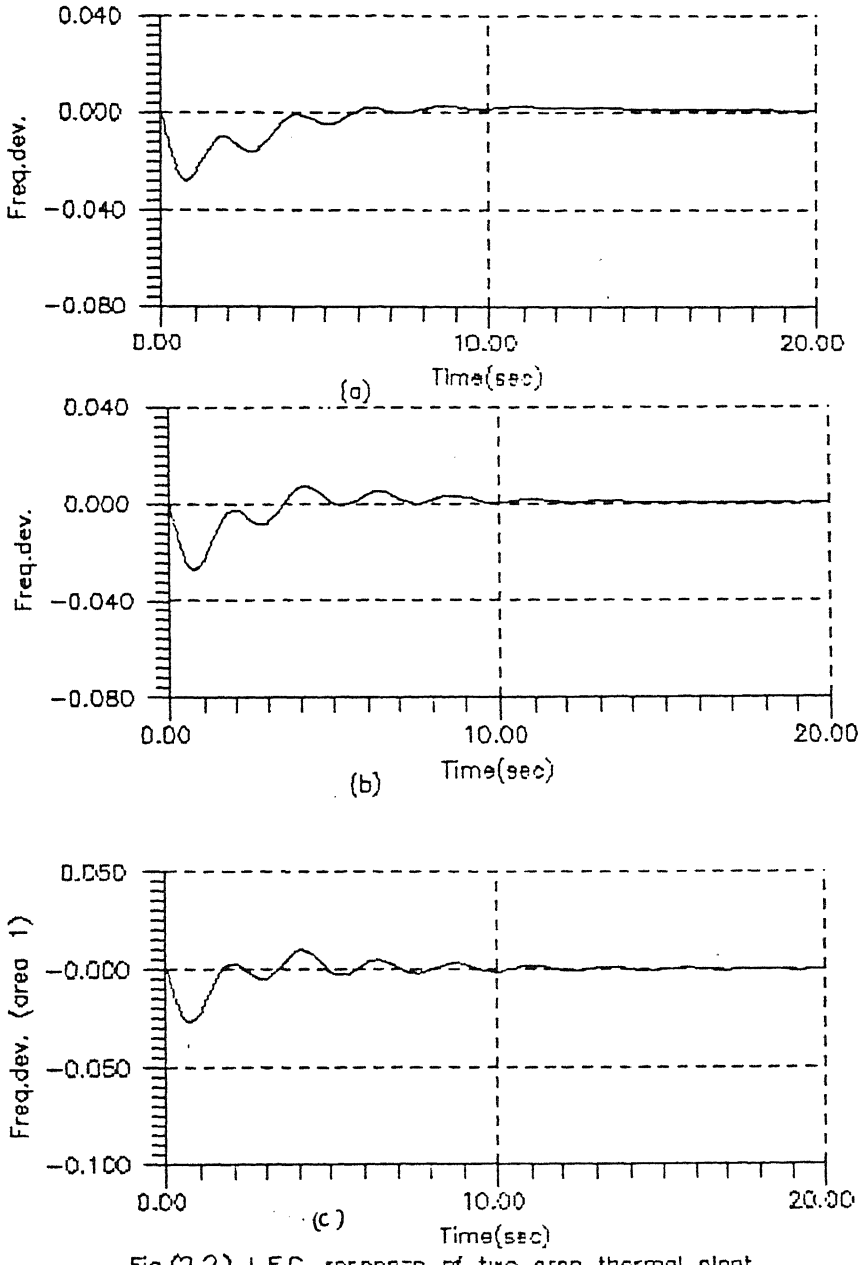

Fig.(3.3) L.F.C. responce of two area thermal plant with only conventional (intg.) controller fig.(a) is with ki=0.3 fig.(b) ki=0.67 and (c) ki=1.0 .

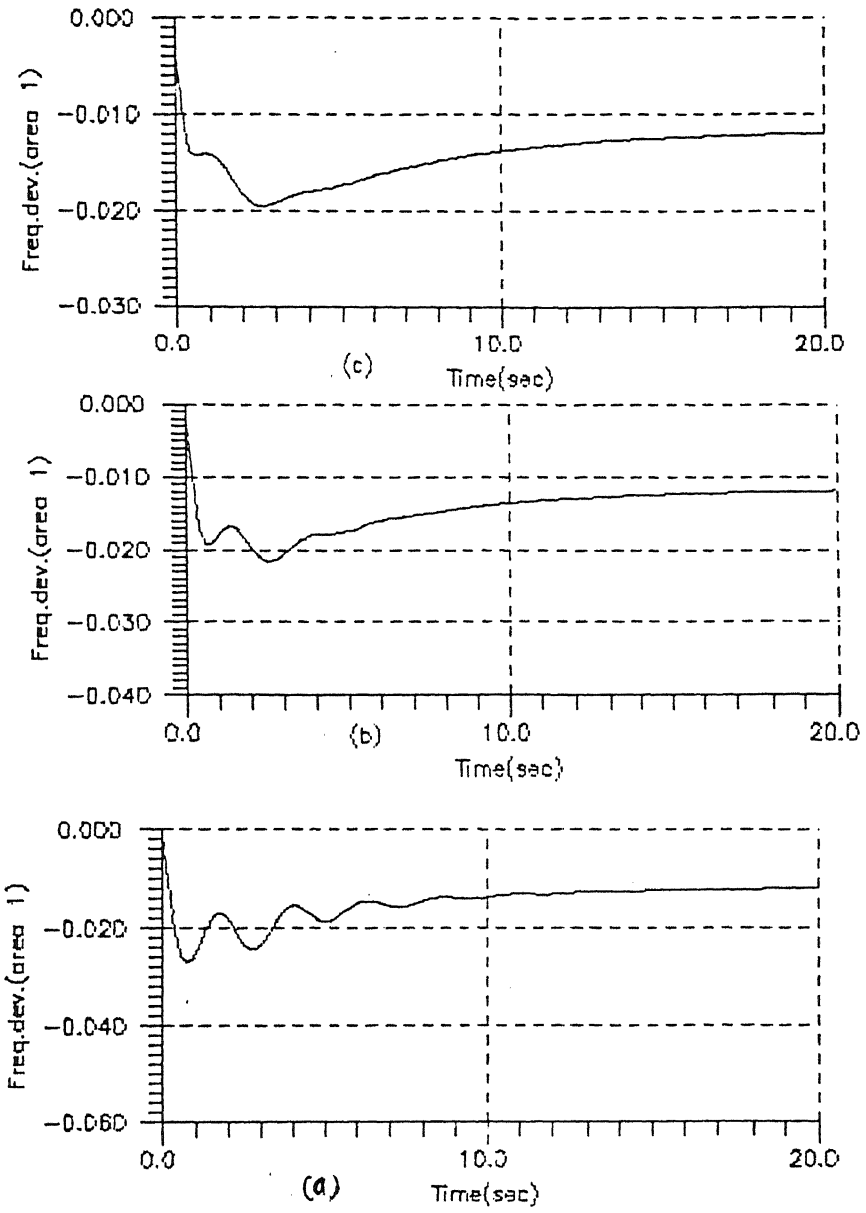

Fig.(3.4)LFC response of two area thermal plant with DERIVATIVE controller fig(a) kd=1.0 ,fig(b) kd=0.5 and fig(c) kd=0.05

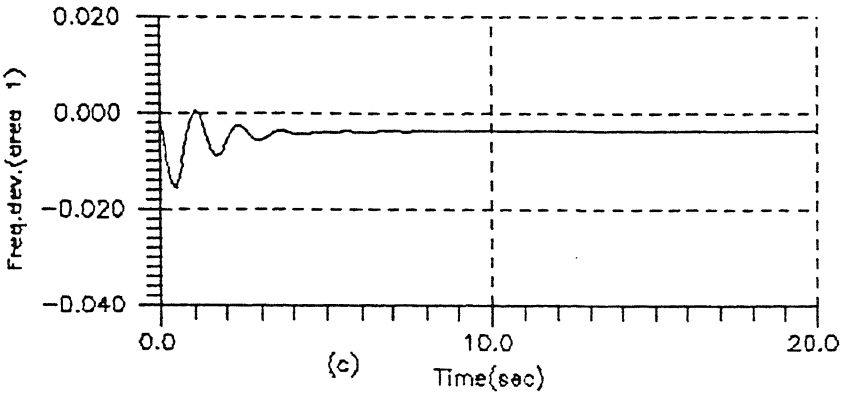

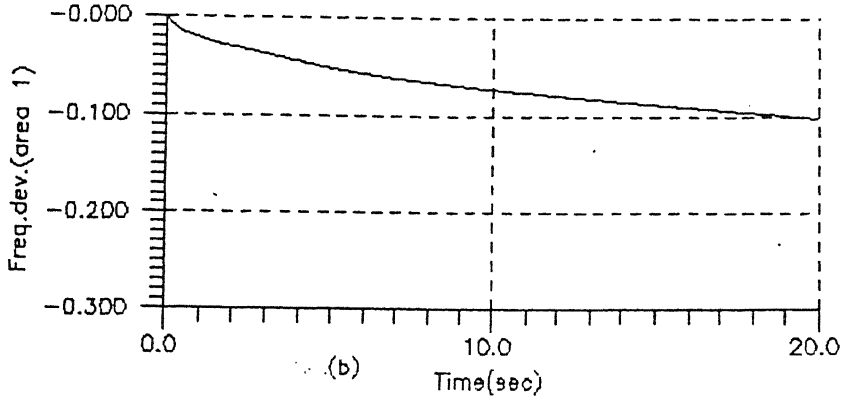

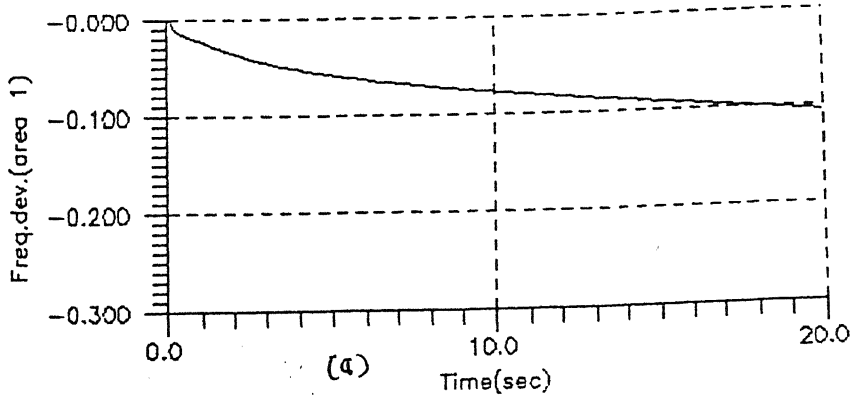

Fig.(3.5) L.F.C. responce of two area thermal plant with controllers in feedback path fig(c) is with proport.(kp=2.5),fig(b)is with integ. ki=0.67 and fig(a) is with derivative kd=0.5 only.

3.5.2 Integral Control: Integral control in forward path, with gain value K_i = 0.3, 0.67and 1.0 have been used to study the load frequency control response of two area-interconnected power plant. The responses have been shown in fig. (3.3). The response with K_i = 0.67 in feed back path is shown in fig. (3.5b). It can be seen that integral control in feed back path is not good, it gives steady state error. A better result is obtained with controller in forward path with gain value 0.67, which has been also found by Fosa & Elgand [6].

3.5.3 Derivative Controller:: This controller alone in forward path or feed back path does not give good response. Simulated responses for gain value K_d = 0.05, 0.5 and 1.0 in forward path has been obtained. The frequency deviation response is shown in figure (3.4). The same with Controller in feed back path with gain value 0.5 is shown in fig. (3.5a).

3.6 CONCLUSIONS

We can conclude from the foregoing results that only conventional controller can be used for load frequency control if we are required to use any single controller. In fact only this controller have been used in the past.

CHAPTER - 4

STUDY OF PROPORTIONAL, INTEGRAL AND DERIVATIVE CONTROL WHEN ANY TWO CONTROLLERES ARE USED SIMULTANEOUSLY

4.1 INTRODUCTION

In this chapter, we shall study the effect of two controllers used in load frequency control of single as well as double area power plants. Two controllers together, normaly proportional plus derivative, proportional plus integral and integral plus derivative are used in forward path as well as feed back path to arrive at appropriate control configuration which yields best response..

4.2 PROPORTIONAL PLUS DERIVATIVE CONTROLLER

With this controller used in single area, it is observed that it gives steady state error in frequency deviation, refer fig. [4.1]. It also gives steady state error in load frequency control of two-area interconnected power system. Fig. [4.2a] shows the frequency deviation when both controllers are in forward path. Fig. [4.2b] shows the response when proportional is in forward path and derivative in feedback path. Fig. [4.2c] shows the response, when derivative is in forward path and proportional controller in feed back path. None of these responses are acceptable since they result in steady state error.

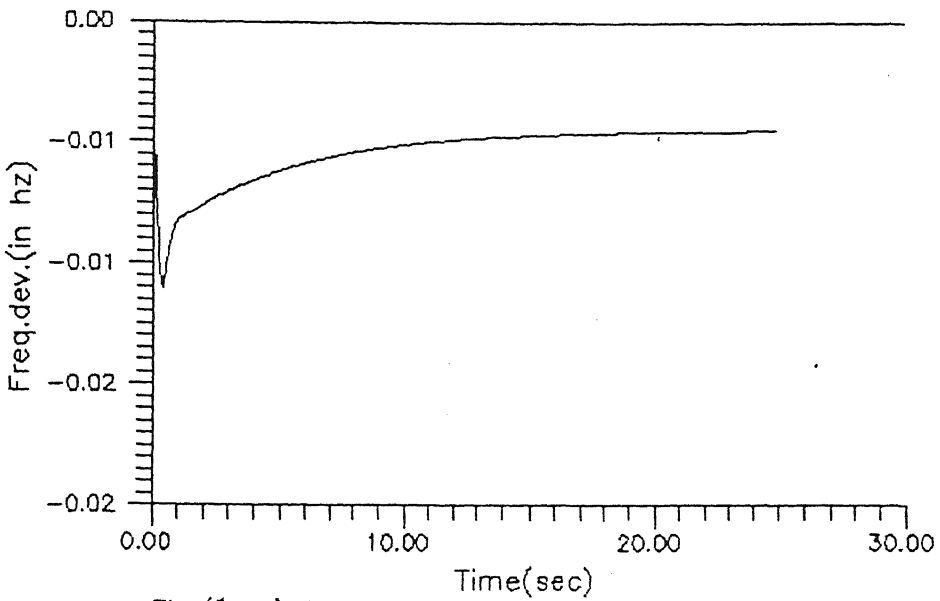

Fig.(4-1)LFC response of one area reheat→thermal plant with propor.+ deriva.controller kp=1.8 kd=0.5

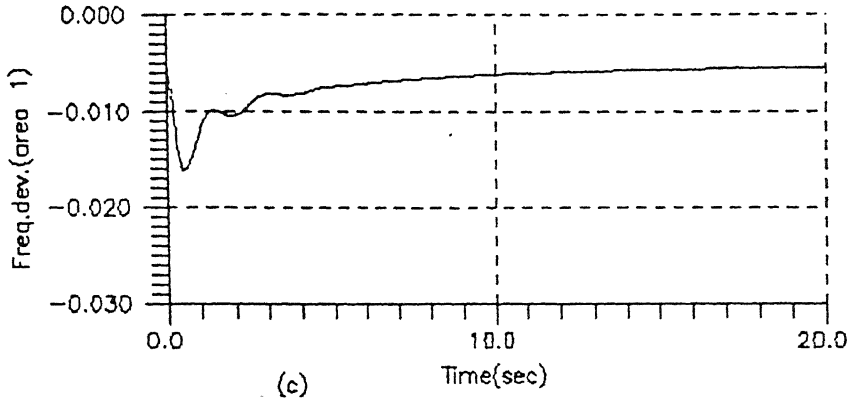

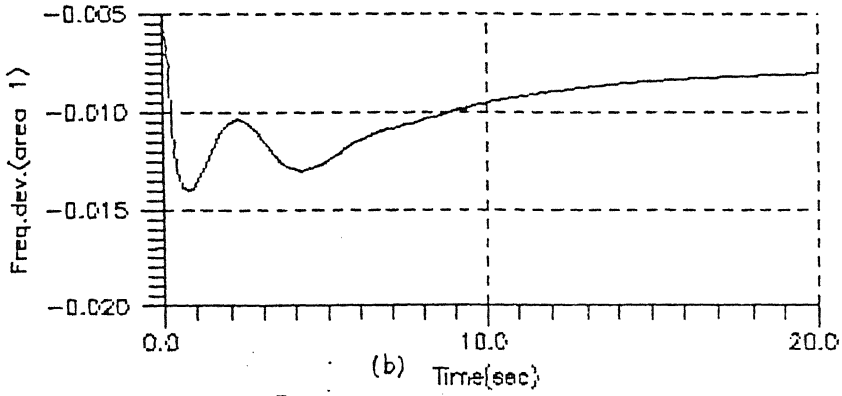

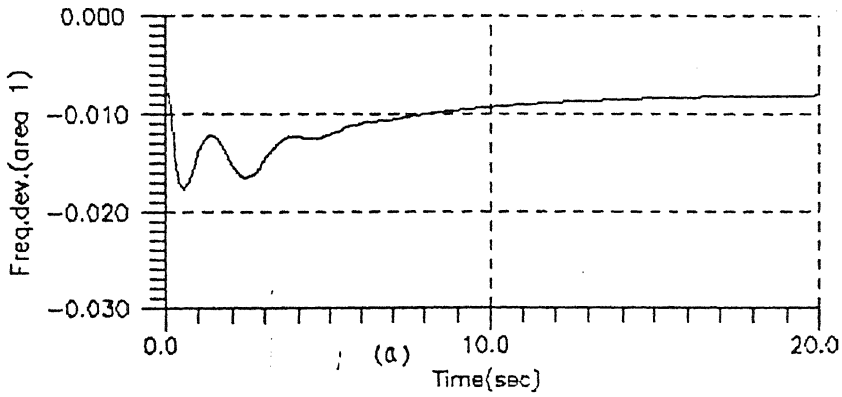

Fig.(4.2)L.F.C. responce of two area thermal plant with combination of two control elements. fig(a)kp=0.5,kd=0.5in forward path fig(b)kp in forward path kd in f.b.path fig(c)kdin f.path kpin f.b.path

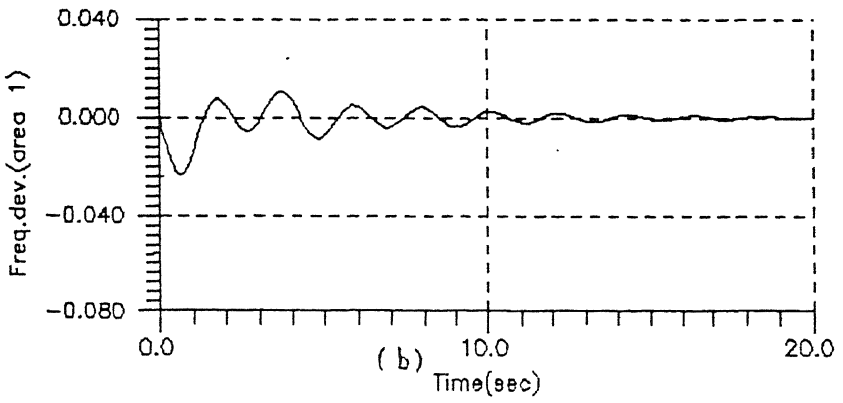

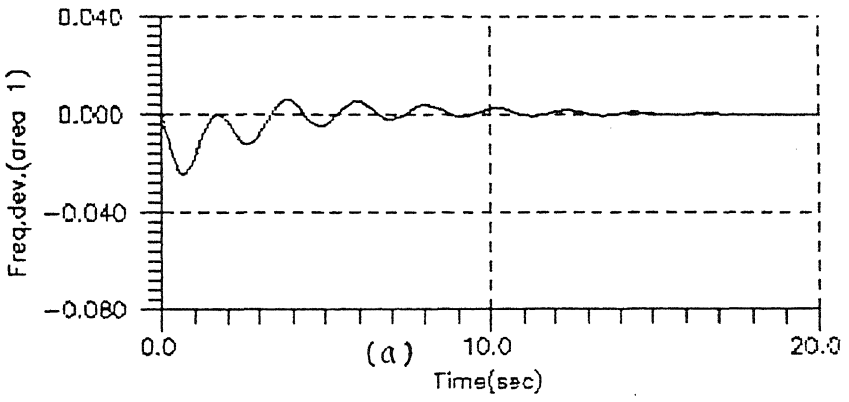

Fig.(4.3)L.F.C. responce of two area thermal plant with combination of two control elements. fig(a) with kp,ki in forward path.fig(b) with kpin forward and ki in feedback path.

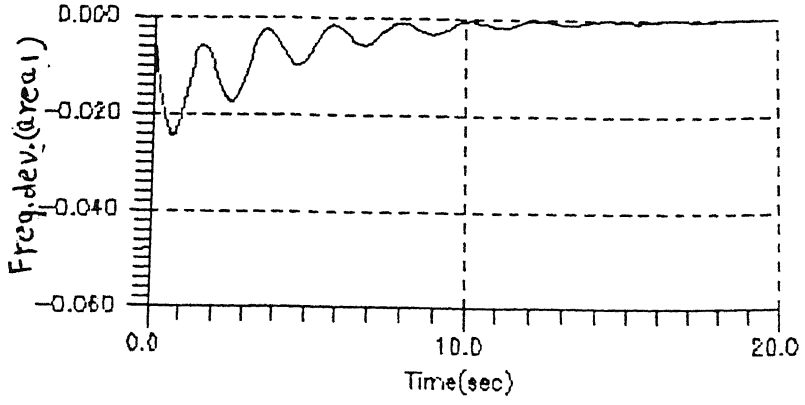

(b)

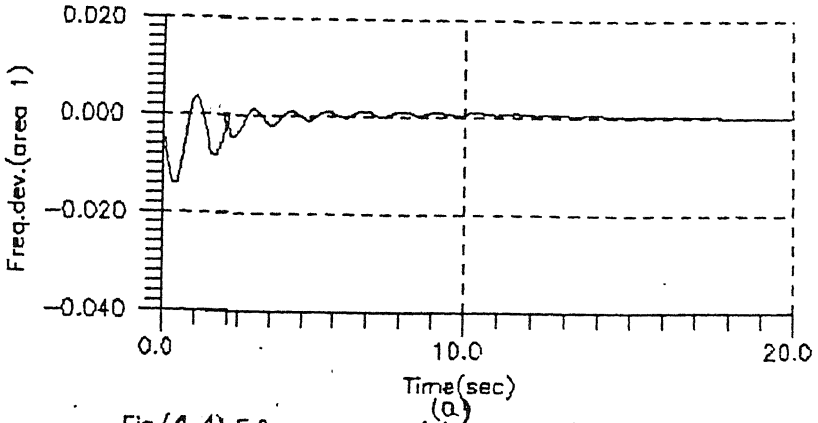

(a)

Fig.(4.4).F.C. responce of two area thermal plant with combination of two control elements. fig(a) ki in f.path & kp in f.b.path, fig(b) with (1+a/s) in f.back path

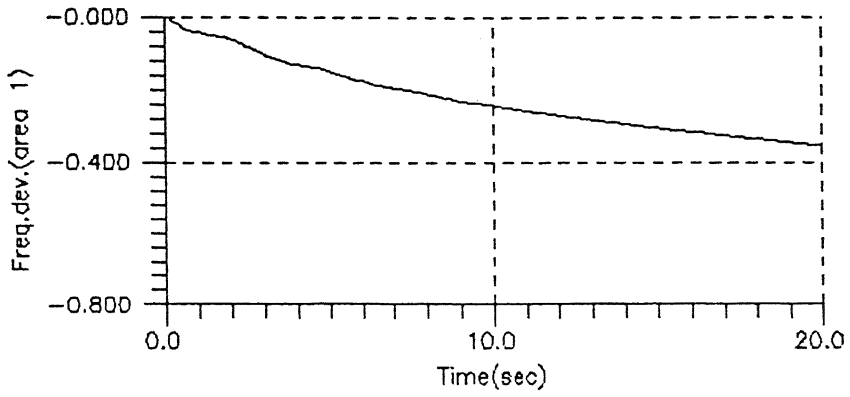

(b)

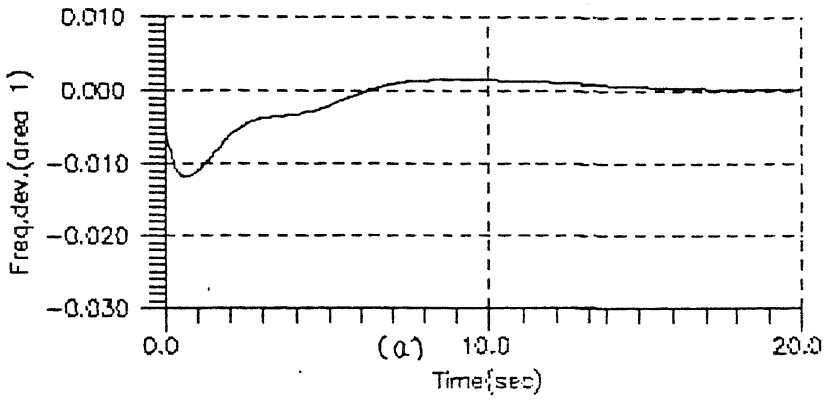

Fig.(4.5) L.F.C. responce of two area plant with combination of two control fig(a)ki in f.path &(1+as) in both f.back fig(b) kp,ki in both feedback path.

4.3 PROPORTIONAL PLUS INTEGRAL CONTROLLER

Only some controller arrangement gives good response, i.e., no steady state error. When proportional and integral both are in forward path with K_p = 0.5 and K_i = 0.67, the response maximum overshoot is 0.024 and sattling time is approximately. 13 sec. (fig. 4.3a). In fig. [4.3b], when proportional is in forward path and integral in feed back path, the maxmimum overshoot is 0.028 but settling time is approximately 11 sec. When proportional is moved to feedback path and integral to forward path, both overshoot and sattling time reduces, (fig. (4.4a)). In fig. (4.4b) it can be seen that with K_p in forward path and (1+A/S) in both the feedback path, the response has 0.024 overshoot and settling time 12 sec. When we use integral controller in forward path and (1+AS) in both feedback path, the response overshoot reduces to 0.012 and transients die out but the settling time is approx. 15 sec.as evident from fig. (4.5).

Therefore, it can be established that I-P arrangement, i.e. integral in forward path and proportional in feedback path results in the best response.

Load frequency responses of single area with different values of proportional gain and integral gain are shown in fig. (4.6) to fig. (4.9).

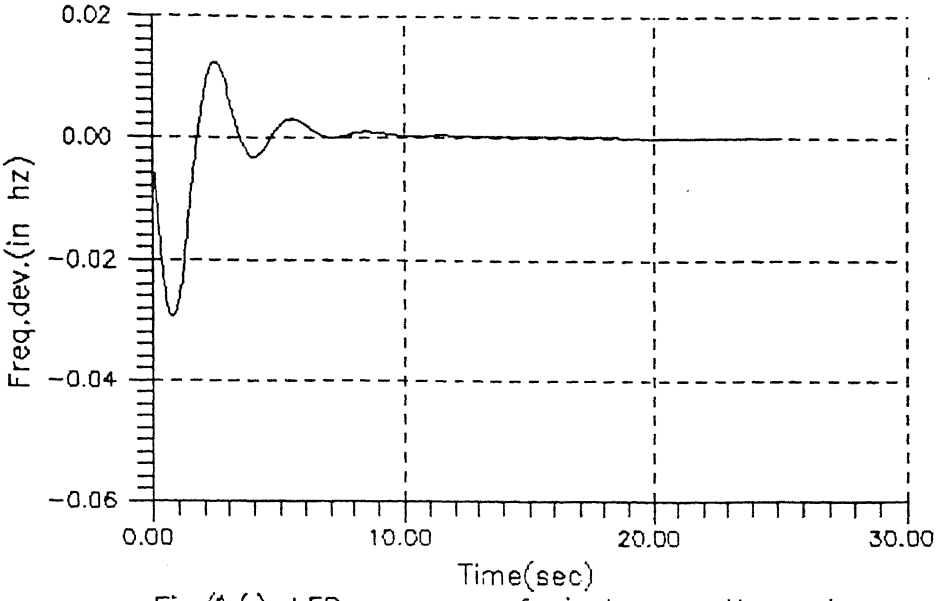

Fig.(4.6)→LFC response of single area thermal plant with integeral+proportional controller
Ki=0.7 kp=0.3

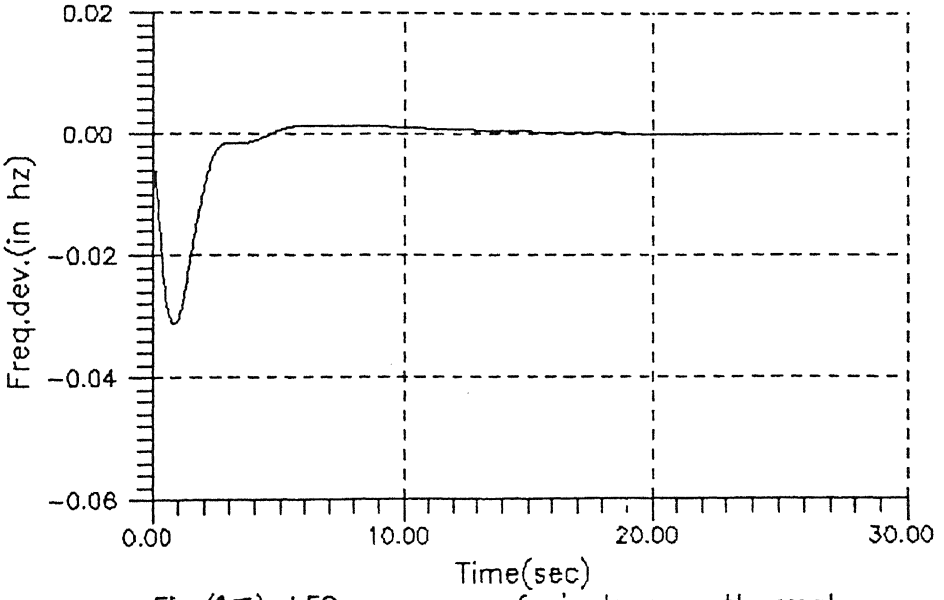

Fig.(4.7)→LFC response of single area thermal plant with integeral+proportional controller
Ki=0.3 kp=0.3

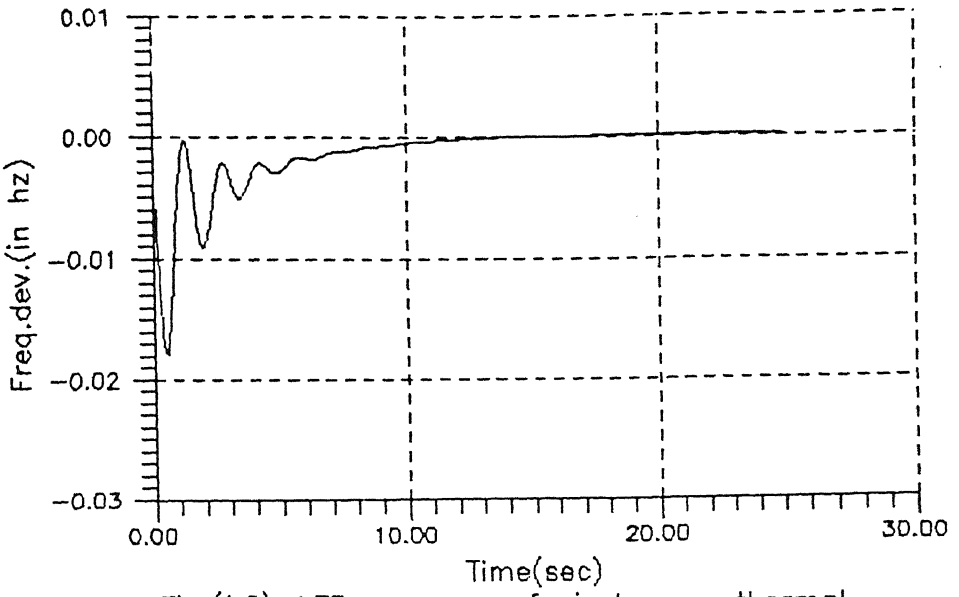

Fig.(4.8)→LFC response of single area thermal plant with integeral+proportional controller
Ki=0.3 kp=1.8

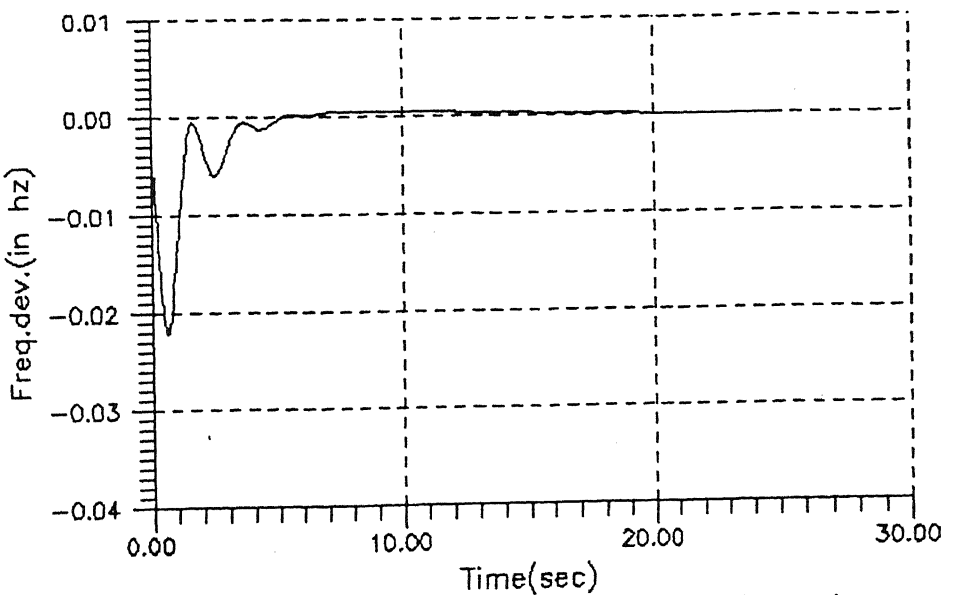

Fig.(4.9)→LFC response of single area thermal plant with integeral+proportional controller
Ki=0.5 kp=1.0

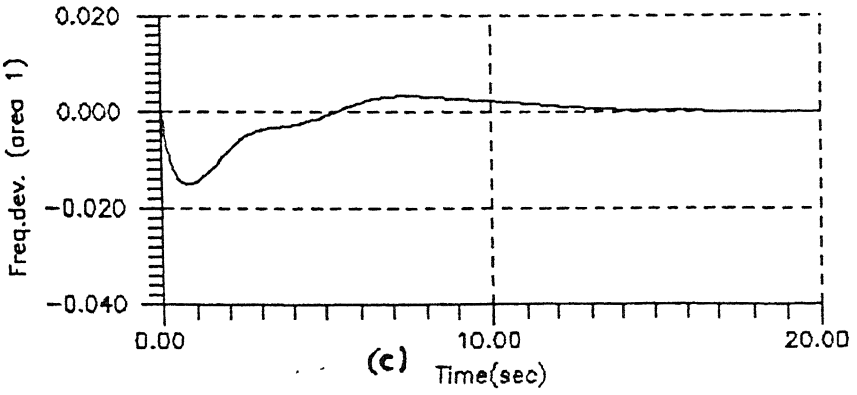

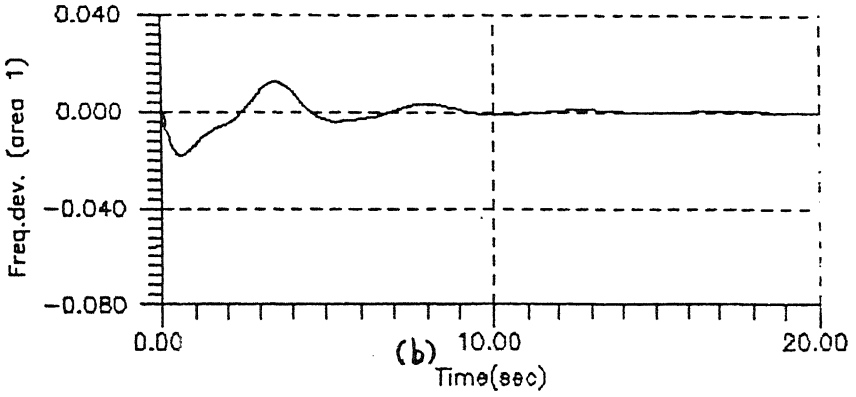

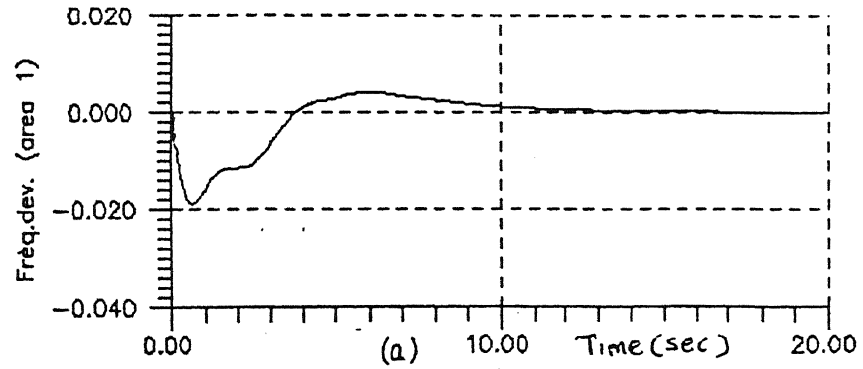

Fig.(4.10) L.F.C. responce of Two area thermal plant with INTEGERAL AND DERIVATIVE controller fig.(a) is with kd=0.5 ,Ki=0.67 in forward path ,fig(b) is kd=0.5 in in forward &ki=0.67 infeedback path.

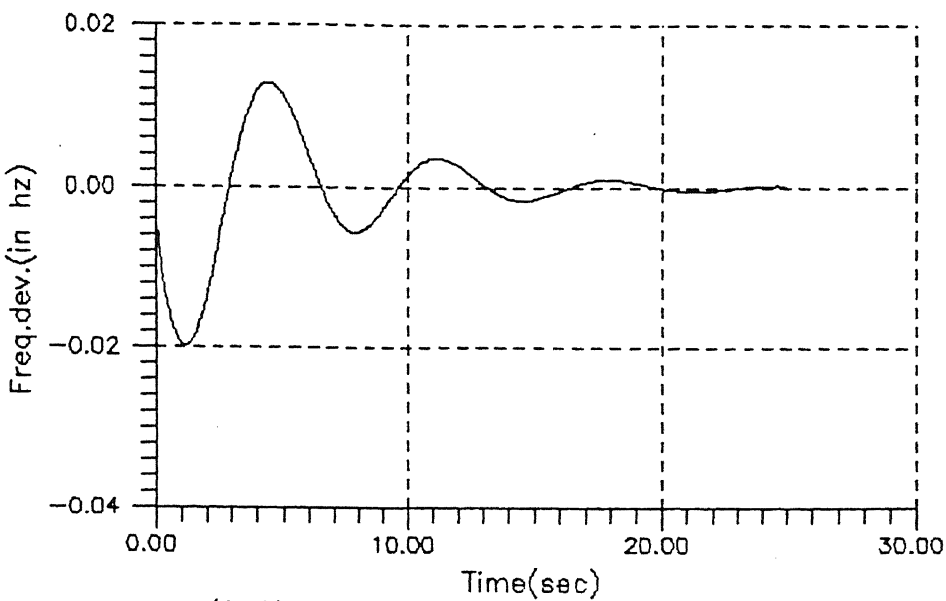

Fig.(4.11) LFC response of single area thermal plant with integeral+derivative controllar
Ki=0.7 kd=0.5

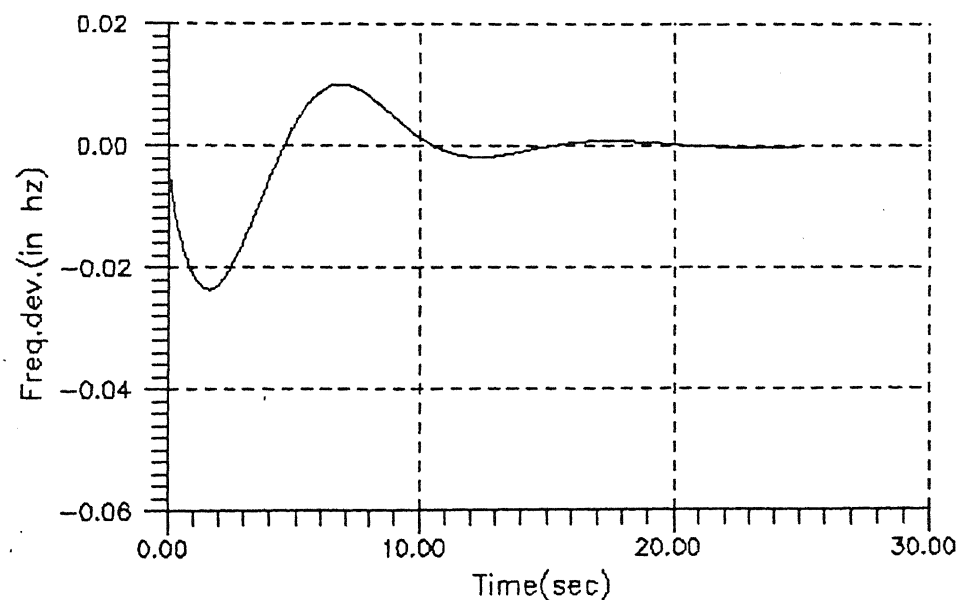

Fig.(4.12) LFC response of single area thermal plant with integeral+derivative controllar
Ki=0.3 kd=0.5

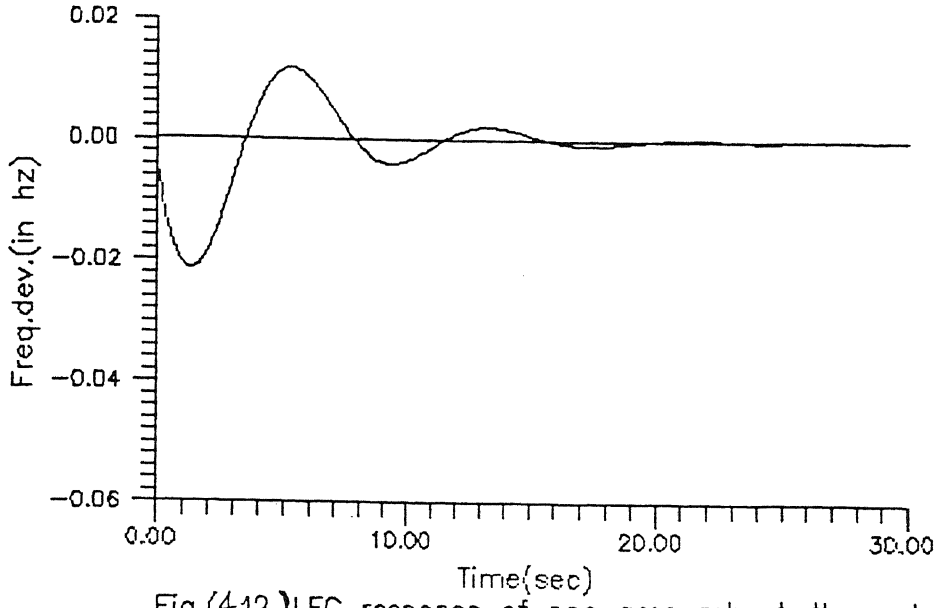

Fig.(4.13)LFC response of one area reheat→thermal plant with Integeral plus derivative controllar ki=0.5 and kd=0.5

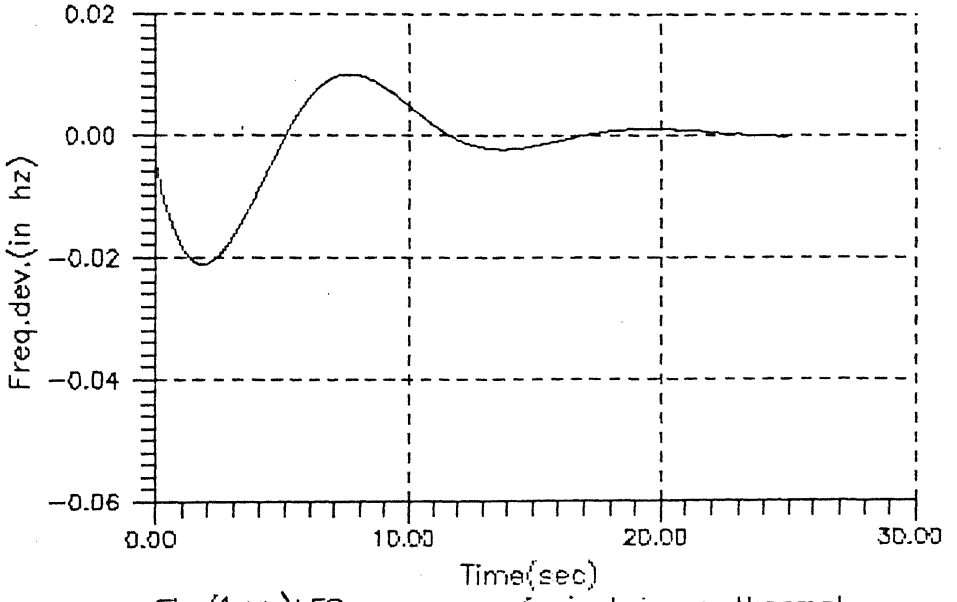

Fig.(4.14)LFC response of single area thermal plant with integeral+derivative controllar
Ki=0.3 kd=0.7

4.4 INTEGRAL PLUS DERIVATIVE CONTROLLER

Since the integral controller brings back the steady state error to zero and derivative controller becomes more effective during high rate of change of error, this combination of controller also gives satisfactory response of load frquency control of single as well as two-interconnected power systems. Figures (4.10) shows the frequency response of two area reheat thermal plant for different configuration of controller. Figure (4.11) to fig. (4.14) gives the frequency responses of single area reheat thermal plant.

4.5 CONCLUSIONS

From the foregoing results, we can conclude that integral controller presence in any combination is a must to bring steady state error to zero. However the I-P configuration, i.e., integral in forward path and proportional in feedback path yields the best response.

CHAPTER - 5

P.I.D. (PROPORTIONAL PLUS INTEGRAL PLUS DERIVATIVE) CONTROLLER APPLIED TO POWER SYSTEMS

5.1 INTRODUCTION

Investigations on load frequency control of power system had been in existance since long [6,14-16]. Various methods have been suggested, like, optimal controller,variable-structure controller and pole-placement techniques. All these methods have certain constraints which has been discussed in chapter-1. To overcome these constraints, a P.I.D. controller approach have been investigated in this chapter. In 1982 Hiyama [5] has suggested P.I.D. controller, but he used it only in forward path. In this chapter different P.I.D. controller configurations will be studied, which are based on the study and results discussed in Appendix 'C'.

5.2 IMPLEMENTATION

P.I.D. controller in different configuration applied to single area thermal plant, two inter-connected thermal plant and hydro-thermal plant is studied. A simple block diagram representation of a particular controller configurations has been shown in the next section. The value of parameters of power systems is given in table (5.1). All other configurations have been shown and discussed in appendix 'D'. For simplicity a single

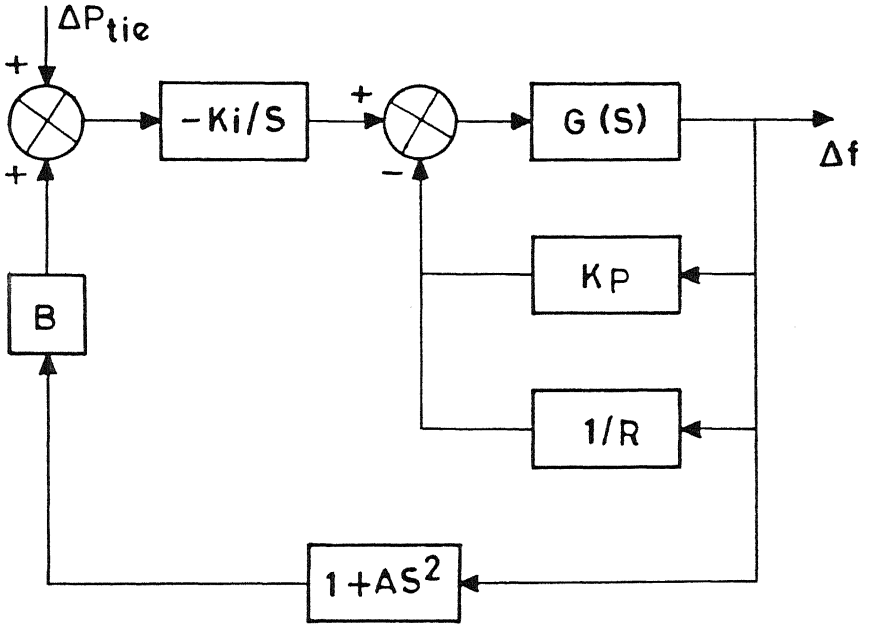

Figure (5.1)

area subsystems, i.e., Governor (Gg(S)), Turbine ($G_T(S)$) and Generator ($G_p(S)$) have been shown as single block (G(S)). One important feature of all configurations is that the overall characteristic polynomial remains of the same order.

5.3 EXAMPLE

One typical example of P.I.D. controller configuration is shown in fig.(5.1). In the secondary feed back path,i.e., 'B_1 feed back path' a second differentiation and a constant gain areused. In forward path only integrator is positioned. With this arrangement, the simulated result of the load frequency control responses of two area thermal plant are shown in fig. (5.2) and fig. (5.3). The response of hydro-thermal plant is shown in fig. (5.4). Block daigram representation of a typical Hydro-Thermal power systems is given in fig.(5.5).

TABLE - 5.1

Thermal plant	Hydro plant
Each area rating = 2000 MW	Each are rating = 2000 MW
Base power = 2000 MVA	Base power = 2000 MVA
R = 2.4 Hz/P.U.MW	R = 2.4 Hz/P.U. MW
B = 0.425 P.U.MW/Hz	T_{12}= 0.545 P.U.MW/Hz
T_g= 0.08 Sec	B = 0.425 P.U.MW/Hz

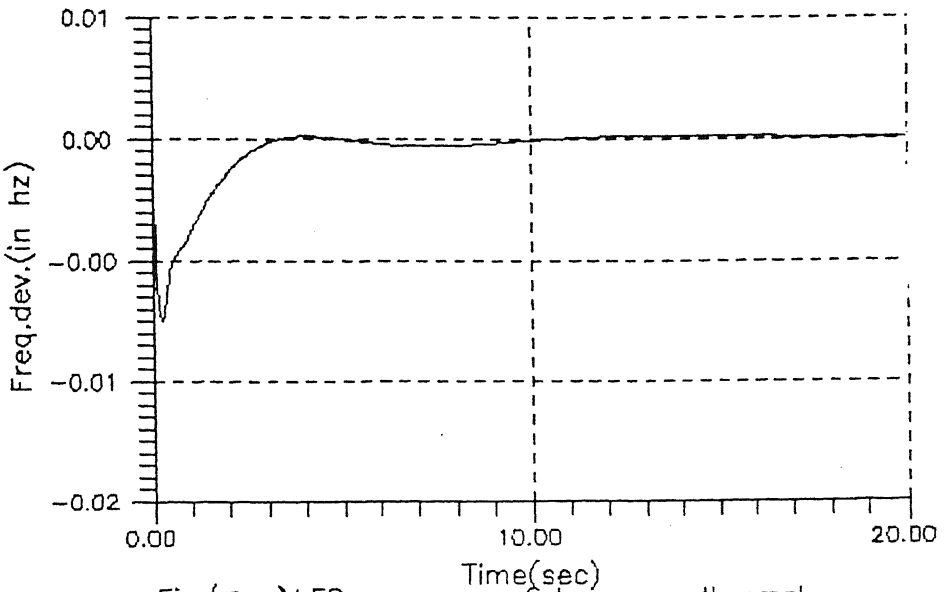

Fig.(5.2)LFC response of two area thermal plant with P.I.D controller (ki/s→in forward path)and((1+a1s*s) in B1 F.B.Path) ki=1.5→kp=2.5,a1=1.5 (kp in'R1'F.B.Path)

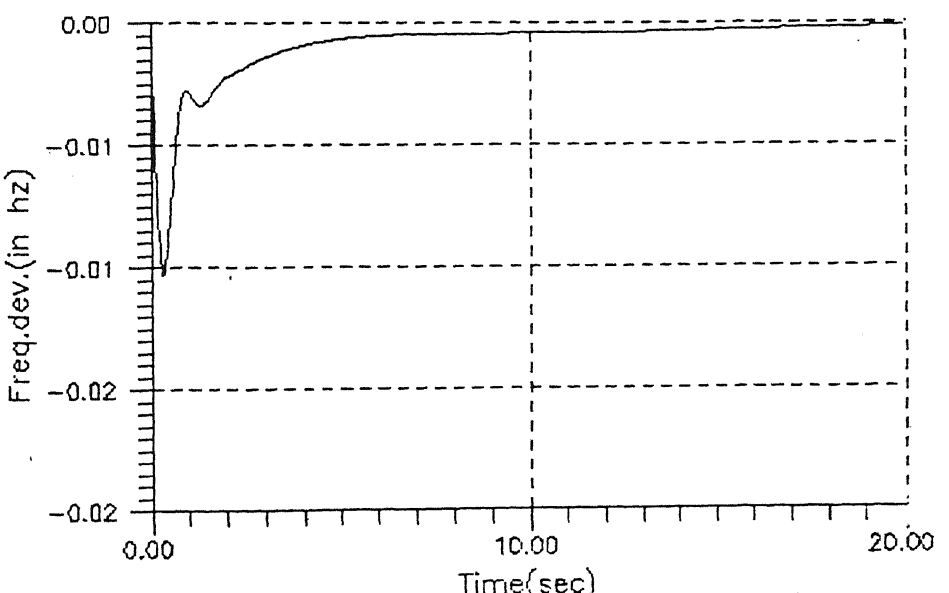

Fig.(5.3)LFC response of two area thermal plant with P.I.D controller (ki/s→in forward path)and((1+a1s*s) in B1 F.B.Path) ki=.67→kp=2.5,a1=1.5 (kp in'R1'F.B.Path)

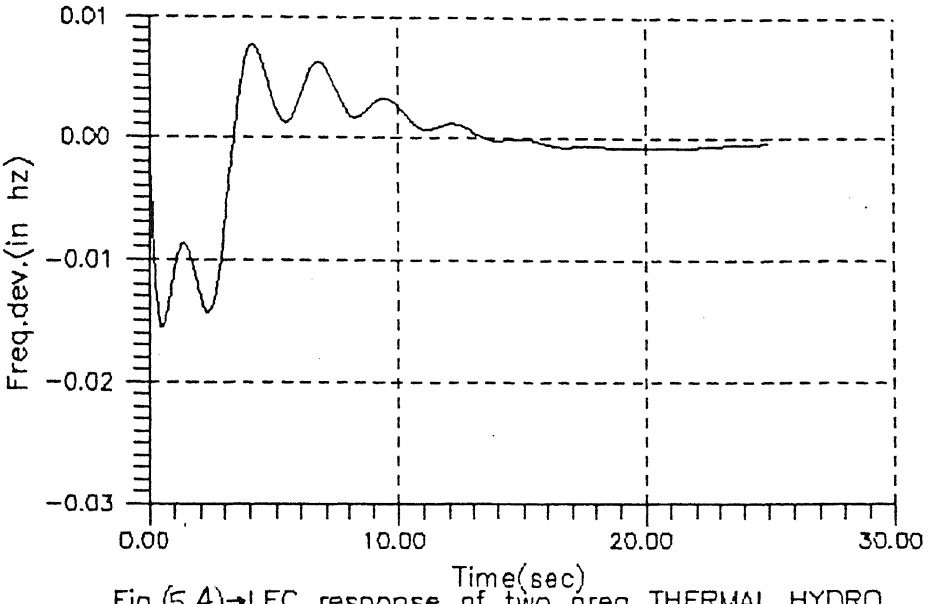

Fig.(5.4)→LFC response of two area THERMAL HYDRO plant with P.I.D controller (ki/s in forward path)and (1+a*s*S) in B_1 f.b.path).
a=0.7 kp=0.5 ki=0.9

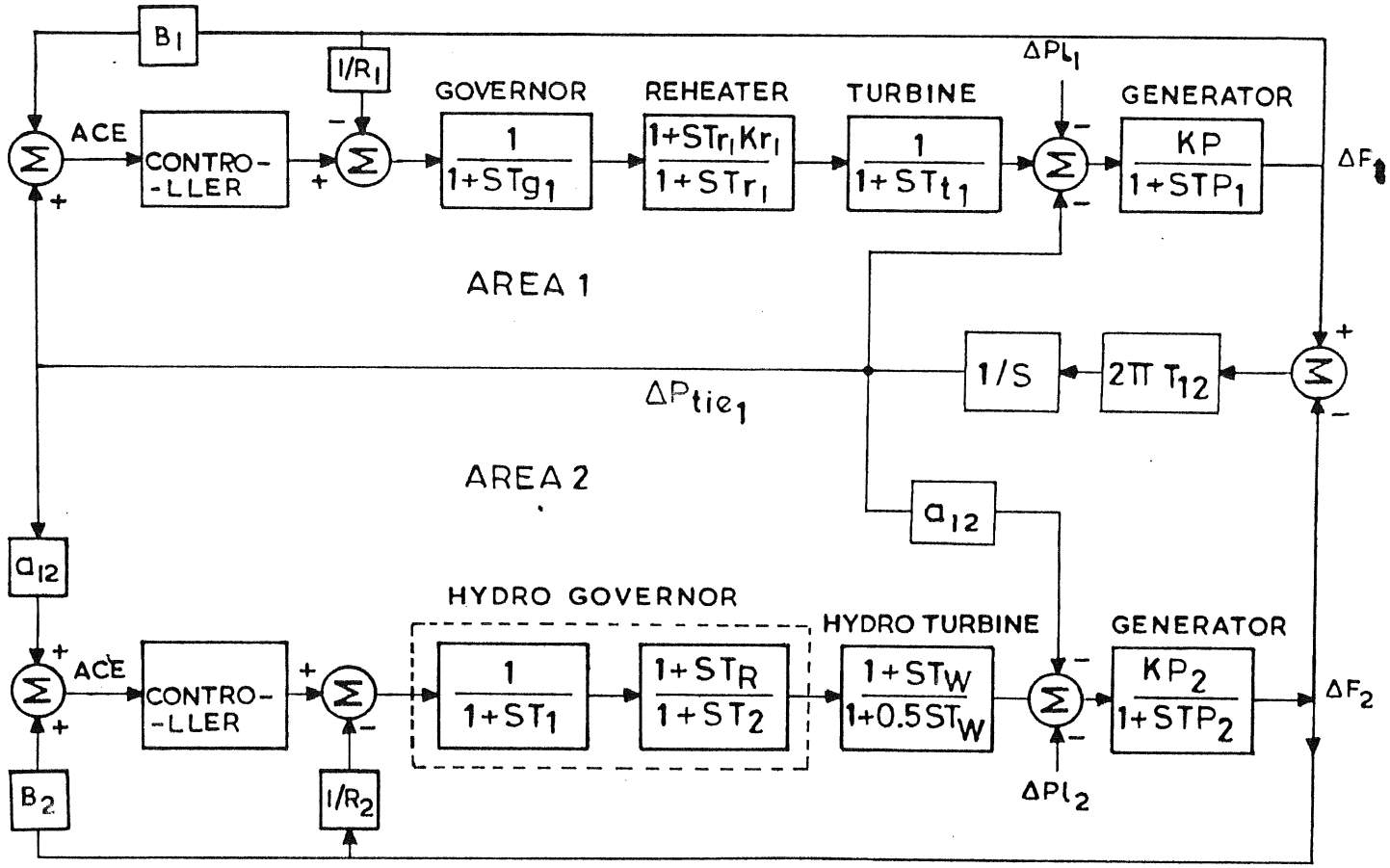

Figure (5.5) Block diagram representation of Hydro-thermal power system

T_t= 0.3 sec

T_r= 10 sec

K_r= 0.5

T_2= 0.545 P.U. MW/Hz

T_P= 20 sec

K_P= 120 Hz/P.U.MW

T_w = 1 sec., T_R = 10 sec

K_r = 0.5, T_1 = 48.7 sec

T_2 = 0.513 sec

K_P = 120 Hz/P.U. MW

T_P = 20 sec

5.4 OBSERVATIONS ON RESULTS

On a close observation of various responses it can be easily seen that maximum undershoot or overshoot is less than 0.02 Hz and setlling time is quiet less. This is as per the 'requirements of controllor' discussed in chapter 1. It can be clearly observed that the responses with proposed controller is better in all respect. All other results of various configuration are shown in appendix 'D'.

To have a brief observation and study of results, the response characteristics have been tabulated and given in table (5.2) to (5.4).

The tie line power deviation, area control error (ACE) and frequency deviation of area '2' have also been shown in appendix 'D' for Reheat\Nonreheat thermal and Hydro plants. It has been compared with Variable-Structure System (VSS) responses. The consolidated results are given in table (5.5).It is also to be noted that controller's gain values have been achieved by trail and error method.

TABLE - 5.2

RESPONSE CHARACTERISTICS OF THERMAL SYSTEM

Configuration No.	Fig. No.	Maximum Undershoot		Maximum Overshoot		Setlling time in sec
		Amplitude in Hz	Duration in sec.	Amplitude in Hz	Duration in sec	
1	D.2	0.017	4.0	0.0025	8.0	13.0
	D.3	0.0175	7.0	0.0	0.0	8.5
2	D.9	0.017	5.0	0.0015	7.0	15.0
	D.10	0.016	1.2	0.0015	0.5	8.0
3	D.13	0.0125	1.5	0.003	1.0	10.0
4	D.16	0.018	1.5	0.0028	0.8	11.0
5	D.19	0.016	6.0	0.004	5.0	11.0
6	D.22	0.0035	1.0	0.0	0.0	1.8
7	D.25	0.008	7.0	0.002	9.0	18.0
8	D.28	0.0045	5.0	0.005	6.0	11.0
9	5.2	0.001	3.0	0.0	0.0	3.0
	5.3	0.0012	7.0	0.0	0.0	7.0

TABLE - 5.3

RESPONSE CHARACTERISTICS OF NON-REHEAT THERMAL POWER SYSTEM

Configuration No.	Fig. No.	Maximum Undershoot		Maximum Overshoot		Setlling time in sec
		Amplitude in Hz	Duration in sec.	Amplitude in Hz	Duration in sec	
6	D.34b	0.0012	5.0	0.0	0.0	5.0
9	D.35a	0.001	3.0	0.0	0.0	11.5

TABLE - 5.4

RESPONSE CHARACTERISTICS OF HYDRO-THERMAL POWER SYSTEM

Configuration No.	Fig. No.	Maximum Undershoot		Maximum Overshoot		Setlling time in sec
		Amplitude in Hz	Duration in sec.	Amplitude in Hz	Duration in sec	
1	D.7	0.00188	3.5	0.0035	5.5	9.0
2	D.11	0.00162	3.2	0.0035	7.5	11.0
3	D14	0.0016	3.5	0.0055	10.0	13.5
4	D.17	0.0088	3.5	0.005	4.0	7.5
5	D.20	0.009	3.8	0.0065	4.0	7.8
6	D.23	0.008	2.0	0.007	2.0	25.0
7*	D.26	0.0013	3.3	0.0095	1.8	13.0
8	D.29	0.0015	3.3	0.008	2.0	11.5
9	5.4	0.0015	3.5	0.008	2.0	13.0

*This configuration is like case 14 of table (C-1).

TABLE 5.5

System responses	Type of system	Controller employed	Fig. No.	Maximum undershoot in Hz	Setlling time in sec.
Frequency deviation area 2	Reheat thermal	P.I.D.	D.31c	0.0022	6.0
		V.S.S.	D.30b	0.0066	15.0
	Non-reheat thermal	P.I.D.	D.35b	0.007	8.0
		V.S.S.	D.37b	0.006	12.0
	Hydro-thermal	P.I.D.	D31a	0.014	8.0

Tie line power deviation	Reheat thermal	P.I.D.	D.31a	0.004	6.0
		V.S.S.	D.30c	0.006	15.0
	Non-reheat thermal	P.I.D.	D.35c	0.003	7.0
		V.S.S.	D.33c	0.005	12.0
	Hydro-thermal	P.I.D.	D.37a	0.0125	8.0
ACE	Reheat thermal	P.I.D.	D.31b	0.001	4.0
		V.S.S.	D.30d	0.018	15.0
	Non-reheat thermal	P.I.D.	D.35d	0.002	8.0
		V.S.S.	D.33d	0.012	10.0

5.5 CONCLUSION

The effectiveness of P.I.D. controller for load frequency control of interconnected power systems has been studied in this chapter. The simulation results (shown in App. 'D') and tables demonstrate the efficiency of the proposed design. It is also shown that the proposed controller satisfies all requirements stated in chapter 1.

CHAPTER - 6

CONCLUSIONS

6.1 GENERAL

This report has been devoted to the Load Frequency Control of single area thermal and hydro plant as well as two area thermal and hydro-thermal power systems. For this purpose proportional, conventional (Integral) and derivative control configurations in various combinations are used. The systems have been simulated on computer and analysed 'EMPIRICALLY'. The following conclusion may be drawn:

(i) The proportional or derivative controller alone does not give good response, i.e., gives steady state error in single area as well as two area power systems.

(ii) Only conventional controller gives steady state zero error.

(iii) When any two controllers are used at a time only integral plus proportional and integral plus derivative controllers yield zero error steady state response in single area. When used in two area power system, these combinations yield good result only in some configurations.

(iv) P.I.D. controller used in single area thermal or hydro plant, shows very satisfactory responses.

(v) P.I.D. controller used in load frequency control of two area interconnected power system shows that only certain control configuration yields good results.

(vi) Load frequency control of interconnected power system when P.I.D. controller is implemented, yields low over shoot (less than

$0.02H_z$), reduced transient oscillations and fast settling time. This is within requirement of standard controller.

(vii) The proposed P.I.D. configuration can be usedd in multi-area (i.e. more than two) interconnected power system [6].

6.2 FUTURE RESEARCH

(a) In this thisis results have been obtained empirically. The mathematical analysis can be carried out on these systems and a formula or theory can be estabalished. This formula might be used for the control of any complex plant.

(b) The P.I.D. controller implementation can be investigated on other area of power generation, transmission and distribution system.

(c) Further investigation can be carried out with consideration of Generation-Rate-Constraints (GRC) in load frequency control of interconnected thermal power plants.

(d) Load frequency control of interconnected hydro plants can be investigated with P.I.D. controller.

REFERENCES

1. ELGERD, O.I.: 'Electric Energy Systems Theory' (McGraw-Hill, 1971) page 315-389.
2. VADHERA, S.S.; Power System Analysis & Stability (Khanna Publishers).
3. OGATA, K.: Modern Control Engg. (Prentice-Hall Englewood Cliffs. N.J. 1970).
4. ROSS, C.W.: 'Error adaptive control of interconnected power systems' IEEE Trans. 1966, PAS-85, pp. 742-749.
5. HIYAMA. T.: 'Design of decentralised load frequency control regulators for Interconnected power system' JEE Proc. C. Gen., Trans., & Distrib, 1982, 129(6), pp. 17-23.
6. FOSHA, C.E. & ELGERD, O.I.: The Megawalt-frequency control problems: a new approach via optimal control theory, IEEE Trans. 192, PAS-91 pp. 563-577.
7. C.K. SANATHANAN,: A Frequency Domain Method for tuning Hydro-Governors: IEEE Trans. on Energy Conversion, Vol. 3, No. 1, March 88. pp 14-17.

8. MURTY, M.S.R. & HARIHARAN, M.V.: Analysis and Improvement of the stability of A Hydro-Turbine generating unit with long Penstock: IEEE Trans. on PAS. Vol. PAS-102, March 1983.

9. IEEE COMMITTEE REPORT: Dynamic Models for Steam and Hydro turbines in power systems studies, IEEE Trans. Power App. Syst. NOV/Dec. 1973.

10. CHAUDHARY, M.H.: Governing stability of a hydroelectric power plant, water power and Dam const., pp. 131-136, April 1970.

11. COLES, H.E. : Effects of Prim-Mover governing and voltage regulation on turbo alternator performance, Proc. IEEE, Vol. 112, No. 7, July 1965.

12. HOVEY, L.M.: "Optimum adjustment of hydro-governors on Manitoba Hydro System", AIEE Trans. Vol. 81, Part III, pp. 581-587, Dec. 1962.

13. HAGIHARA, S., YOKOTA, H., GODA, K. an ISOBE, K.: "Stability of a Hydroulic turbina generating unit controlled by P.I.D. governor" IEEE Trans. on Power App. System, Vol. PAS-98, no. 6, Nov/Dec 1979, pp. 2294-2298.

14. ASHOK KUMAR, MALIK, O.P. and HOPE, G.S.: "Variable structure system control applied to AGC of an interconnected power system", IEEE Proceedings, Vol. 132, Pt. C, No. 1, Jan. 1985.

15. RAMAR, K. and VELUSAMI, S.: "Design of decentralized Load-frequency controllers using pale placementtechnique, Electrical machine and power systems, vol. 16, No. 3, 1989, pp. 193-207.

16. CHAN, W.C., and HSU, Y.Y., 'Automatic generation control of interconnected power systems using variable structure controllers, IEEE Proc. C, Gen. Trans & Distrib, 1981, 128 (5), pp. 269-279.

APPENDIX A

MODELLING FOR LOAD-FREQUENCY CONTROL STUDY

The load frequency control system consists of various subsystems mentioned below.

(i) Governor system

(ii) Turbine system

(iii) Generator and Load system

A-1 Governor System

The governor is the primary tool for the load frequency control. Governing system is basically of two types:

(i) Mechanical-Hydraulic governor

(ii) Electro-Hydraulic governor/P.I.D. governor.

A-2 Mechanical-Hydraulic Governor

A schematic arrangement of the main features of a speed governing system of the kind used on steam turbine is shown in fig. (A.1).

The main components of governor system are listed below

(a) Centrifugal Governor: This is purely mechanical speed sensitive device coupled directly to the prime-mover. As the speed increases the fly balls moves upwards and the point 2 on linkage mechanism moves upwords.

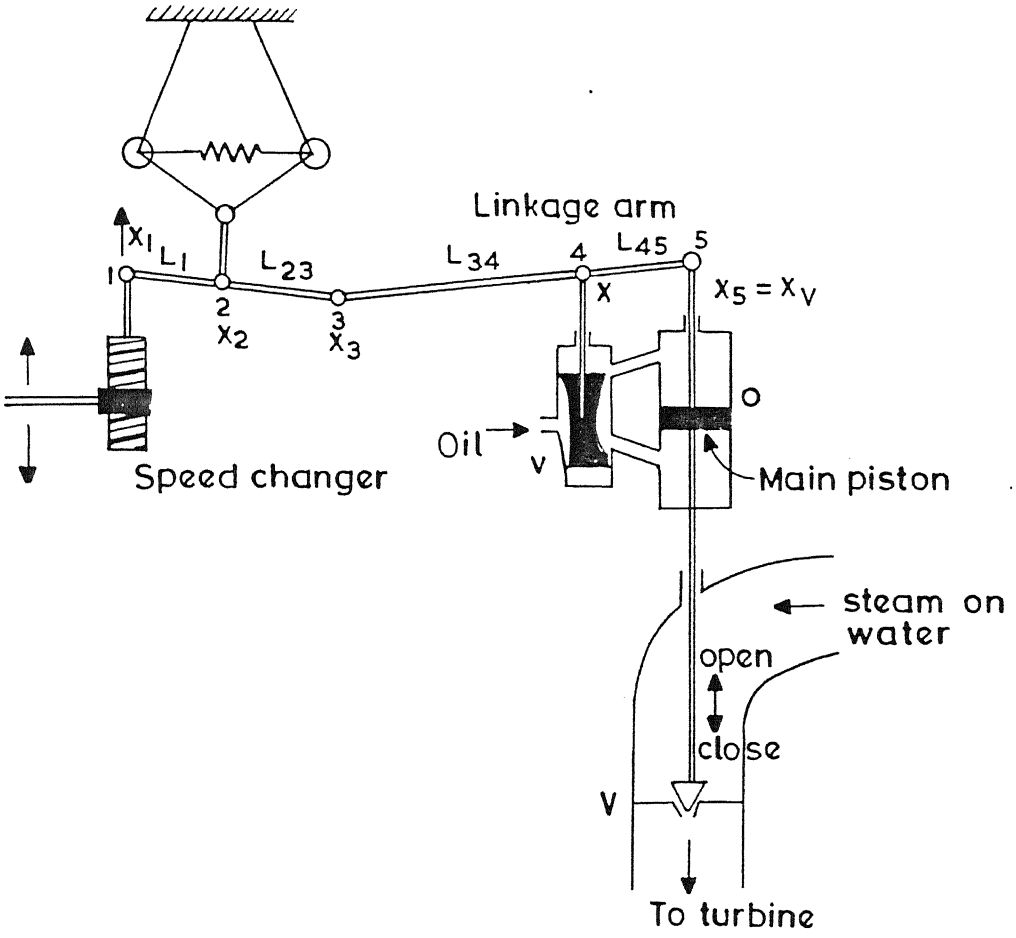

Figure (A-1) Steam turbine speed governor system

(b) Hydraulic Amplifier: It consists of pilot valve (v) and oil servomotor (O). A low power pilot valve movement is converted into high power level piston valve (servomotor) movement. This is necessary for closing and opening the steam valve against high pressure steam.

(c) Linkage Mechanism: 1-2-3 is a rigid link pivoted at point 2. For point 3-4-5, another rigid link pivot is provided at point 4. The function of linkage mechanism is to control the steam valve 'V'. It also provides a feedback from the steam valve movement.

(d) Speed Changer: It provides a steady state power output setting for the turbine. Its downward movement opens the upper pilot valve so that more steam can be admitted to turbine under steady condition.

To develop the mathematical representation of the system, let us assume that the system is operating under steady-state condition i.e. the linkage mechanism is stationary, pilot valve is closed, the steam valve is opened by a definite magnitude, turbine is running at constant speed and the turbine output is balancing generator load.

Thus the nominal conditions are;

Power delivered = P_G^o

Speed = w^o

frequency = f^o

Primemover valve position = X_5^o

Let us change the speed changer to command a power increase (ΔP_c). The speed changer movement gives rise to the linkage point '1' moves upwards a small distance (ΔX_1). We may establish:

$$\Delta X_1 = K\Delta P_c$$

The link point "3" will move downward because of Linkage (1-2-3) action. Let it be ($\Delta X_3'$). Further, the link point "4" moves downward by an amount ($\Delta X_4'$) which moves the piston in pilot servo (v), resulting in high pressure oil flow in the bottom of piston of servomotor 'O'. The piston moves upwards by an amount ($\Delta X_5'$) and steam valve opening increases. Thereby increasing the torque developed by turbine. This increased torque increases the speed of generators i.e. frequency (Δf).

This change of speed results in the outward movement of flyball of the governor. Thus the link point '2' moves slightly upward a small distance (ΔX_2).

Due to the movement of link point 2, the link point 3 also moves upward by an amount $\Delta X_3''$ which is also proportional to Δf.

Thus the net movement of link point 3 is

$$\Delta X_3 = \Delta X_3' + \Delta X_3'' \qquad \text{(A.1)}$$

where $-X'_3(l_{12}) = X_1(l_{23})$

or $$\Delta X_3' = -\frac{l_{23}}{l}\Delta X_1$$

$$= -K_1 \Delta Pc$$

and

$$\Delta X_3'' = K_2 \Delta f$$

Thus we can write: $\Delta X_3 = -K_1 \Delta Pc + K_2 \Delta f$ (A.2)

Again

$$\Delta X_4 = \Delta X_4' + \Delta X_4'' \quad (A.3)$$

where $\Delta X_4'(l_{34}+l_{45}) = \Delta X_3(l_{45})$

$$\Delta X_4'' (l_{34}+l_{45}) = \Delta X_5(l_{34})$$

Thus we can write (A.3) as

$$\Delta X_4 = K_3 \Delta X_3 + K_4 \Delta X_5 \quad (A.4)$$

Now if we make our assumption that the flow of oil into the servo-motor is proportional to position ΔX_4 of the pilot valve v, then the movement ΔX_5 of the piston (or valve opening) can be expressed as

$$\Delta X_5 = \Delta X_v = K_5 \int_0^t (-\Delta X_4) dt \quad (A.5)$$

Taking Laplace transform of eqn. (A.2), (A.4) and (A.5) we get

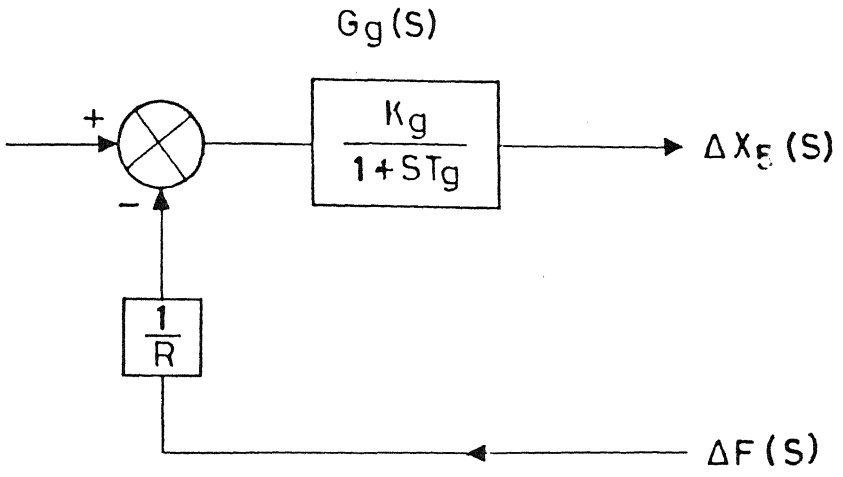

Figure (A-2) Block diagram representation of governor

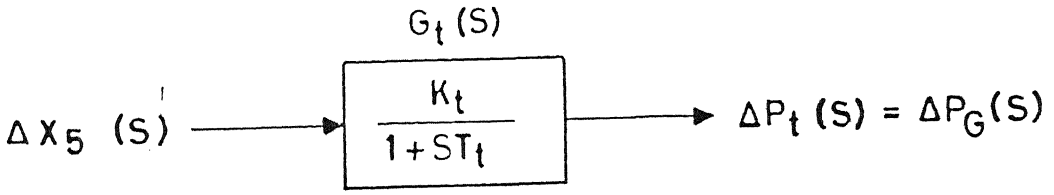

Figure (A-7) Block diagram representation of a linearised model of nonhreheat turbine

$$\Delta X_3(s) = -K_1 \Delta Pc(s) + K_2 \Delta F(s) \qquad (A.6)$$

$$\Delta X_4(s) = K_3 \Delta X_3(s) + K_4 \Delta X_5(s) \qquad (A.7)$$

$$X_5(s) = -K_5 \frac{1}{s} X_4(s) \qquad (A.8)$$

eliminating $\Delta X_3(s)$ and $\Delta X_4(s)$, we obtain the following equation

$$\Delta X_5(s) = \frac{K_1 K_3 \Delta P_c(s) - K_2 K_3 \Delta F(s)}{(K_4 + \frac{s}{K_s})}$$

or $$\Delta X_5(s) = [\Delta P_c(s) - \frac{1}{R} \Delta F(s)] \times \frac{K_g}{1+sT_g} \qquad (A.9)$$

where $R \triangleq \frac{K_1}{K_2}$ = speed regulation of the governor

$K_g \triangleq \frac{K_1 K_3}{K_4}$ = gain of speed governor

$T_g \triangleq \frac{1}{K_4 K_5}$ = time constant of speed governor.

In standard block diagsram symbol we can represent equation (9) as in fig.(A.2).

A-3 Modified Models of Mechanical Governors

Many authors have considered various other parametersof generating station to consider different requirements. For example Chowdhary [10], Hovey [12] have modelled for stability

boundary of governors of hydroplant.

As per Hovey Governor Response is

$$-\delta T_\gamma \frac{dz}{dt} = T_\gamma \frac{dw}{dt} + w \qquad (A.10)$$

and as per Chowdhary Governor Response is

$$(\delta - \sigma) T_\gamma \frac{dz}{dt} = - T_\gamma \frac{dw}{dt} - (w - \sigma 2) \qquad (A.11)$$

where δ is temporary speed droop

σ is permanent speed droop

z is incremental gate position

T_γ is dashpot reset time

w is incremental machine speed.

H.E. Coles [11] modelled steam terboalternator by linearising the nonlinear differential equations. The transfer function relating throttle-valve opening to changes in set speed has been obtained by linearising these equations giving

$$\frac{\Delta z}{\Delta \omega}(P) = \frac{G_3 G_4 G_5}{(1+\tau_\gamma P)(1+\tau_1 P)(1+\tau_2 P)} \qquad (A.12)$$

where τ_g = governor relay time constant

τ_1 = primary relay time constant

τ_2 = secondary valve time constant

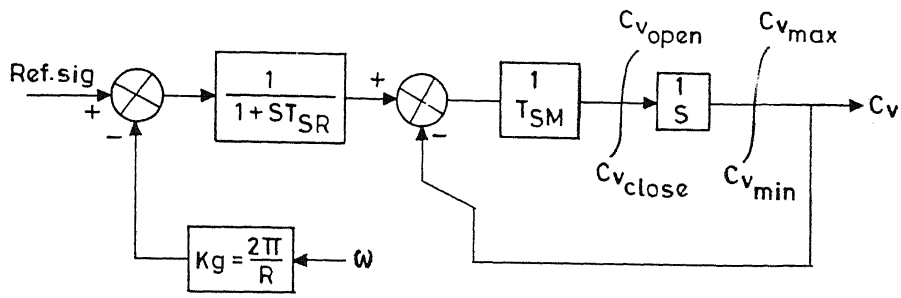

Figure (A.3) Mechanical-hydro governor for steam turbine

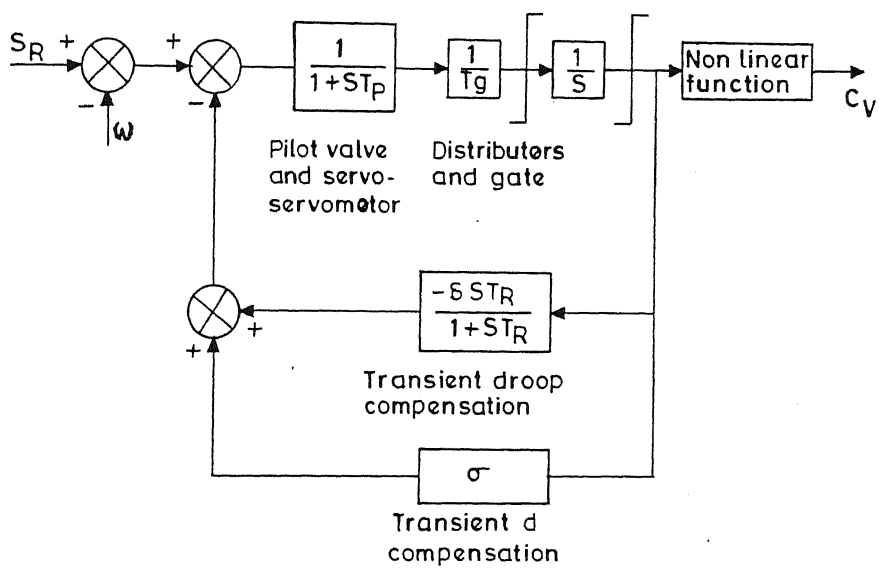

Figure (A-4) Mechanical-hydro governor for steam turbine

$G_3G_4G_5$ = constants which relates the steam valve lift to the change in speed, at any perticular operating load.

z = throttle value displacement

ω = machine speed rad/sec.

$P = \frac{d}{dt}$.

In 1973 IEEE committee report was published on dynamic models for steam and hydro turbines. As per this report steam turbine mechanical-hydroaulic governor was represented as in fig. (A.3) and (A.4).

A.4 ELECTRO-HYDRAULIC SPEED GOVERNOR

An electro-hydraulic speed control mehanism provides flexibility through the use of electronic circuits in place of mechanical components in the low power portions.

A typical Electro-hydrautic is PID governor represented as in fig. (A.5).

Hagihera et al [Ref.] have modeled the governor with other systema with following assumptions: See fig. (A.6).

(1) The hydrosystem operates in linear mode with small load perturbations.

(2) The water column is inelastic

(3) the load is isolated..

where σ = governor permanant speed droop

δ = temporary speed droop

T_w = water starting time

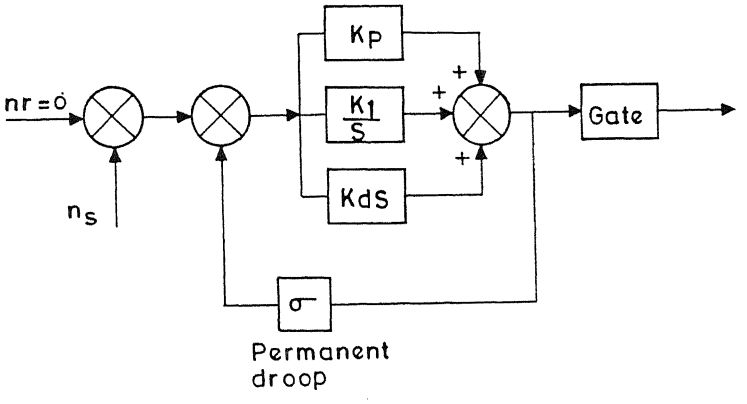

Figure (A-5) Electro-hydraulic governor

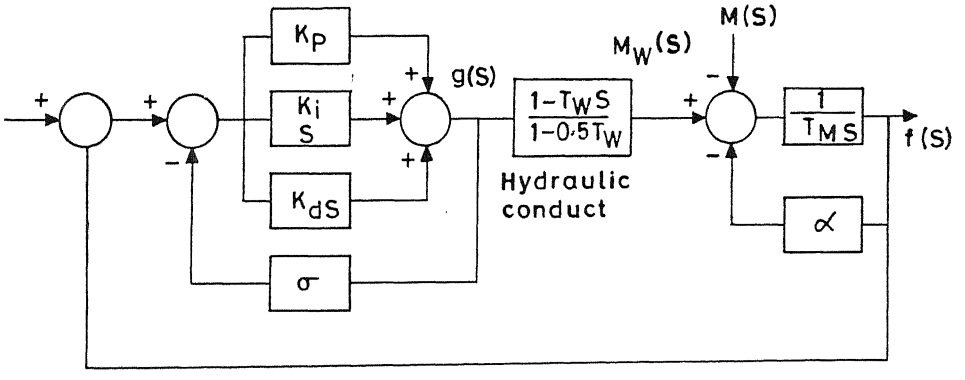

Figure (A-6) Electro-hydraulic governor

T_m = mechanical starting time

α = load self regulation factor

T_γ = dashpot time constant of temporary droop governor.

If we adjust the gains K_p, K_i and K_d of the PID governor to the values as below:

$$K_p = \frac{1}{\delta},\ K_i = \frac{1}{\delta T_\gamma} \text{ and } K_d = 0$$

Murthy & Hariharan [8] has shown the Temporary droop governor is:

$$K_p = \frac{1}{\delta}\ ,\ K_i = \frac{1}{\delta T_\gamma}\ ,\ K_d = \frac{T_n}{\delta}$$

where T_n is derivative feed back in temporary droop governor.

A.5 MODELLING OF TURBINE

STEAM TURBINE: All compound steam turbine systems utilize governor-controlled valves at the inlet to the high presure (or very high pressure) turbine to control steam flow. The steam chest and inlet piping to the first turbine cylinder and reheater and cross over piping downstream all introduce delays between valve movement and change in steam flow. The principal objective in modelling the steam system for stability studies is to account for these delays.

The continuity equation is

$$\frac{dW}{dt} = Q_{in} - Q_{out} \qquad \text{(A.13)}$$

where W is the weight of steam in volume V(ft^3), t is time in seconds and Q_{in} and Q_{out} are flows assuming the weight flow out of the vessel is proportional to pressure in the vessel.

$$Q_{out} = \frac{P}{P_o} \; Q_o$$

$$\frac{dQ_{out}}{dt} = \frac{Q_o}{P_o} \; \frac{dP}{dt}$$

where P is variable vessel pressure and P_o is steady state vessel pressure, Q_o is steady state weight flow out at P_o

$$\text{Thus} \quad \frac{dW}{dt} = \frac{\partial W}{\partial P} \; \frac{dP}{dt} = V \frac{\partial}{\partial P} \left(\frac{1}{V}\right) \frac{dP}{dt} \qquad (A.14)$$

where V is specific volume (ft^3/wt) of steam in vessel

$$Q_{in} - Q_{out} = \frac{P}{Q} V \left(\frac{V\partial}{\partial P}\right) \left(\frac{1}{V}\right) \frac{dQ_{out}}{dt} \qquad (A.15)$$

$$\text{Let} \quad T = \frac{P_o}{Q_o} V \frac{\partial}{\partial P} \left(\frac{1}{V}\right)$$

$$\text{Then} \quad Q_{in} - Q_{out} = T \frac{dQ_{out}}{dt}$$

$$\text{or} \quad \frac{Q_{out}}{Q_{in}} = \frac{1}{1+ST} \qquad (A.16)$$

This model is without reheater and shown in figure (A.7)

H.E Coles [11] has modelled steam turbine as:

$$\frac{\text{steam pressure}}{\text{throttle-valve opening}} - \frac{\Delta P_t}{\Delta z}(P) = \frac{G_1}{1+\tau P_t}$$

where G_1 is intrained-steam gain constant.

With reheater ,it is modelled as:

$$\frac{\text{Prime mover torque}}{\text{pressure at inlet}} = \frac{\Delta T_o}{\Delta P_t}(P) = \frac{G_2(1+n\tau_\gamma P}{1+\tau_\gamma P} \qquad \text{(A.17)}$$

$$n = \frac{\text{effective heat drop in H.P. turbine}}{\text{total heat drop}} = \text{Reheat coefficient}$$

where P_t = steam pressure at the inlet to the high pressure turbine, lb/in^2

G_2 is Reheater gain constant

z = throttle-value displacement,

τ_τ = entrained-steam time-constant

τ_γ = reheater time constant

T_o = primemover torque P.U.

$P = \frac{d}{dt}$

Both (A.16) and (A.17) are same except the parameters of Reheater is included in (A.17). If there is no radiation, i.e.,n=0 then (A.16) becomes equal to (A.17).

Modelling of Hydro-turbine

The transient characteristics of hydroturbine are determined by the dynamics of water flow in the penstock. The conversion of flow and head (h) to power by the turbine involves only non-dynamic relationships. The most precise models of water pressure and flow in the penstock are those which treat the travelling-wave phenomena. But usually it is not necessary to use travelling wave models for stability studies, although they are used regularly for detailed plant design studies.

The approximate linear model desired by Murthy and Hariharan [8] & IEEE committee report [9] , Hoavey [10] and Chowdhary [12] is given below:

The turbine flow is given by

$$q_t = g + 0.5h \qquad \text{(A.18)}$$

and torque $M = g+1.5h$ (A.19)

where g is gate position and h is head of water.

For inelastic water column the head and flow are related by the impedance function,

$$\frac{h}{q_t} = T_w S \text{ where } T_w \text{ is water starting time}$$

by algebraic manipulation we get

$$\frac{M}{g} = \frac{1-T_w S}{1+(T_w/2)S} \qquad \text{(A.20)}$$

is the turbine transfer function with long penstock and elastic

water column.

Murty et al [8] have derived modified transfer function

$$\frac{M}{g} = \frac{1-(T_w/T_e)\tanh(T_e S)}{1+(T_w/2T_e)\tanh(T_e S)} \qquad (A.21)$$

where T_e pipe line reflection time.

Again C.K. Sanathanam [7] have considered the detailed model of Hydroturbine as:

$$T_{(S)} = \frac{1-1.9865+0.36065^2}{1+0.99325+0.36065^2} \qquad (A.22)$$

A.6 GENERATOR LOAD MODELLING

We shall develop mathematical modelling of an isolated generator, which is only supplying local load and is not supplying power to another area via a tie-line.

Suppose there is real load change of ΔP_D.

Due to the action of turbine controllers, the generator increases its output by the amount ΔP_G. The net surplus power $\Delta P_G - \Delta P_D$ will be absorbed by the system in two ways.

1. By increasing the kinetic energy W_{Kin} in the rotor generator at the rate $\left[\frac{d(W_{Kin})}{dt}\right]$

2. By an increased load consumption. All typical loads experiences on increase

$$B = \frac{\partial P_D}{\partial d} \text{ MW/H}_z$$

B is called damping coefficient.

Thus we can express this surplus power

$$\Delta P_G - \Delta P_D = \frac{d}{dt} W_{Kin} + B\Delta f \ MW \qquad (A.23)$$

As the kinetic energy is proportional to the square of the speed, we can thus write

$$W_{Kin} = W^o_{Kin} \left(\frac{f}{f^o}\right)^2 \ M.W.S$$

as $f = fo+\Delta f$ where f^o nominal frequency. and f is new frequency after disturbance.

$$W_{Kin} = W^o_{Kin}\left(\frac{fo+\Delta f}{f^o}\right)^2 = W^o_{Kin}\left[1+ \frac{2\Delta f}{f^o} + \left(\frac{\Delta f}{f^o}\right)^2\right]$$

$$\cong W^o_{Kin}\left(1+2\ \frac{\Delta f}{f^o}\right)$$

$$\frac{d(W_{kin})}{dt} = \frac{2W^o_{Kin}}{f^o}\ \frac{d(\Delta f)}{dt} \qquad (A.24)$$

Substituting (A.24) in (A.23) we get

$$\Delta P_G - \Delta P_D = \frac{2W_{Kin}}{f^o}\ \frac{d(\Delta f)}{dt} + B\Delta f \ MW \qquad (A.25)$$

By dividing this equation by the generator rating P_r and by introducing the perunit inertia constant

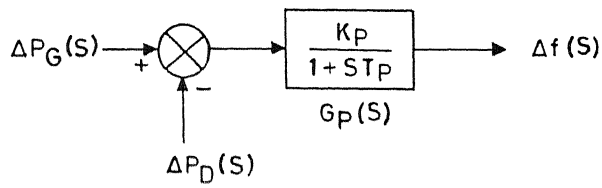

Figure (A-8) Representation of generator load model

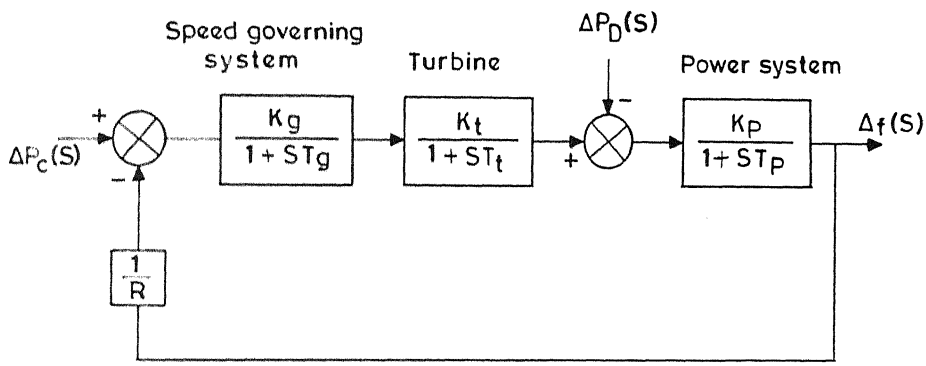

Figure (A-9) Block diagram representation of power system

$$H = \frac{W^{o}_{Kin}}{P_r} \text{ MWS/Mw}$$

(A.25) becomes

$$\Delta P_G - \Delta P_D = \frac{2H}{f^{o}} \frac{d\Delta f}{dt} + B\Delta f \quad \text{per MW}$$

Taking the Laplace transform,

$$\Delta P_G(S) - \Delta P_D(S) = \frac{2H}{f_o} S\Delta f(S) + B\Delta f(S)$$

or we can write $\Delta f\ (S) = G_P(S)[\Delta P_G(S) - \Delta P_D(S)]$ (A.6)

$$G_P(S) \triangleq \frac{K_P}{1+ST}$$

$$\frac{1}{K_p} = \frac{2H}{f^{o}B} \text{ sec.}$$

$$T_P = \frac{1}{B} \text{ } H_z/\text{P.U. MW}$$

Thus the block diagram representation will be as in fig. (A.8).

A.7 Block Daigram Representation of single area power system

We can easily obtain its model by combining the block diagrams. Shown in figure (A.2), (A.6) and (A.7). By properly connecting these block diagram, we get fig. (A.9) which is a single area representation.

APPENDIX B

MODELING OF INTERCONNECTED POWER POOLS

B.1 LOAD FREQUENCY CONTROL OF TWO-AREA SYSTEM

From a practical point of view, the problem of frequency control of inter-connected areas, or power pools, are more important than those of isolated areas. Practically, all power systems today are tied together with neighbourig areas, and the problem of load-frequency control becomes a joint undertaking. Closely associated is the problem of controling the power flows on the inter-ties.

Since peak demands occurs at various hours of the day in various areas, the ratio between peak and average load for a large pool is smaller than that of the individual systems. It is obvious, therefore, that all pool members can benefit from a reduced need of reserve capacity by a scheduled arrangement of energy interchange.

B.2 Modelling of the tie-line

As per well known power transfer equation

$$P_{12}^{o} = \frac{|V_1^o| \; |V_2^o|}{X} \sin (\delta_1^o - \delta_2^o) \qquad (B.1)$$

where δ_1^o and δ_2^o are the angles of end voltages V_1 and V_2

respectively. The order of the subscripts indicates that the tie-line power is defined positive in direction 1 to2.

For small deviation in the angles δ_1 and δ_2 the tie-line power changes with the amount

$$\Delta P_{12} \approx \frac{|V_1^o|\ |V_2^o|}{X} \cos\ (\delta_1^o - \delta_2^o)\ (\Delta\delta_1 - \Delta\delta_2) \qquad \text{(B.2)}$$

Analogous to the concept of "electric stiffness" of synchronous machines we define the "synchronizing coefficient" of a line

$$T^o \triangleq \frac{|V_1^o|\,|V_2^o|}{X} \cos(\delta_1^o - \delta_2^o) \quad \text{MW/rad} \qquad \text{(B.3)}$$

Thus we can write equation (B.2), tie-line power deviation

$$\Delta P_{12} = T^o(\Delta\delta_1 - \Delta\delta_2) \quad \text{MW}$$

The frequency deviation Δf is related to the reference angle $\Delta\delta$ by the formula

$$\delta f = \frac{1}{2\pi} \frac{d}{dt} (\delta^o + \Delta\delta) = \frac{1}{2\pi} \frac{(\Delta\delta)}{dt} \quad \text{Hz}$$

or $$\frac{d(\Delta\delta)}{dt} = 2\pi\Delta f$$

or $$\Delta\delta = 2\pi \int_0^t \Delta f\ dt$$

respectively. The order of the subscripts indicates that the tie-line power is defined positive in direction 1 to2.

For small deviation in the angles δ_1 and δ_2 the tie-line power changes with the amount

$$\Delta P_{12} \approx \frac{|V_1^o|\ |V_2^o|}{X} \cos\ (\delta_1^o - \delta_2^o)\ (\Delta\delta_1 - \Delta\delta_2) \qquad \text{(B.2)}$$

Analogous to the concept of "electric stiffness" of synchronous machines we define the "synchronizing coefficient" of a line

$$T^o \triangleq \frac{|V_1^o||V_2^o|}{X} \cos(\delta_1^o - \delta_2^o) \quad \text{MW/rad} \qquad \text{(B.3)}$$

Thus we can write equation (B.2), tie-line power deviation

$$\Delta P_{12} = T^o(\Delta\delta_1 - \Delta\delta_2) \quad \text{MW}$$

The frequency deviation Δf is related to the reference angle $\Delta\delta$ by the formula

$$\delta f = \frac{1}{2\pi}\frac{d}{dt}\ (\delta^o + \Delta\delta) = \frac{1}{2\pi}\ \frac{(\Delta\delta)}{dt} \quad \text{Hz}$$

or $$\frac{d(\Delta\delta)}{dt} = 2\pi\Delta f$$

or $$\Delta\delta = 2\pi \int_0^t \Delta f\ dt$$

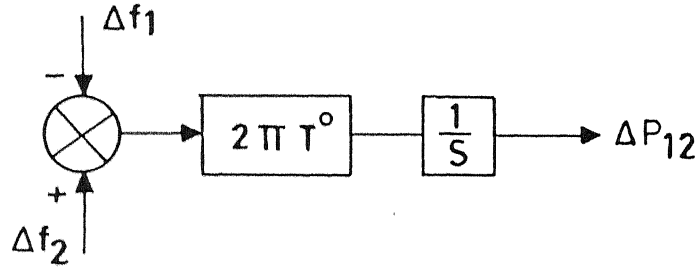

Figure (B-1) Representation of tie line

By expressing tie-line power deviation in terms of Δf rather than $\Delta\delta$ we thus get

$$\Delta P_{12} = 2\pi T^{o}\left(\int^{t} \Delta f_1 dt - \int^{t} \Delta f_2 dt\right) \text{ MW} \qquad \text{(B.4)}$$

Laplace transformation of the last formula yields

$$\Delta P_{12}(S) = \frac{2\pi T^{o}}{S}\left(\Delta f_1(S) - \Delta f_2(S)\right) \qquad \text{(B.5)}$$

Representing this equation in terms of block diagram symbols yields the diagram is given in fig. (B.1).

Similar like equation (5) the incremental tie-line power expected from area 2 is given by

$$\Delta P_{21}(S) = \frac{2\pi T^{o}}{S}\left(\Delta f_2(S) - \Delta f_1(S)\right) \qquad \text{(B.6)}$$

The power balance equation for single area is

$$\Delta P_G - \Delta P_D = \frac{2H}{f^{o}} \frac{d(\Delta f_1)}{dt} + B\Delta f_1$$

Now in case of two area we must modify the same equation for area 1 and area 2 accordingly.

Thus we must clearly add ΔP_{12} to right side of this equation that is,

$$\Delta P_{G1} - \Delta P_{D1} = \frac{2H_1}{f^{o}} \frac{d(\Delta f_1)}{dt} + B_1\Delta f_1 + \Delta P_{12} \qquad \text{(B.7)}$$

Taking Laplace transform of this equation

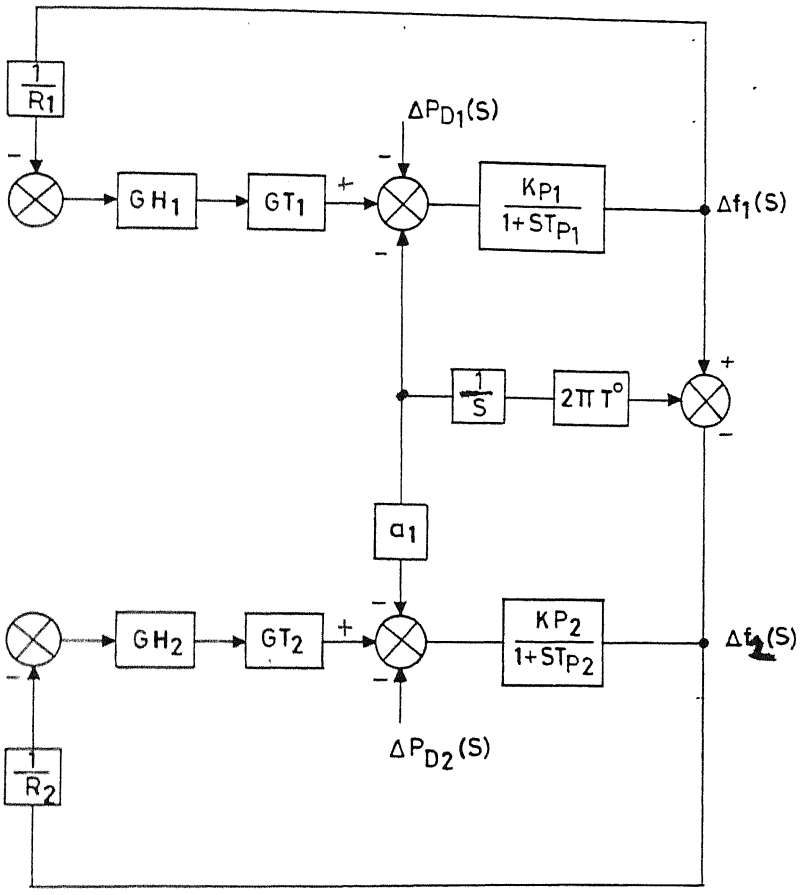

Figure (B-2) Block diagram representation of two inter-connected power plant

$$[\Delta P_{G1}(S)-\Delta P_{D1}(S)-\Delta P_{12}(S)] = \frac{2H_1}{f^o} S\Delta f_1(S)+B_1\Delta f_1(S)$$

$$= \frac{2H_1}{f^o} \Delta f_1(S)(S+B_1)$$

$$= \frac{2H_1}{f_o} B_1\Delta f_1(S)(\frac{1}{B_1} S+1)$$

Putting $\frac{2H_1B_1}{f_o} = \frac{1}{K_{P1}}$, $\frac{1}{B_1} = T_{P1}$

We get $\Delta f_1(S) = G_{P1}(S)[\Delta P_{G1}(S)-\Delta P_{D1}(S)-\Delta P_{12}(S)]$ (B.8)

where $GP_1(S) = \frac{K_{P1}}{1+ST_{P1}}$.

Thus the complete Block diagram representation of two area LFC is as given in figure (B.2).

APPENDIX C

ANALYSIS OF STEADY STATE RESPONSE OF A FIRST ORDER LEAD-LAG SYSTEM WITH P.I.D. (PROPORTIONAL PLUS INTEGRAL PLUS DERIVATIVE) CONTROL

C.1 GENERAL

In literature , the performance and design procedures for P.I.D. controller have been discussed [3 & 5]. However, various methods to implement P.I.D. controllers have not been given much attention. In this appendix, an attempt has been made to determine the possible methods for implementing the P.I.D. controllers, and selecting the feasible methods. The selection of feasible methods has been done by determining the steady-state error. Normally, it is desired that the steady-state error must be zero for given control scheme. To investigate the feasible methods for implementing the P.I.D. controllers, the system transfer function considered is given below:

$$G(S) = \frac{1-T_w S}{1+T_w S}$$

The criterion for choosing the configuration for the PID scheme has been based on characteristic equation, i.e. same characteristic equation must be obtained for various configuration, that is:

$$P(S = 1+[(K_P+K_d S+K_i/S)G(S)]$$

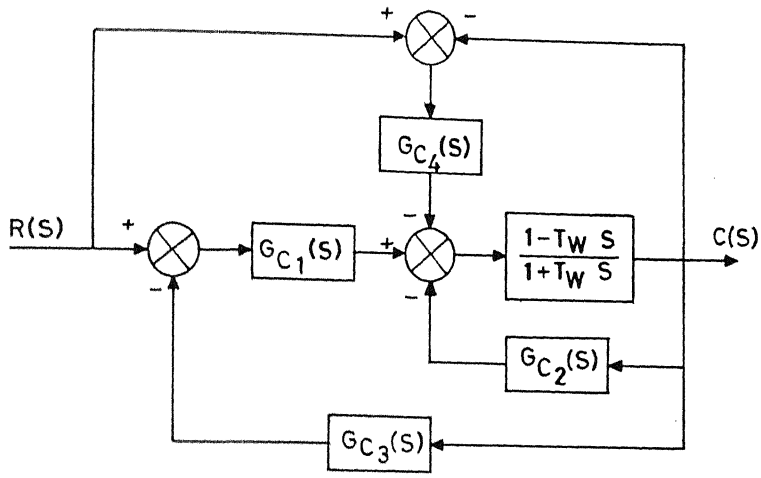

Figure (C.1)

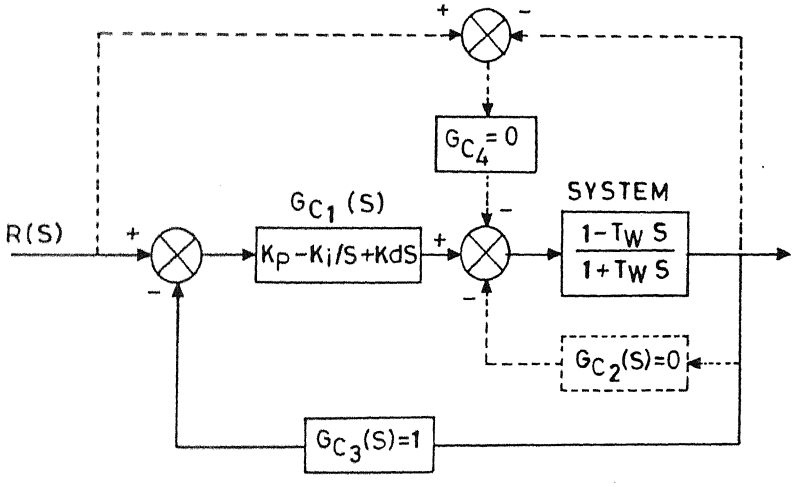

Figure (C.2)

C.2 SYSTEM REPRESENTATION

Fig.(C.1) shows the general block diagsram of the system. The block $G_{c1}(S)$, $G_{c1}(S)$, $G_{c3}(S)$ and $G_{c4}(S)$ is the various controller implementation positions. In any one configuration, a single control block or combination of blocks can be used. Further, a single block may contain single control element or combination of three controller, proportional, integeral and derivative.

For illustration, an example is shown in figure (C.2). In this configuration

$$G_{c1}(S) = K_P + K_i/S + K_d S \qquad \text{and}$$

$$G_{c2}(S) = G_{c3}(S) = G_{c4}(S) = 0$$

To analyse the steady state error of this system we can proceed as follows:

It can be found that

$$\frac{C(S)}{R(S)} = \frac{(K_P + K_i/S + K_d S)(G(S)}{1+(K_P+K_i/S + K_d S)(G(S)}$$

$$\text{error } E(S) = R(S) - C(S)$$

$$= 1+[(K_P+K_i/S+K_d S)G(S)-(K_P+K_I/S+K_D S)G(S)$$

or

$$\frac{E(S)}{R(S)} = 1 - \frac{C(S)}{R(S)}$$

Hence

$$\frac{E(S)}{R(S)} = \frac{1}{1+(K_P+K_i/S+K_d S)G(S)} \qquad (C.1)$$

From Final value theorem, when $R(S) = \frac{1}{S}$ (step input)

(1) steady state error $e_{SS} = \lim_{S \to 0} SE(S)$

$$= \lim_{S \to 0} \frac{S}{1+(K_p+K_i/S+K_dS)G(S)} S\frac{1}{}$$

$$= \frac{0}{0+K_i} = 0 \qquad \text{(C.2)}$$

(2) Steady state error with R(S) = 1 (Impulse input)

$$e_{SS} = \lim_{S \to 0} SE(S)$$

$$= \lim_{S \to 0} \frac{S}{1+(K_p+K_i/S+K_dS)} = \frac{0}{K_i} = 0$$

C.3 BRIEF STUDY

It can be seen from the foregoing example that likewise number of configuration can be studied. To avoid exhaustive study, the configuration and results has been presented in tabulated form. Refer Table (C.1). Total 28 configuration were investigated and 14 were found satisfactory i.e. steady state error zero. It is to be remembered that in all systems, the characsteristics polynomial remains same.

TABLE C.1

Case No.	$G_{c1}(S)$	$G_{c2}(S)$	$G_{c3}(S)$	$G_{c4}(S)$	S.S.error when R(S)=1	S.S. error when R(S)= $\frac{1}{s}$
1.	$K_P+K_i/S+KdS$	open	1	open	0	0
2.	$K_i/S+KdS$	K_P	1	open	0	0
3.	K_i/S	K_P+KdS	1	open	0	0
4.	$K_i/S+K_P$	KdS	1	open	0	0
5.	K_i/S	open	$1+As+A_2S^2$	open	0	0
6.	K_P	open	A_1+A_2S	KdS	0	0
7.	$K_i/S+K_e$	open	1+AS	open	0	0
8.	K_i/S	KdS	1+AS	open	0	0
9.	K_i/S	K_P	$1+AS^2$	open	0	0
10.	K_i/S	open	$1+AS^2$	K_P	0	0
11.	K_i/S	open	1+AS	KdS	0	0
12.	1	open	KdS	K_P+K_i/S	0	0
13.	KdS	open	A_1+A_2/S	K_i/S	0	0
14.	K_P	open	1+AS	K_i/S	0	0
15.	1	open	K_i/S	K_P+KdS	0	1
16.	K_P	$K_i/S+KdS$	1	open	0	1
17.	K_P+KdS	K_i/S	1	open	0	1
18.	1	K_P	K_i/S	KdS	0	1
19.	KdS	$K_i/S+K_P$	1	open	0	1
20.	KdS	open	$\frac{A_1}{2}+A_2+\frac{A_3}{S}$	open	0	1
21.	K_P	open	$\frac{A_1}{2}+A_2+\frac{A_3}{S}$	open	0	1

21.	K_P	open	$\frac{A_1}{S}+A_2+\frac{A_3}{S}$	open	0	1
22.	$KdS+K_P$	open	$\frac{A_1}{S}+A_2$	open	0	1
23.	KdS	K_i/S	$\frac{A_1}{S}+A_2$	open	0	1
24.	1	$KdS+K_P$	$\frac{A_1}{S}$	open	0	1
25.	.1	$K_P+\frac{K_i}{S}$	A_1S	open	0	1
26.	$K_dS^2+K_PS+K_i$	open	K_i/S	open	0	1
27.	K_dS	open	A_1+A_2/S	K_P	0	1
28.	1	KdS	K_i/S	K_P	0	1

C.4 OBSERVATIONS

From the study of above all configurations, we find that only 28 configurations are possible, keeping the order of characteristic polynomial same. Out of these possible configurations, 14 are found to be suitable to yield steady state error zero with step input.

APPENDDIX - D

CONTROL CONFIGURATIONS

The various controller configurations are illustrtated below:

D.1 CONFIGURATION ONE

The controller is simply positioned in forward path, as shown in fig. (D.1). The frequency response of two area reheat thermal plant with P.I.D. controller is shown in fig. (D.2) and (D.3) for different value of gains. It can be compared with frequency response with conventional controller in fig. (D.4). In fig. (D.5) and (D.6), the freuency response of single area thermal plant is shown with P.I.D. controller and conventional controller respectively. The response of hydro-thermal is shown in Fig. (D.7).

D.2 CONFIGURATION TWO

For this case the P.I.D. controller configuration for the power plant is shown in fig. (D.8).

The load frequency control response of the power system in the above configuration, is shown in fig. (D.9), (D.10) and (D.11) for different value of gains.

D.3 CONFIGURATION THREE

In this case the P.I.D. components have been arranged as shown in fig. (D.12). The load frequency control response of this system is shown in fig. (D.13) and (D.14).

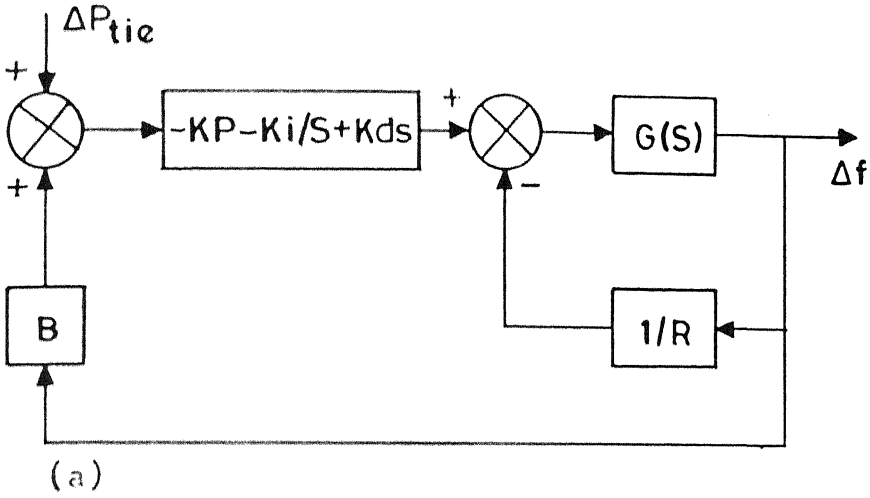

(a)

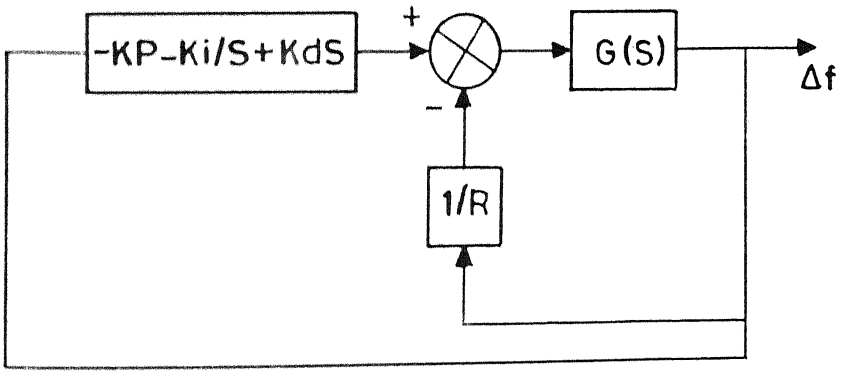

(b)

Figure (D.1) Controller configuration
(a) For two area
(b) For single area

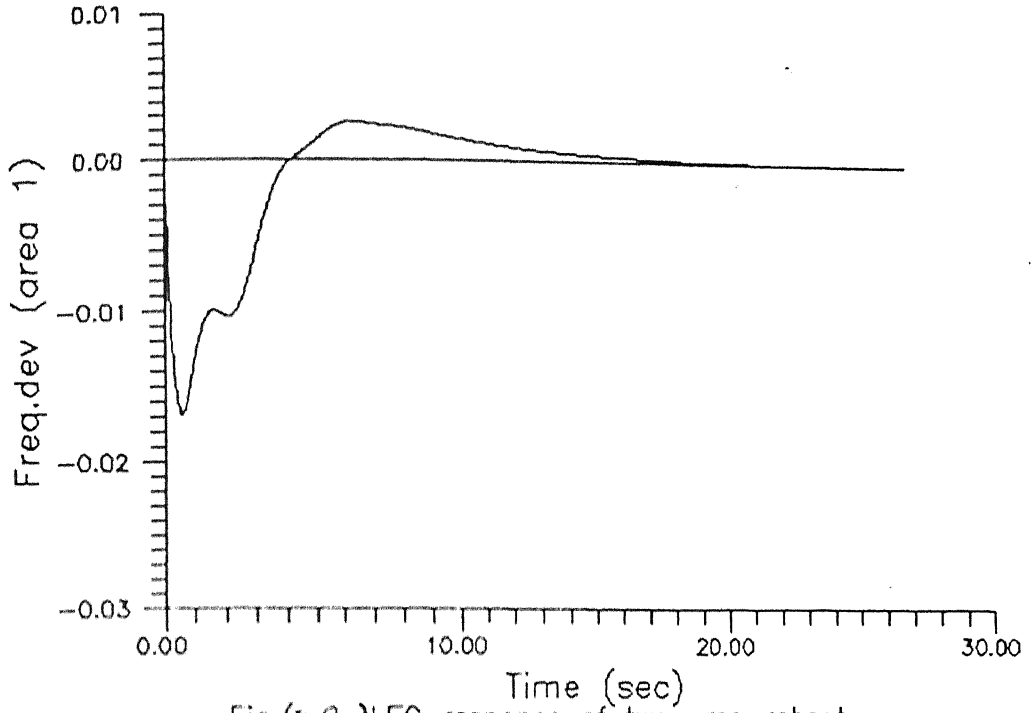

Fig.(D.2)LFC response of two area reheat thermal plant with PID controller(in forward path) kp=0.3 ki=0.67 and kd=0.6

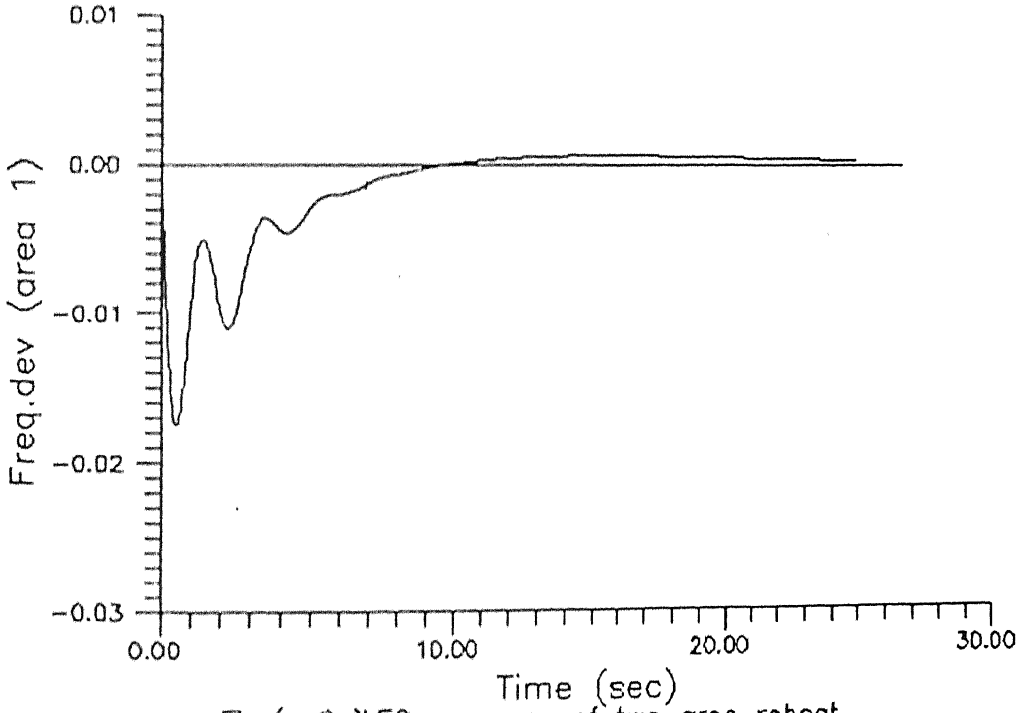

Fig.(D.3)LFC response of two area reheat thermal plant with PID controller(in forward path) kp=1.2 ki=0.35 and kd=0.35

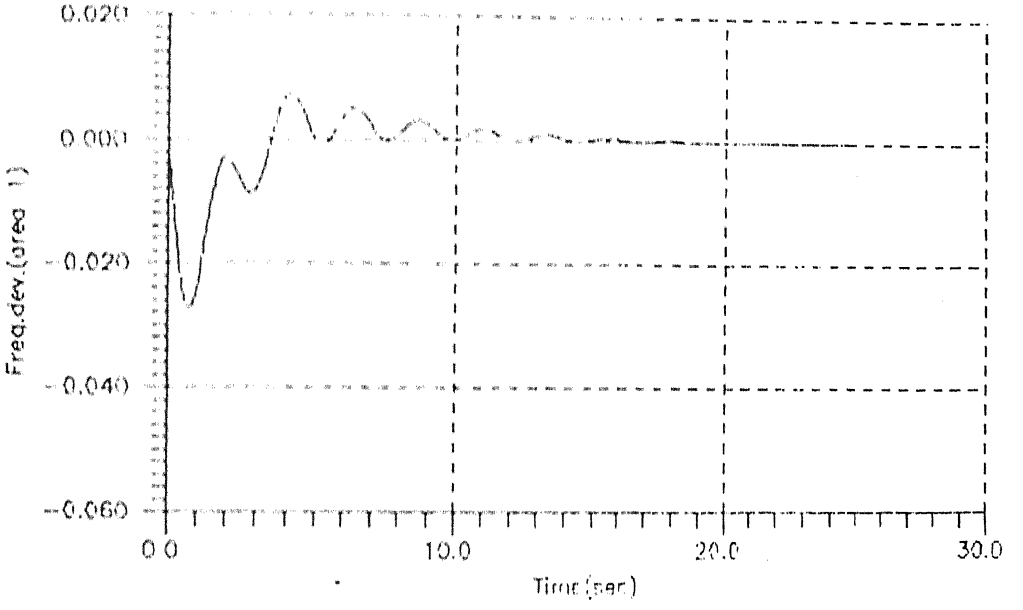

Fig.(D-4)Freq.Response of two area thermal plant with CONVENTIONAL controller ki=0.67

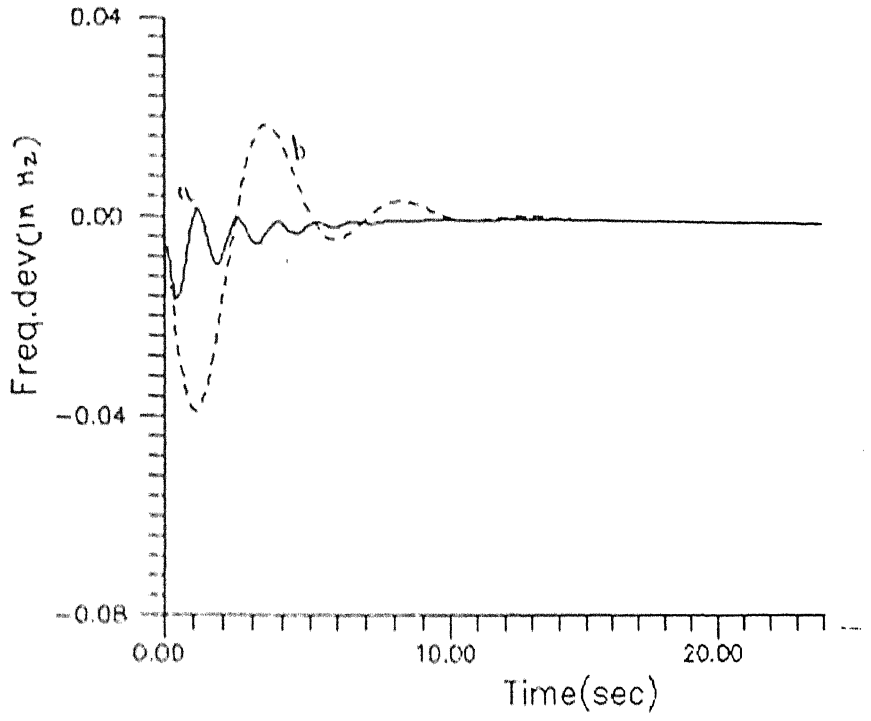

Fig (D-5) LFC Response of Single Area Thermal Plant
a-PID control b-conventional (int.)control

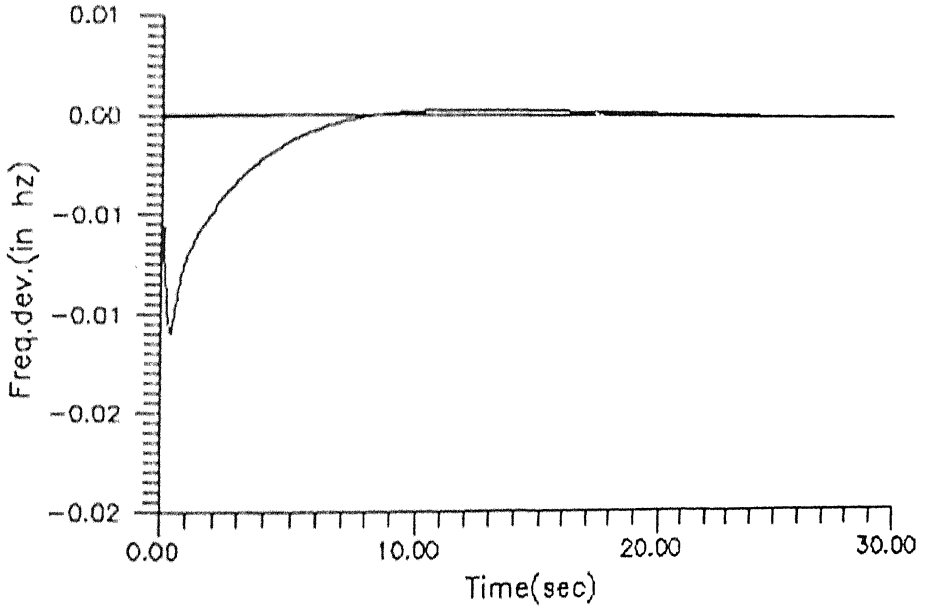

Fig.(D-6)LFC response of one area reheat→thermal plant with PID controller kp=1.8,ki=0.5 and kd=0.5

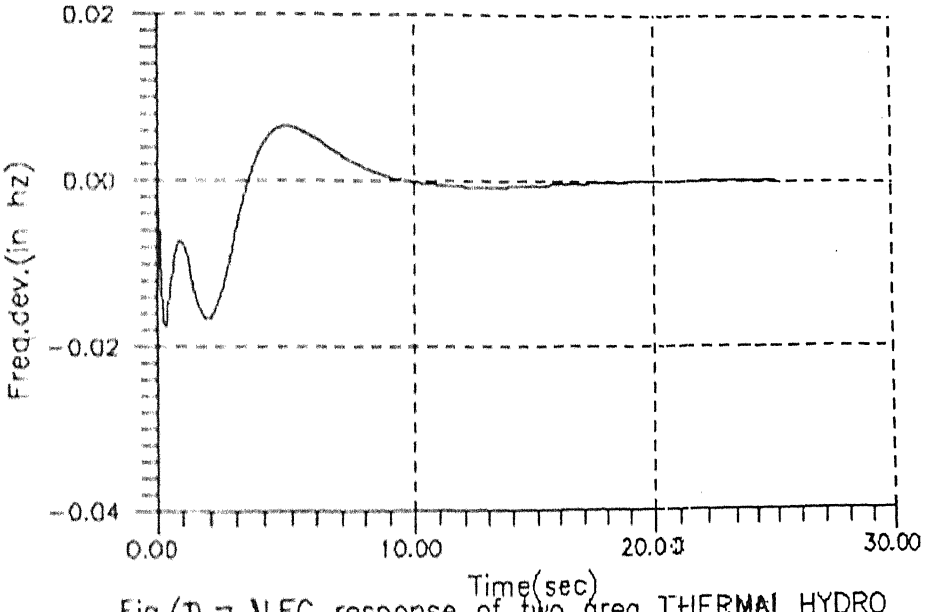

Fig.(D.7)LFC response of two area THERMAL HYDRO plant with P.I.D controller (→kp+ki+kd in forward path)
kd=0.7→kp=0.8 ki=0.67

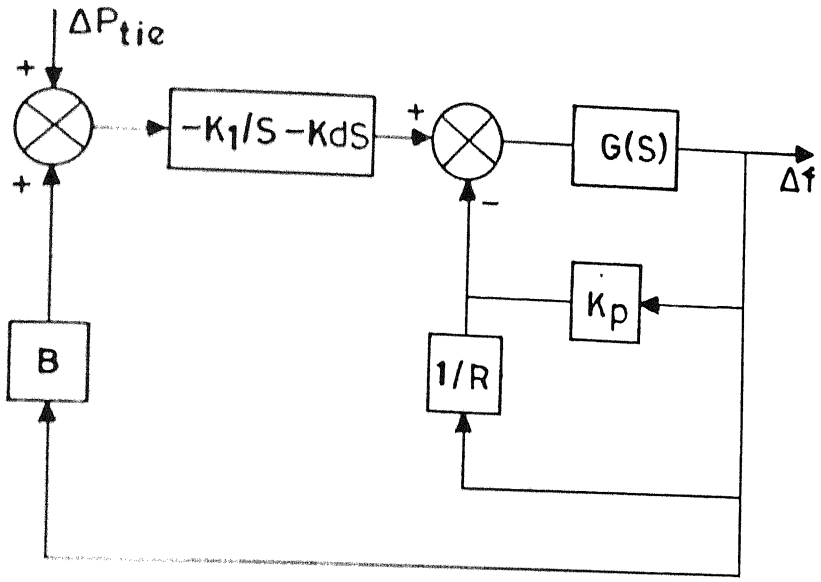

Figure (D.8)

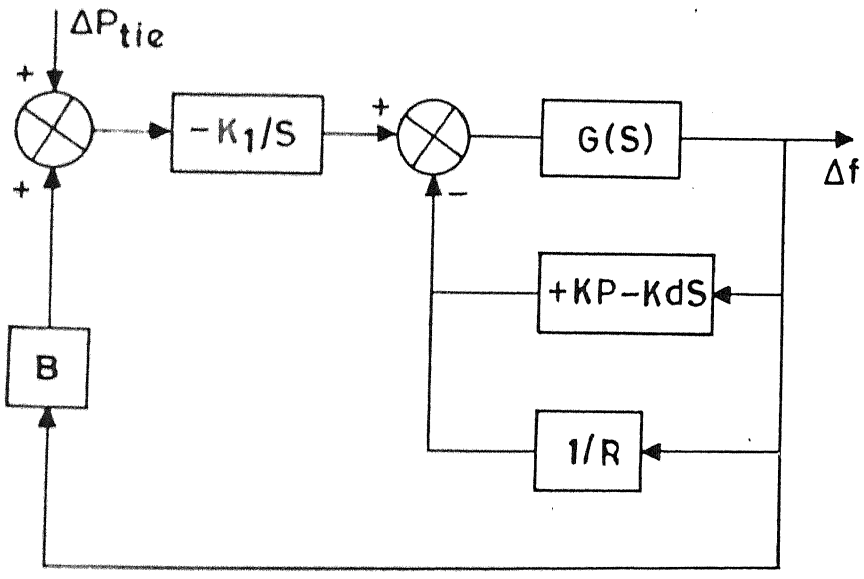

Figure (D.12)

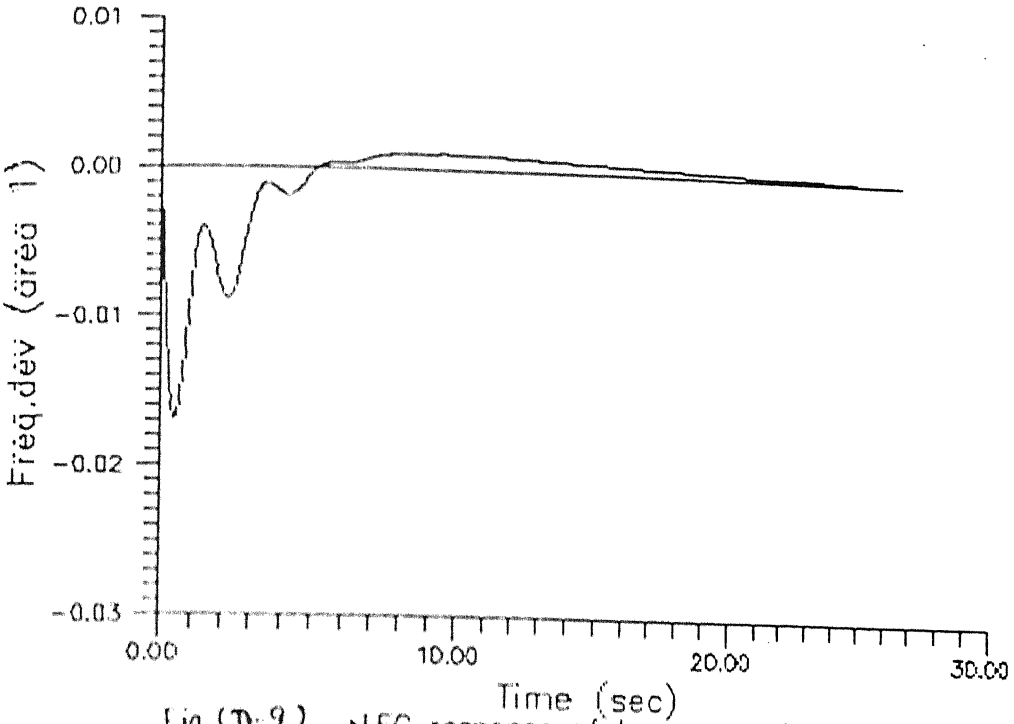

Fig (D·9) ▸LFC response of two area reheat→thermal plant with PID controller (ki+kd in forward path) kp=5.0 ki=0.5→ and kd=0.04(kp in feedback path)

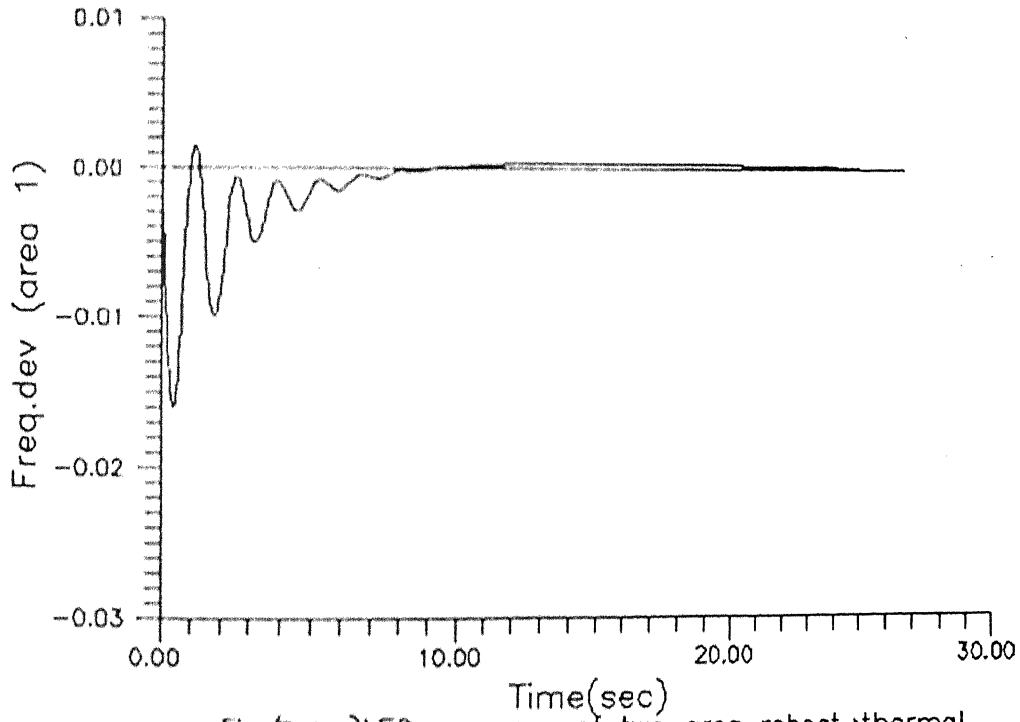

Fig.(D.10)LFC response of two area reheat→thermal plant with PID controller (ki+kd in forward path) kp=1.8 ki=0.67 and kd=0.05(kp in feedback path)

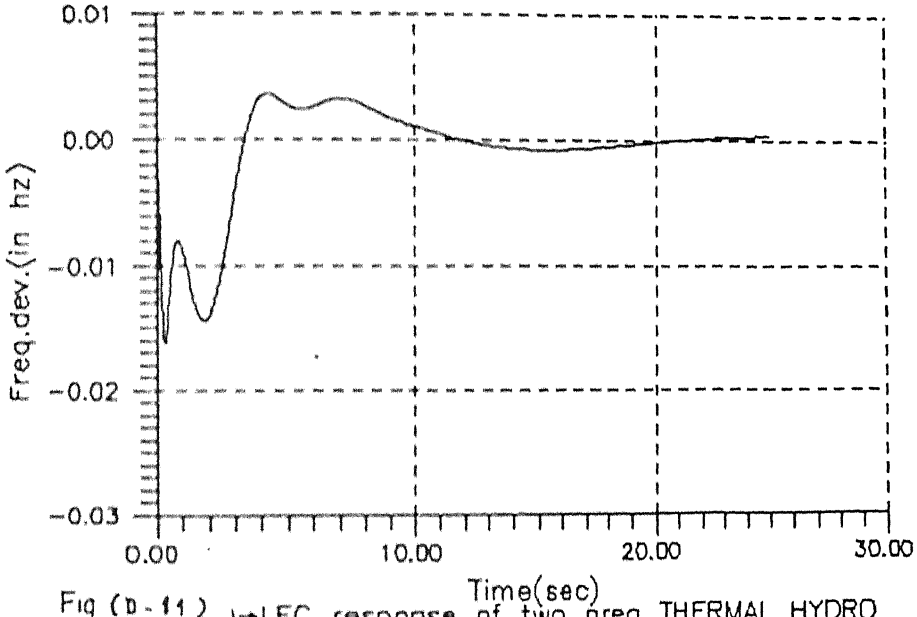

Fig (D-11))→LFC response of two area THERMAL HYDRO plant with P.I.D controller (ki/s+kds in forward path)and (kp in f.b.path)
kd=0.8→kp=0.5 ki=0.67

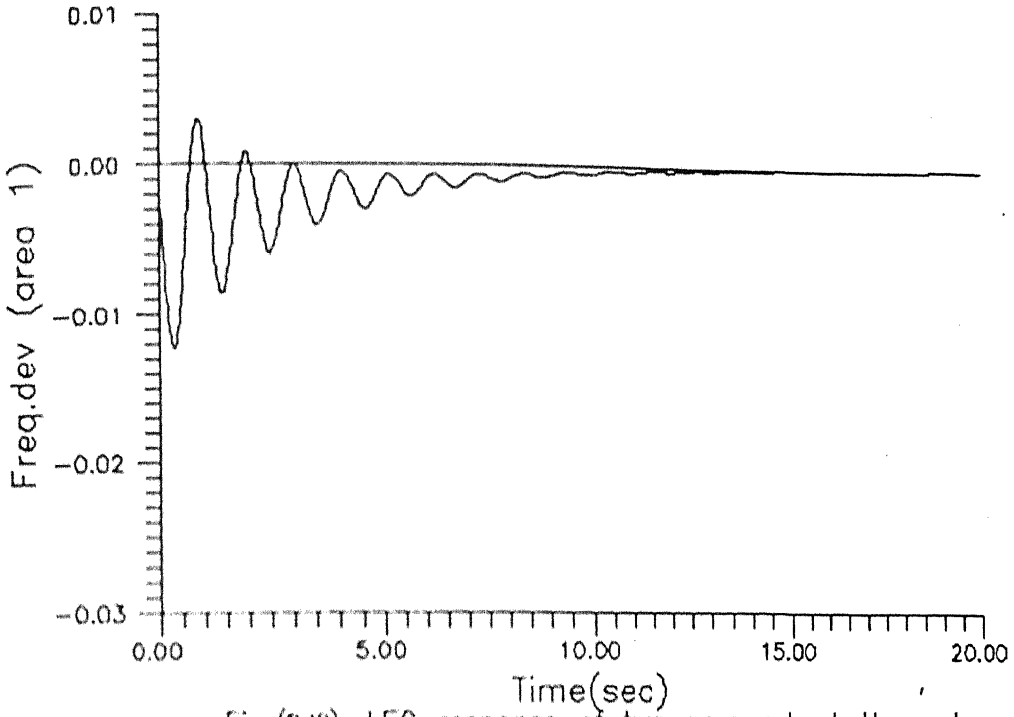

Fig.(D.13)→LFC response of two area reheat→thermal plant with PID controller (kp+kd in feedpath→path) kp=3.5 ki=0.67 and kd=0.08(ki in forward→ path)

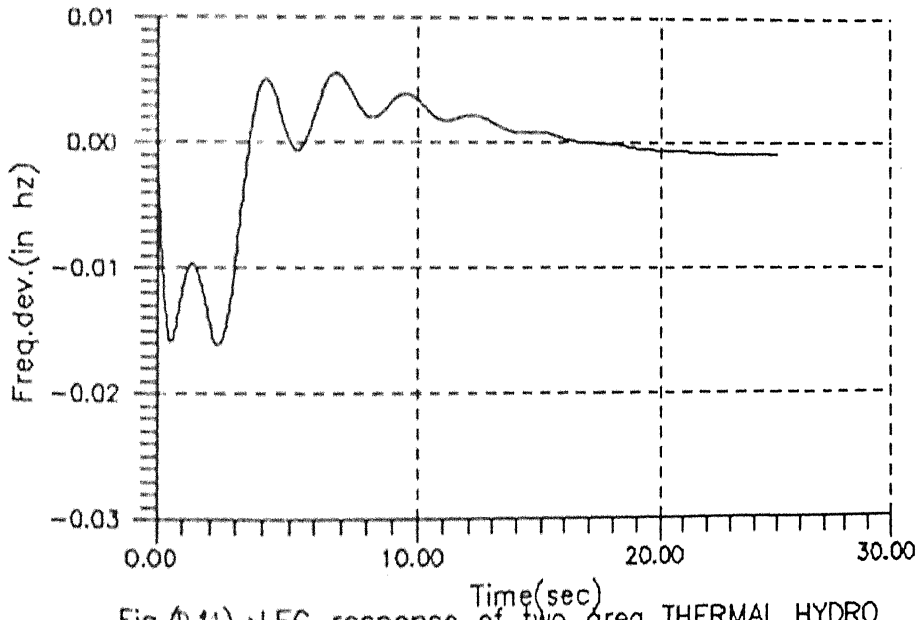

Fig.(D.14)→LFC response of two area THERMAL HYDRO plant with P.I.D controller (ki/s only in forward path)and (kp +kds in f.b.patn) kd=0.25kp=0.5 ki=0.67

D.4 CONFIGURATION FOUR

The arrangement of P.I.D. controller is shown in fig. (D.15) and the load frequency control response is shown in fig. (D.16) and (D.17).

D.5 CONFIGURATION FIVE

This is the most complex of all the systems due to the double differentiation in the secondary feedback path. The implementation is shown in fig. (D.18).The load frequency control response is shown in fig. (D.19) and (D.20).

D.6 CONFIGURATION SIX

In this case both the feedback path and forward path have been implemented with components of P.I.D. controller as shown in figure (D.21). The load frequency control response is shown in fig. (D.22) and (D.23).

D.7 CONFIGURATION SEVEN

In this controller configuration, a differentiation is positioned in secondary feedback path and effective P.I.D. controller is implemented as shown in fig. (D.24) and the load frequency response for different value of integral gain, is shown in fig. (D.25) and (D.26).

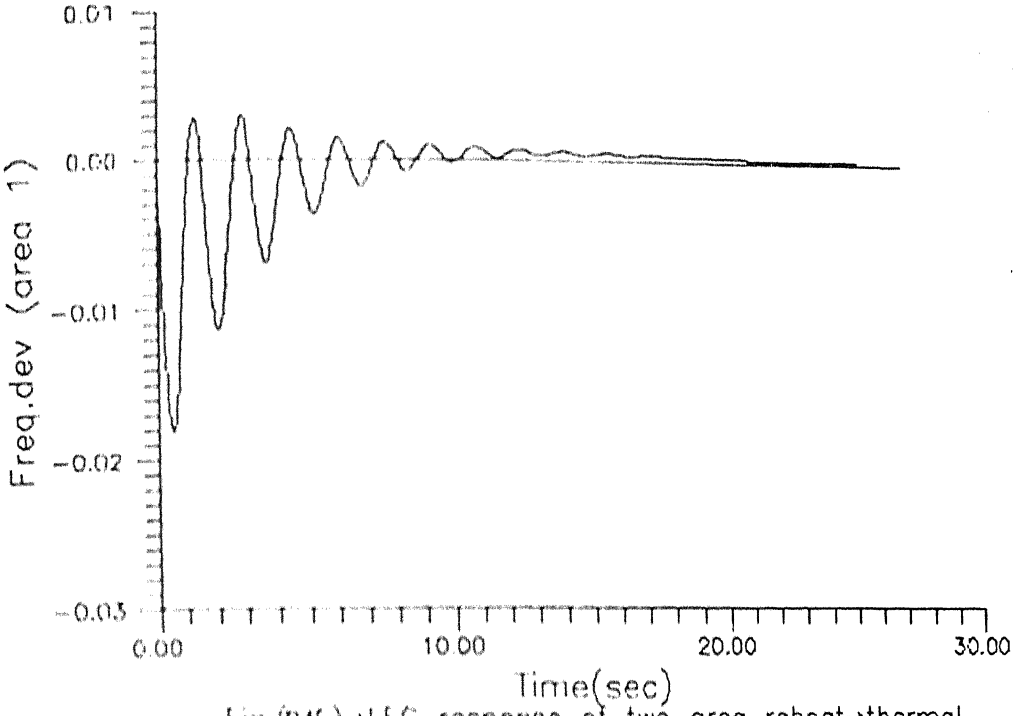

Fig.(11.16) →LFC response of two area reheat→thermal plant with PID controller →→(→kd in feedpath→path) kp=1.0 ki=0.67 and kd=.008(ki+kp in forward path)

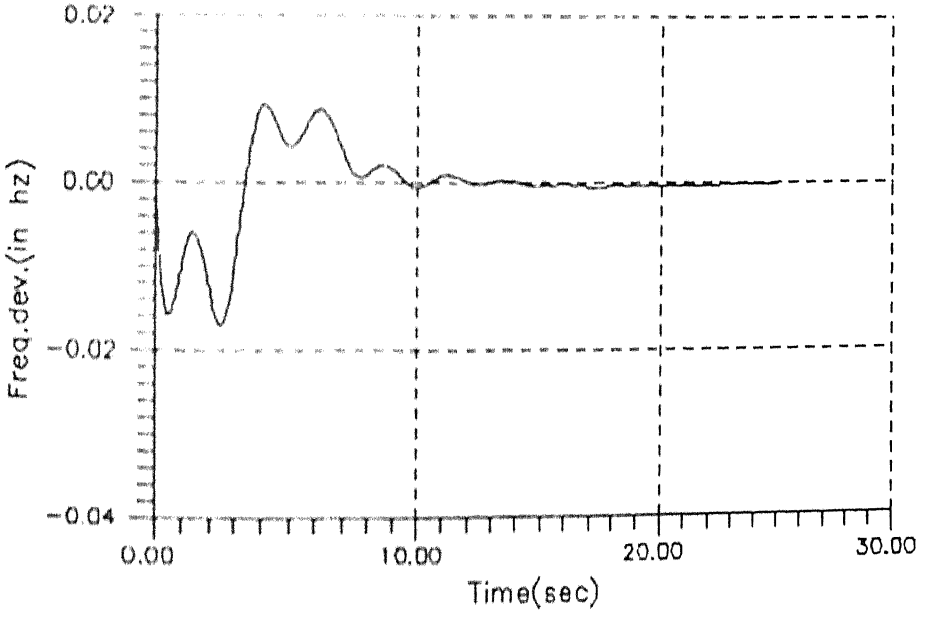

Fig.(11.17)→LFC response of two area THERMAL HYDRO plant with P.I.D controller(ki+kpinforward path) (Kds in R1 f.b.path) kp=1.0 ki=1.0 kd=0.25

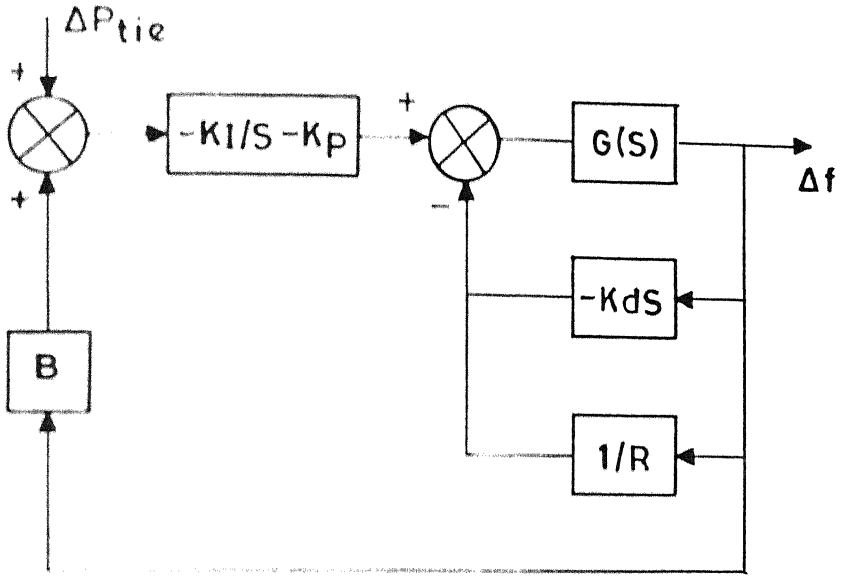

Figure (D.15)

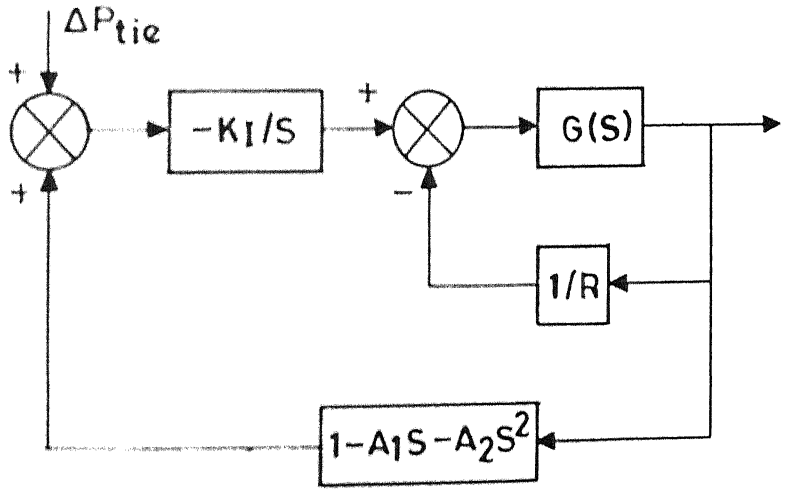

Figure (D.18)

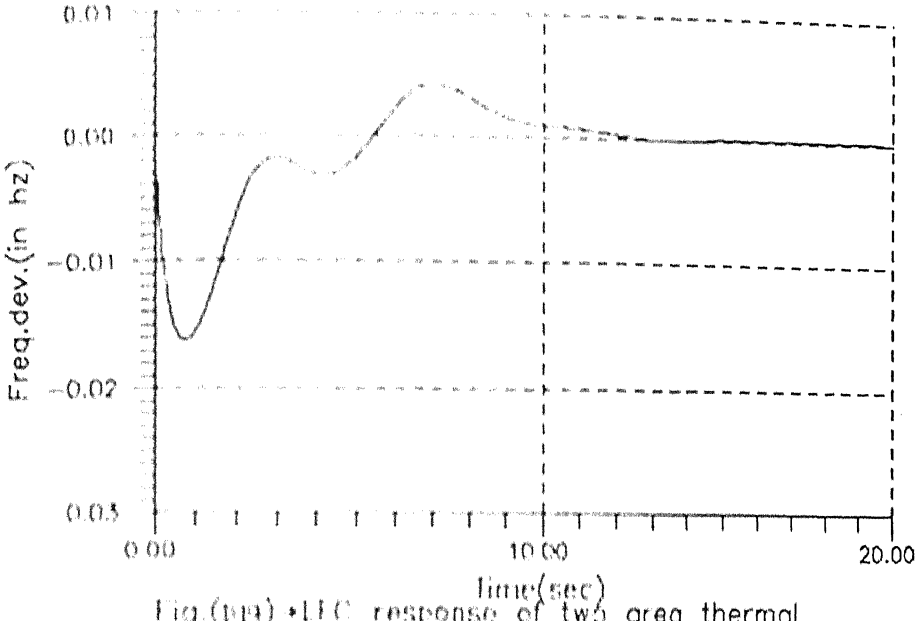

Fig.(D.19)→LFC response of two area thermal plant with P.I.D controller (ki/s→in forward path)and((1+a1s+a2s*s)f.backpath))
ki=0.67a2=1.5,a1=0.1

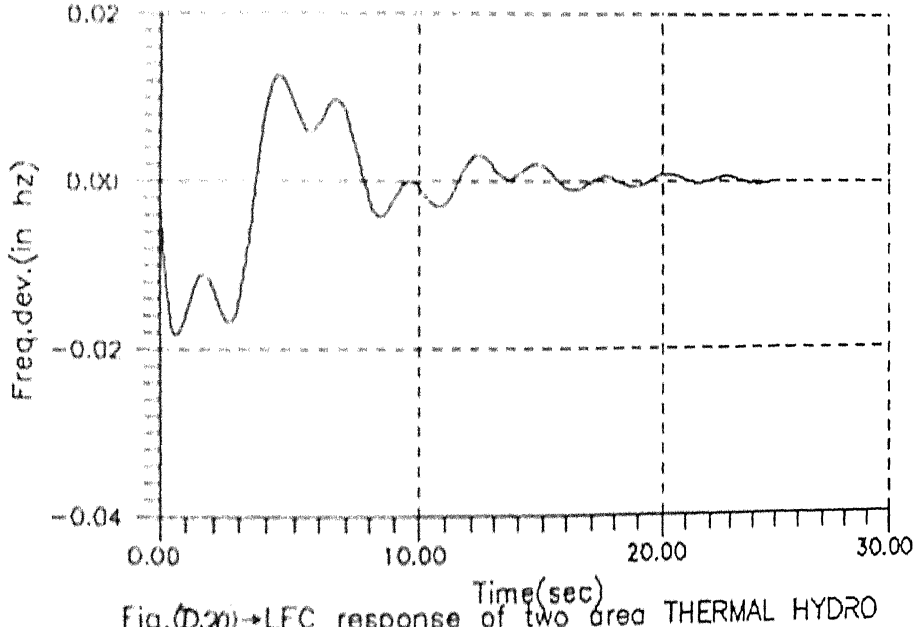

Fig.(D.20)→LFC response of two area THERMAL HYDRO plant with P.I.D controller (ki/s in forward path)and (1+as+a1s*s inθ_1f.b.path)
a=0.01 a1=0.55 ki=1.1

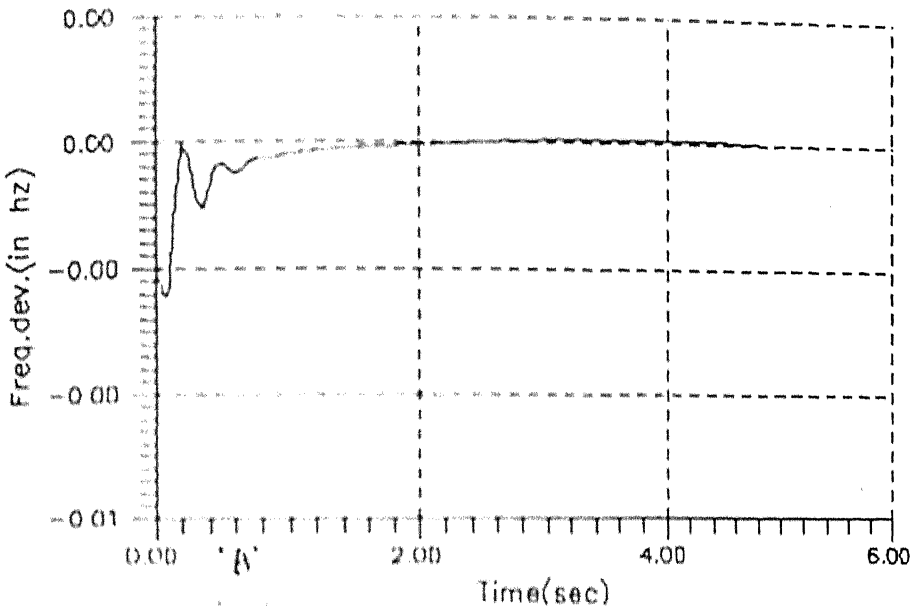

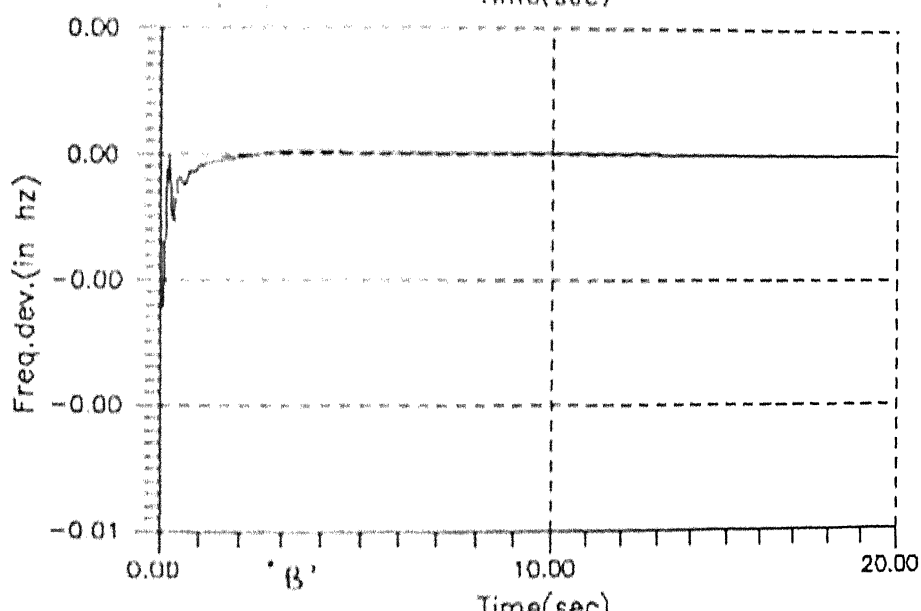

Fig.(5.22)→I.F.C response of two area thermal plant with P.I.D controller (→kp→→in forward path)and((a1+a2/s) in B1 F.B.Path) kd=5.0→kp=10.0a1,a2=5.0(kds in B1 F.B.Path)

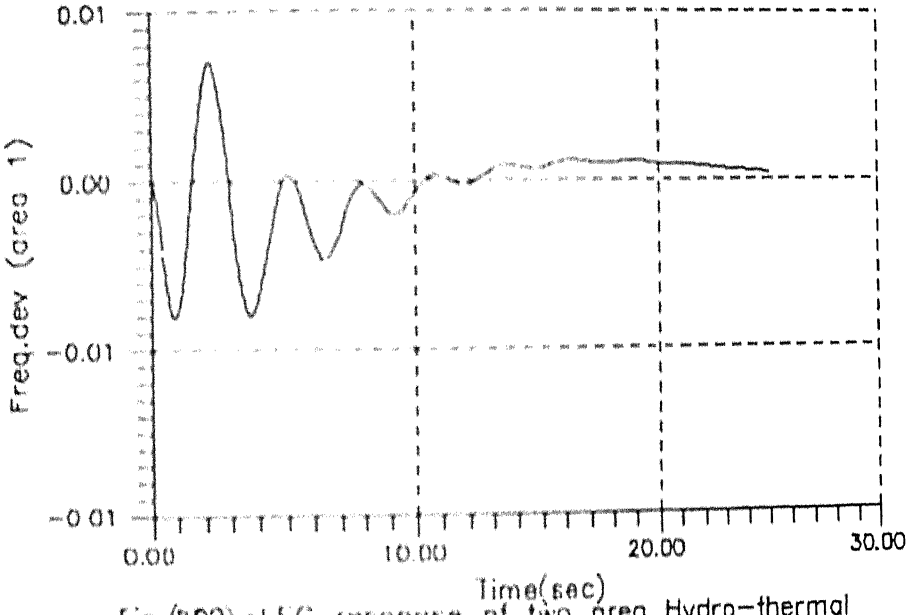

Fig.(D.23) ▸LFC response of two area Hydro-thermal plant with P.I.D controller (kp in forward path) (kds in R1 f.b.path) (a1+a2/s in B1 f.b. path) kp= 5.8 a1=4.0 a2= 4.0 kd=0.3

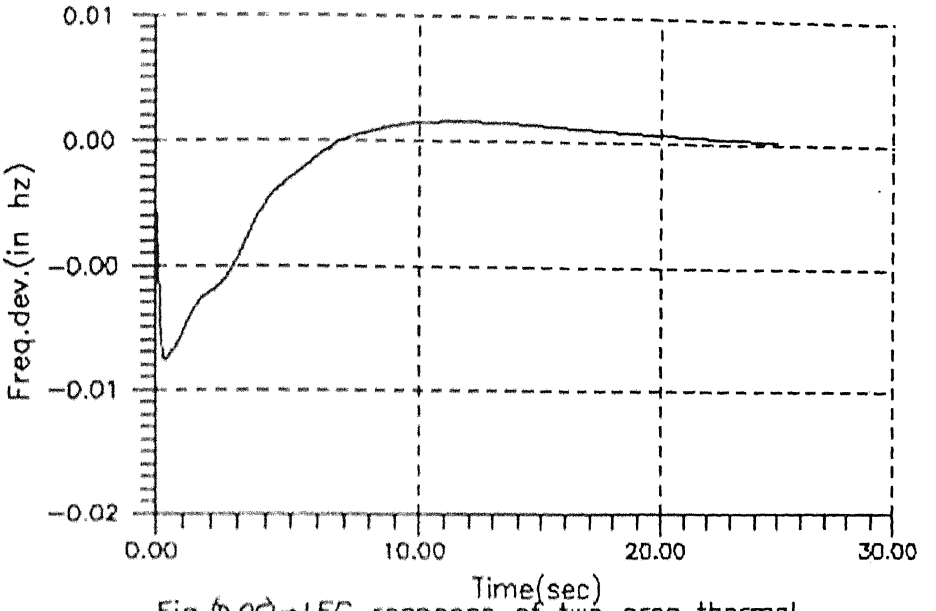

Fig.(D.25)→LFC response of two area thermal plant with P.I.D controller (ki/s+ke in forward path and (1+as) in feedback path) ki=0.67ke=1.5,a=2.0

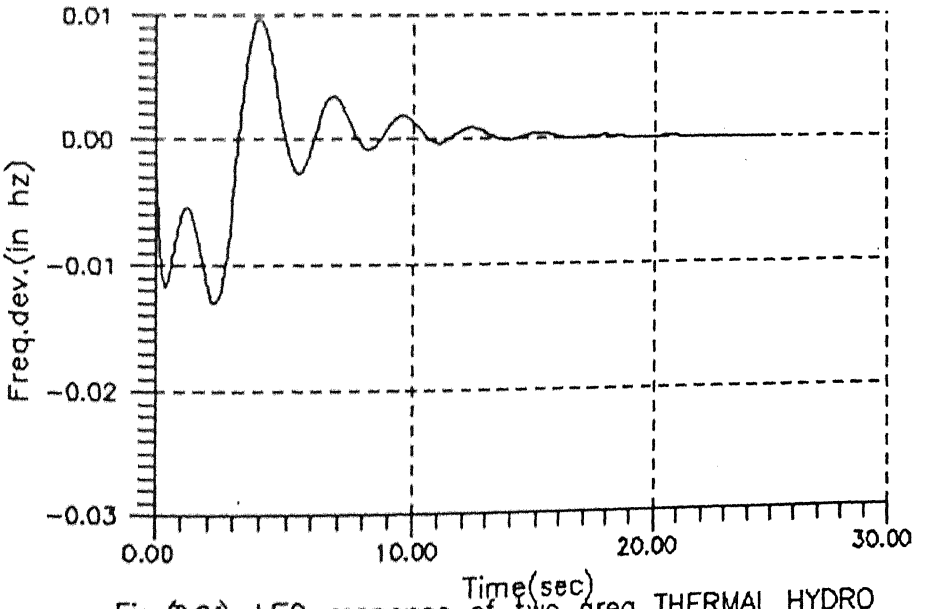

Fig.(D.26)→LFC response of two area THERMAL HYDRO plant with P.I.D controller (kp in forward path) (Ki/s in R1 f.b.path) (1+a*s inB1 f.b.path) a=0.55 kp=2.0 ki=0.55

D.8 CONFIGURATION EIGHT

This configuration , P.I.D. controlller is shown as in fig. (D.27) and load frequency control response is shown in figure (D.28) and (D.29) for different Ki & Kd.

D.9 CONFIGURATION NINE

It is shown and discussed as an example in chapter 5.

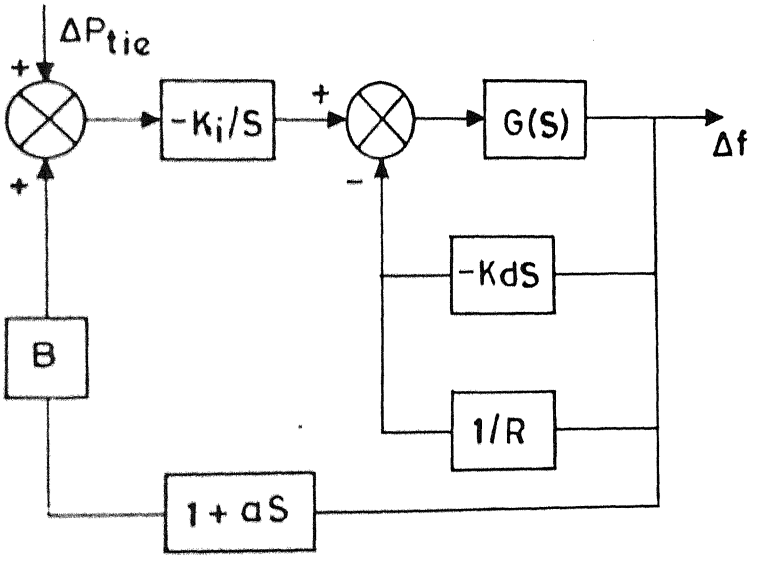

Figure (D.27)

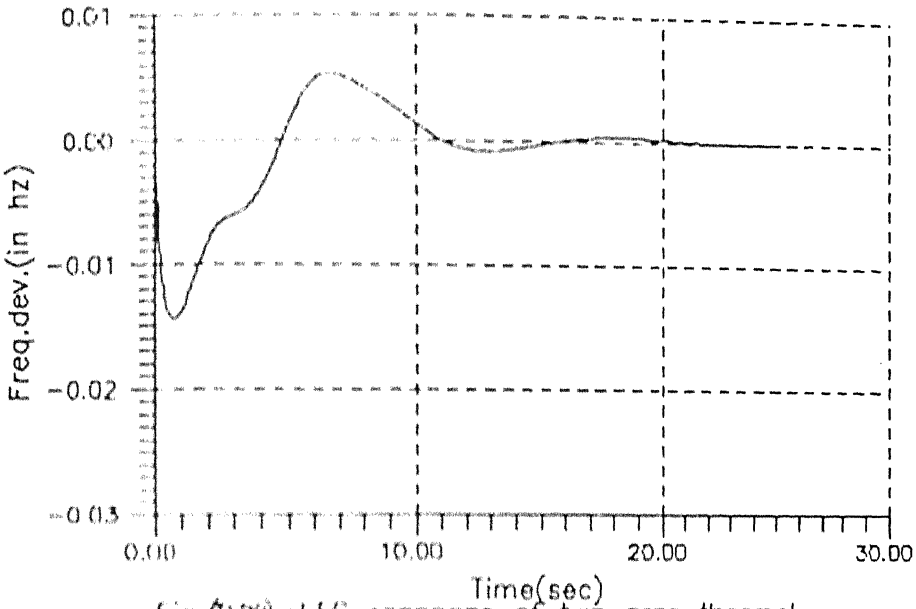

Fig.(5.28)→LFC response of two area thermal plant with P.I.D controller (ki/s→in forward path)and((1+a*s)in'B1'F.backpath)) ki=.67 ,kd=0.5,a1=.001(kds in'R1'F.backpath)

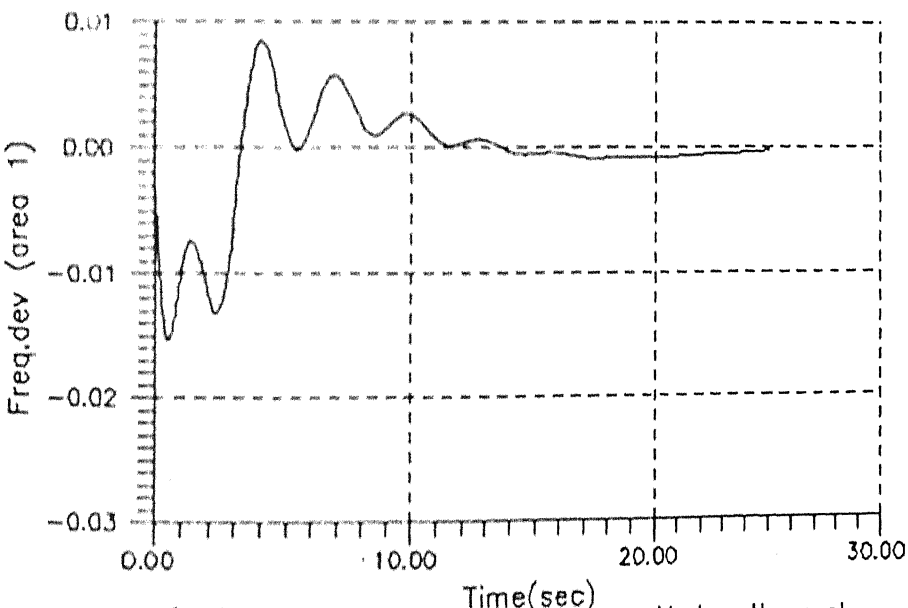

Fig.(5.29)→LFC response of two area Hydro-thermal plant with P.I.D controller (ki/sinforward path) (kds in R1 f.b.path) (1+a*s in B1 f.b. path) ki=1.0 a=-1.5 . kd=0.25

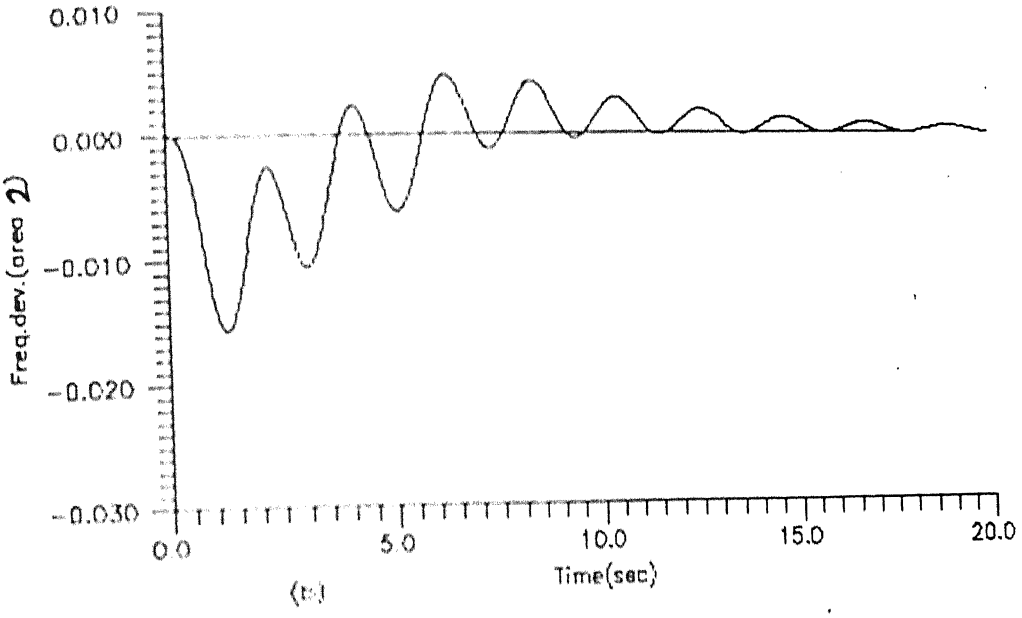
0.010
0.000
-0.010
-0.020
-0.030
Freq.dev.(area 2)
0.0
5.0
10.0
15.0
20.0
Time(sec)

(b)

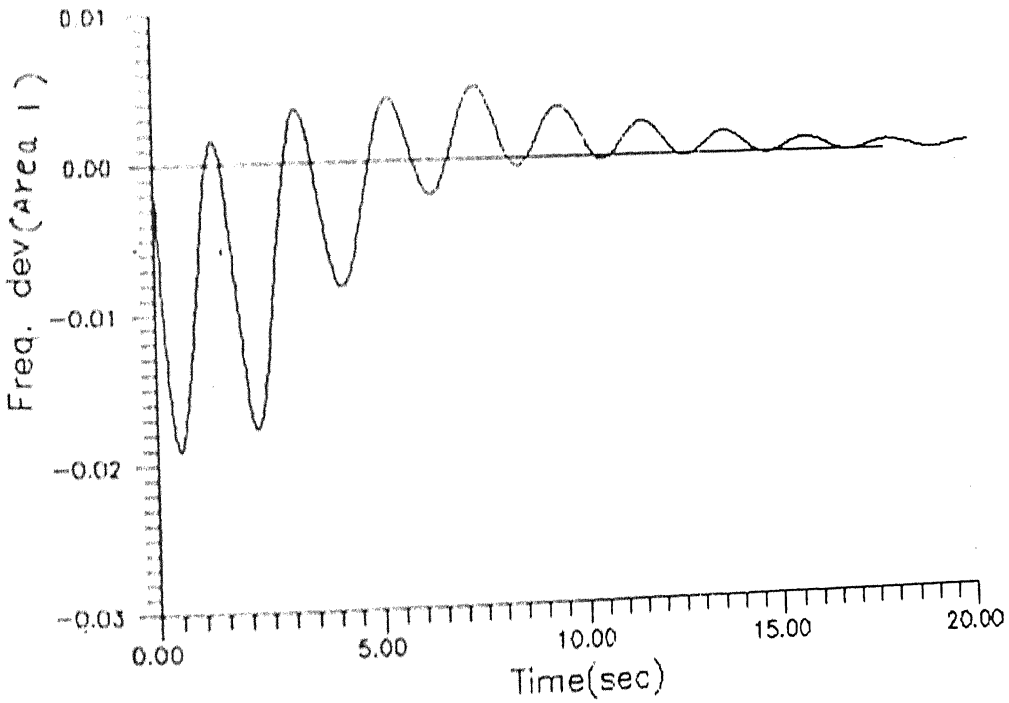
0.01
0.00
-0.01
-0.02
-0.03
Freq. dev(Area 1)
0.00
5.00
10.00
15.00
20.00
Time(sec)

(a)

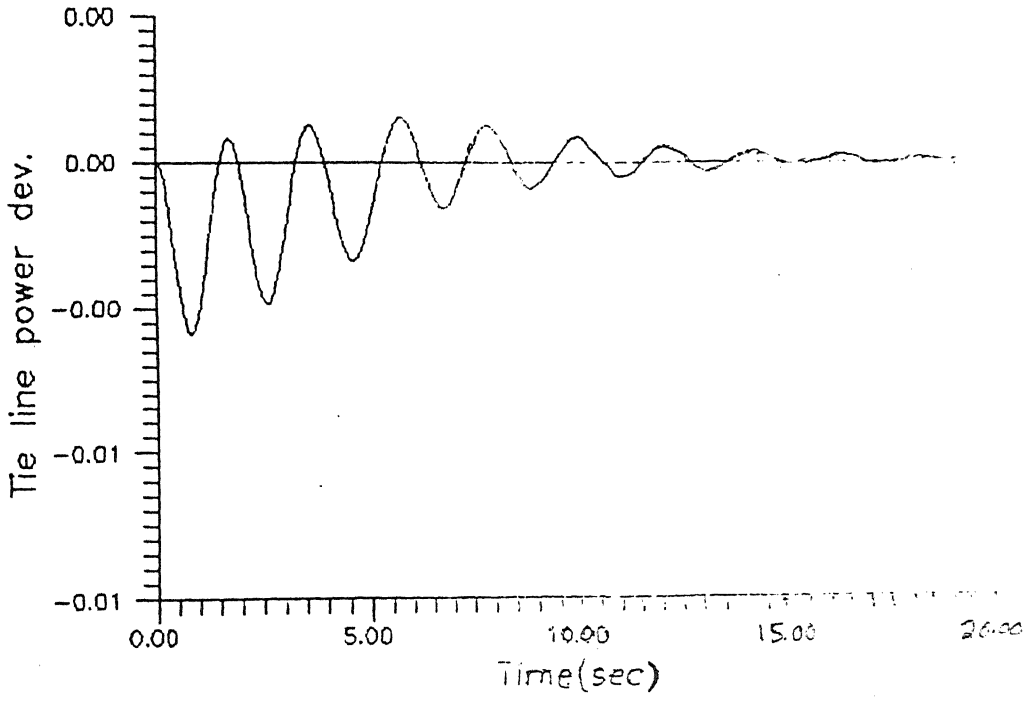

(c)

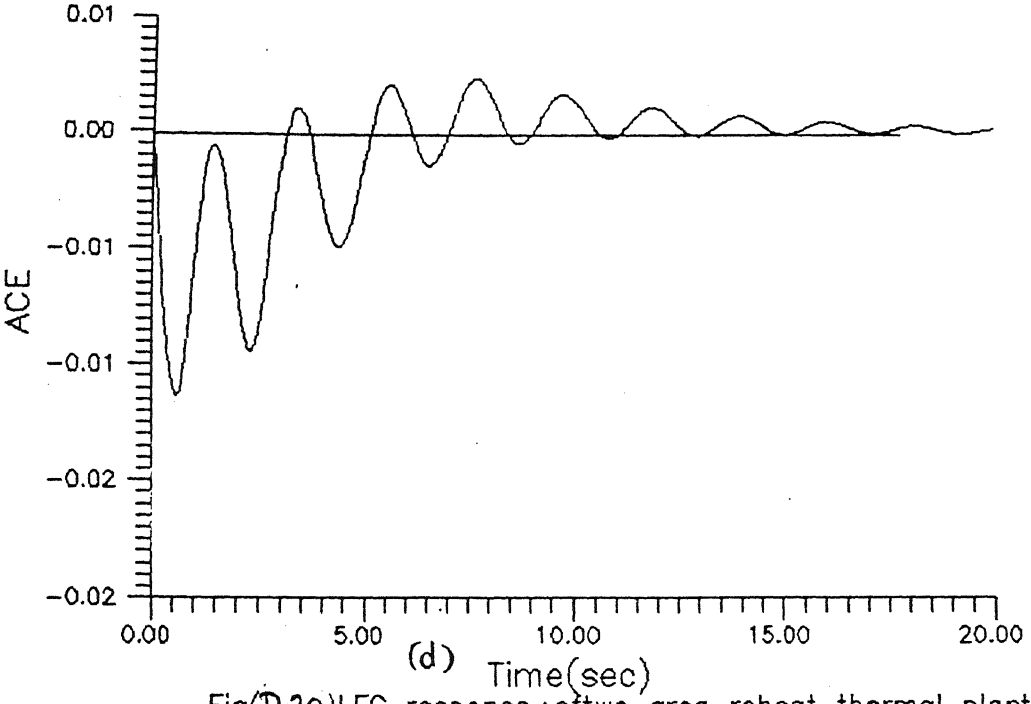

(d)

Fig(D.30)LFC responce→oftwo area reheat thermal plant variable structure system control kp=2.5 ki=0.67 and abs(ACE)=0.006

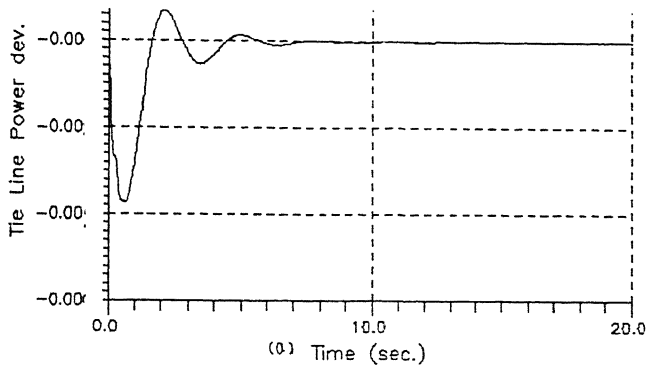

Two Area reheat thermal plant
Response with P I D CONTROLLER
kp in f.path ,kdsin R1 f.b.path,a1+a2/s
in B1 f.b.path kd=5.0 kp=10.0a1=5.0a2=5.0

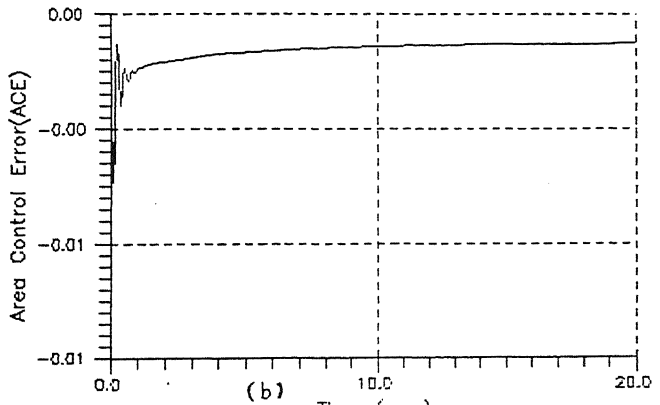

Two Area Reheat thermal plant
Response with P I D CONTROLLER
kp in f.path ,kdsin R1 f.b.path,a1+a2/s
in B1 f.b.path kd=5.0 kp=10.0a1=5.0a2=5.0

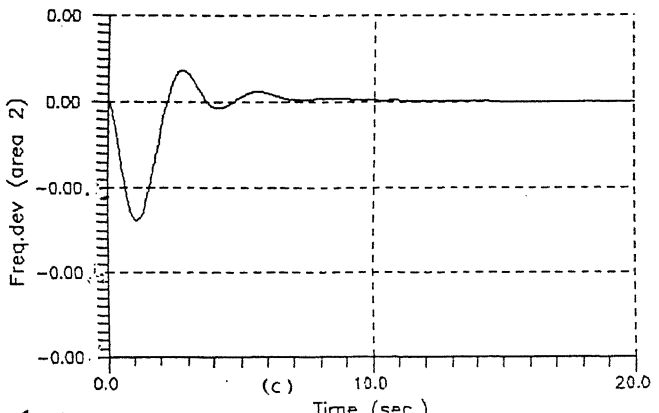

Fig.(6.31) Two Area Reheat thermal plant
Freq. Response with P I D CONTROLLER
kp in f.path ,kdsin R1 f.b.path,a1+a2/s
in B1 f.b.path kd=5.0 kp=10.0a1=5.0a2=5.0

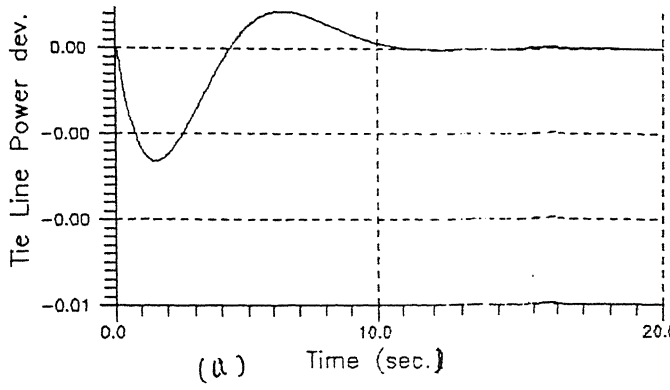

Two Area Reheat thermal plant
Response with P I D CONTROLLER
ki/s in f.path ,kp in R1 f.b.path, 1+A*S*S
in B1 f.b.path ki=1.5 kp=2.5 a=1.5

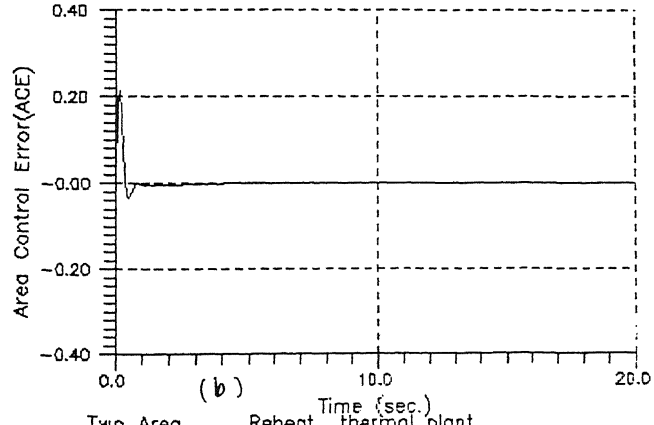

Two Area Reheat thermal plant
Response with P I D CONTROLLER
ki/s in f.path ,kp in R1 f.b.path, 1+a*s*s
in B1 f.b.path kp=2.5 ki=1.5 a=1.5

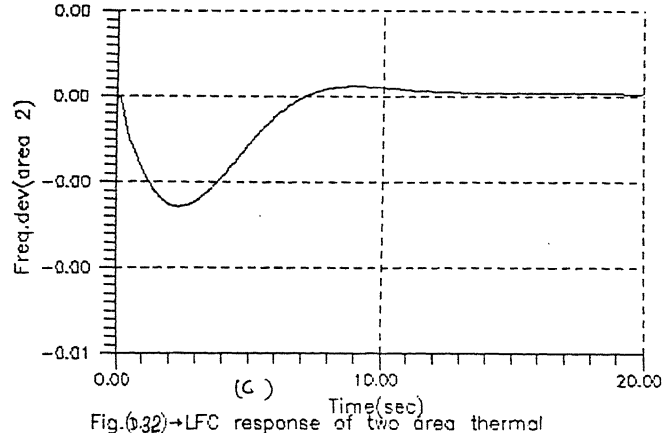

Fig.(3.32)→LFC response of two area thermal plant with P.I.D controller (ki/sinforward path) (kp in R1 f.b.path) (1+a*s*sin B1 f.b. path) kp=2.5 a=1.5 ki=1.5

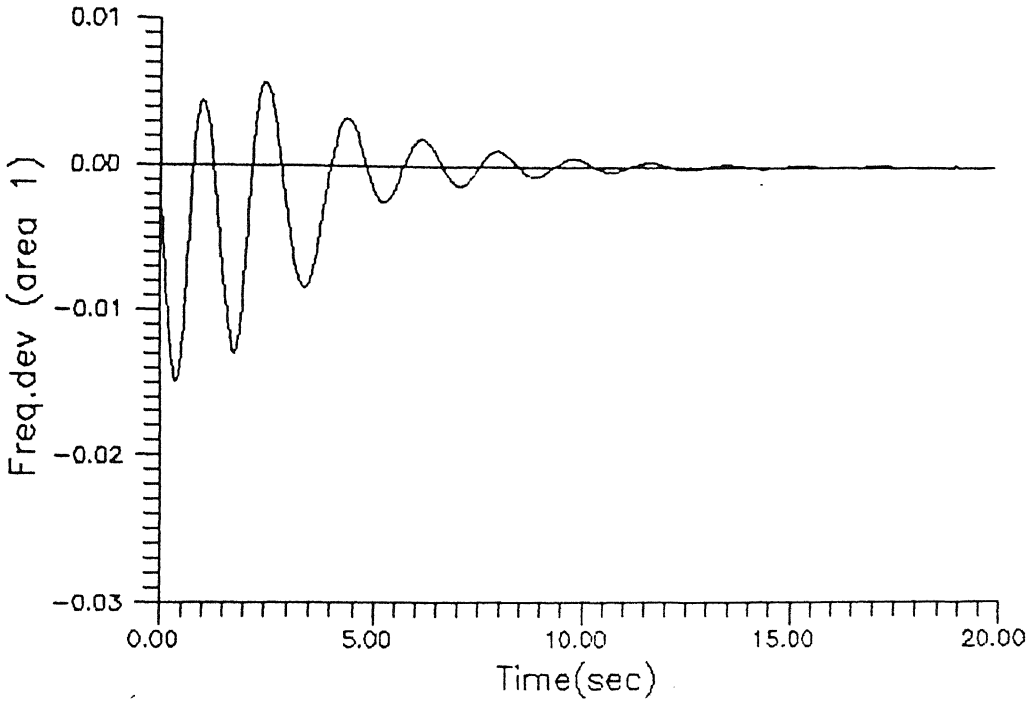
0.01
0.00
-0.01
-0.02
-0.03
Freq.dev (area 1)
0.00
5.00
10.00
15.00
20.00
Time(sec)

(a)

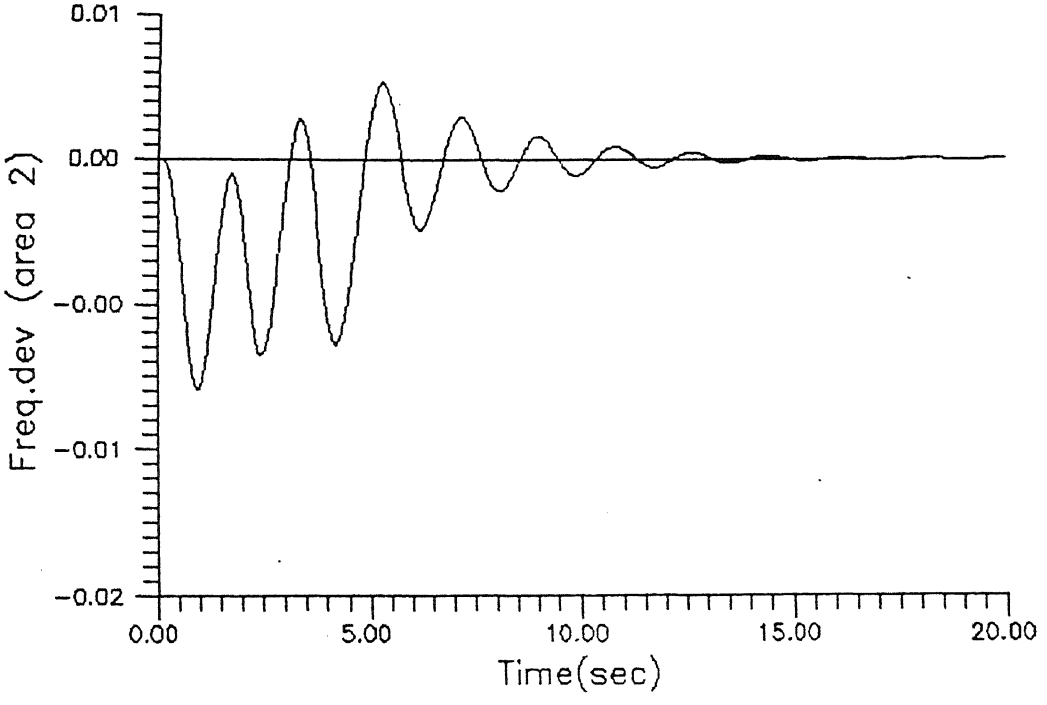
0.01
0.00
-0.00
-0.01
-0.02
Freq.dev (area 2)
0.00
5.00
10.00
15.00
20.00
Time(sec)

(b)

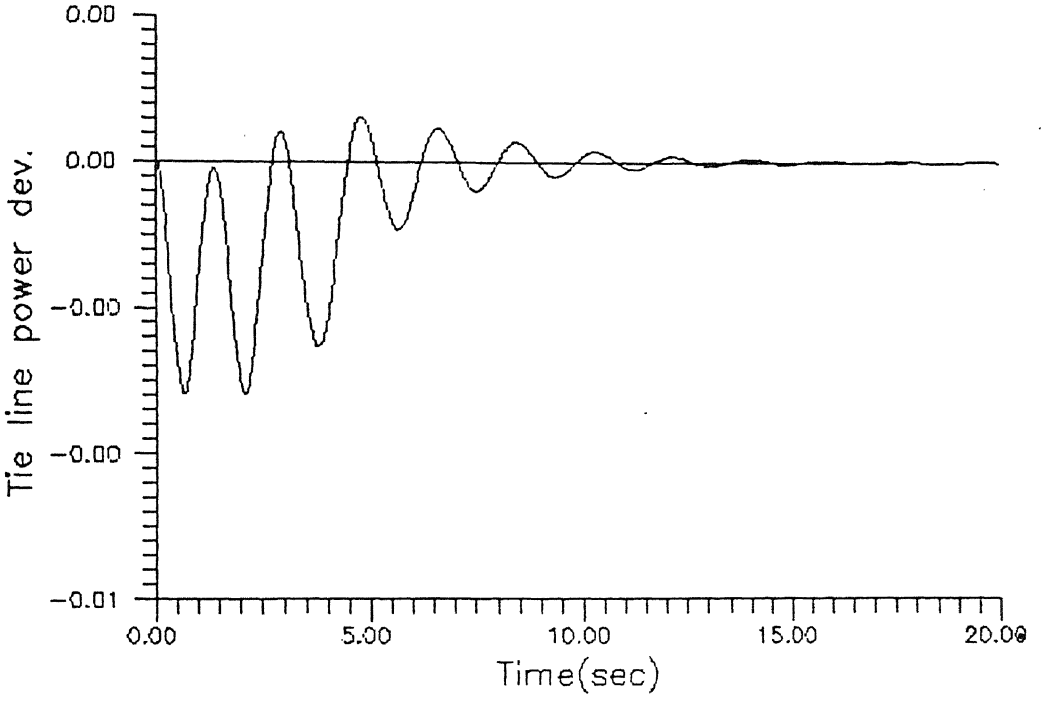

(c)

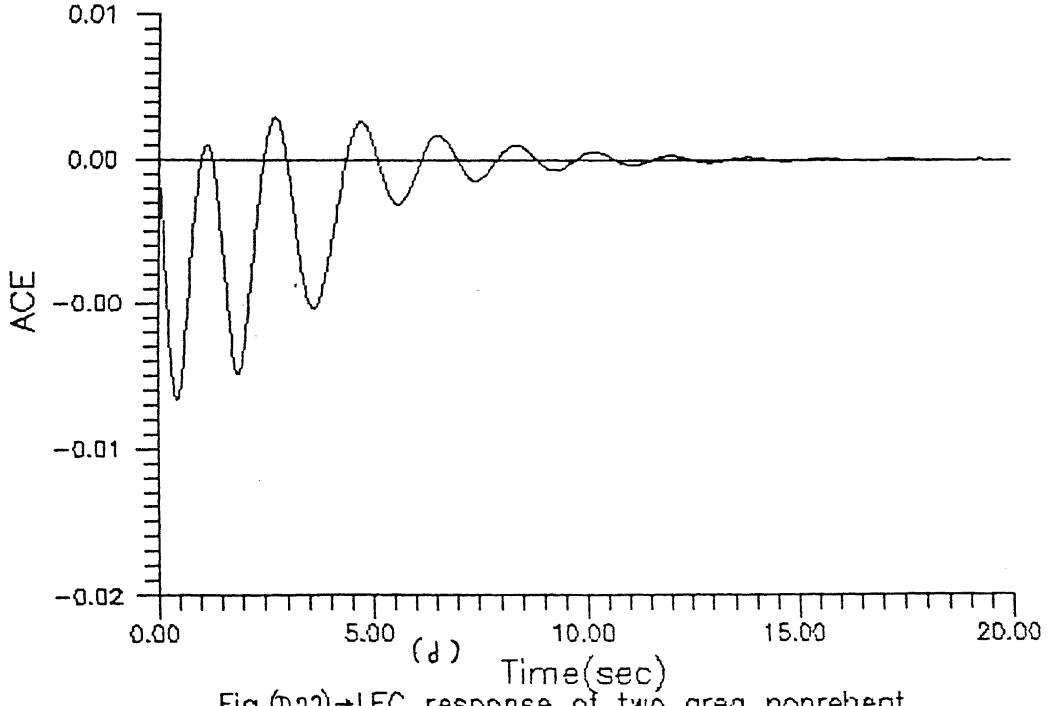

(d)

Fig.(D.33)→LFC response of two area nonreheat thermal plant variable structure control with kp=2.0 ki=0.75 abs(ace)=0.006

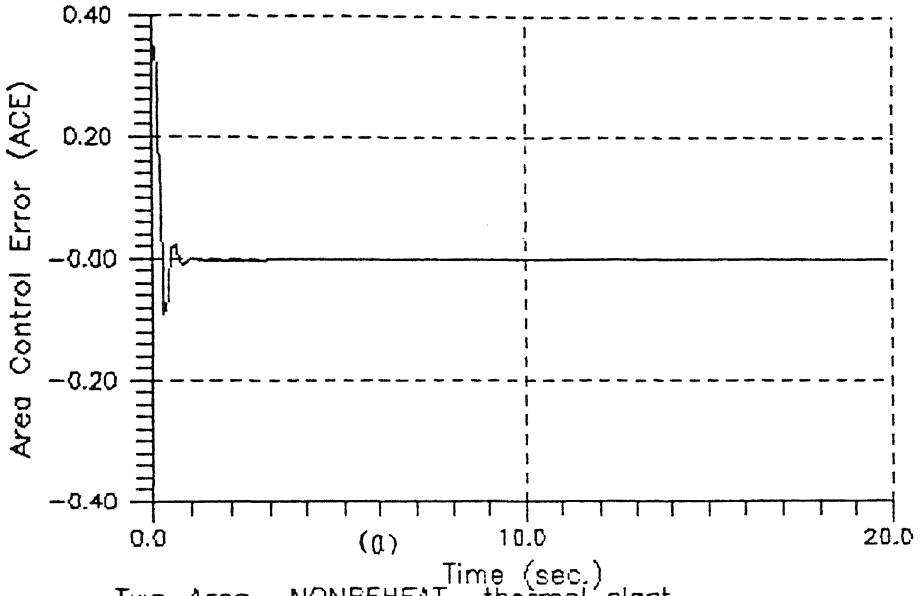

Two Area NONREHEAT thermal plant
Response with P I D CONTROLLER
ki/s in f.path ,kp in R1 f.b.path, 1+a*s*s
in B1 f.b.path kp=2.5 ki=1.5 a=1.5

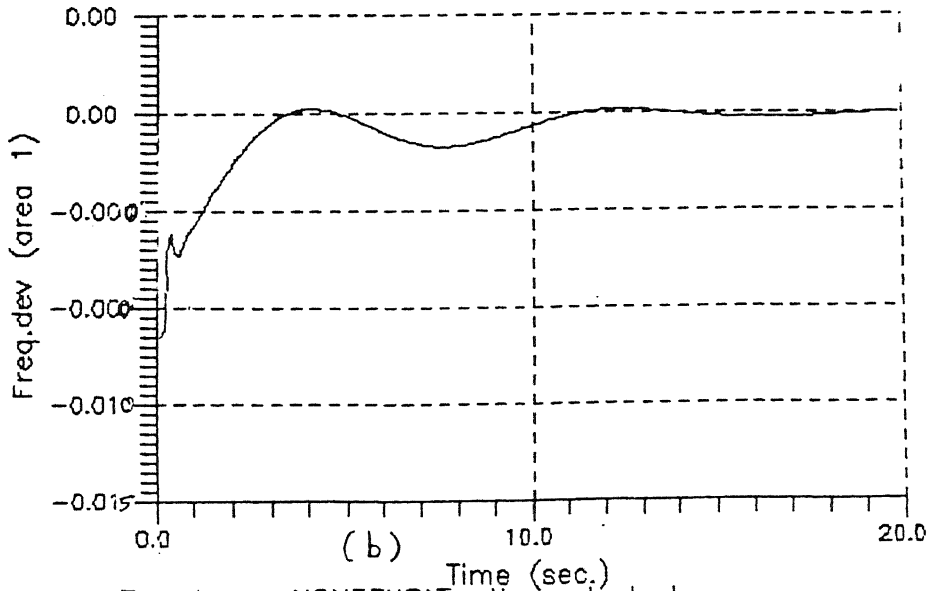

Two Area NONREHEAT thermal plant
Freq. Response with P I D CONTROLLER
ki/s in f.path ,kp in R1 f.b.path, 1+a*s*s
in B1 f.b.path kp=2.5 ki=1.5 a=1.5

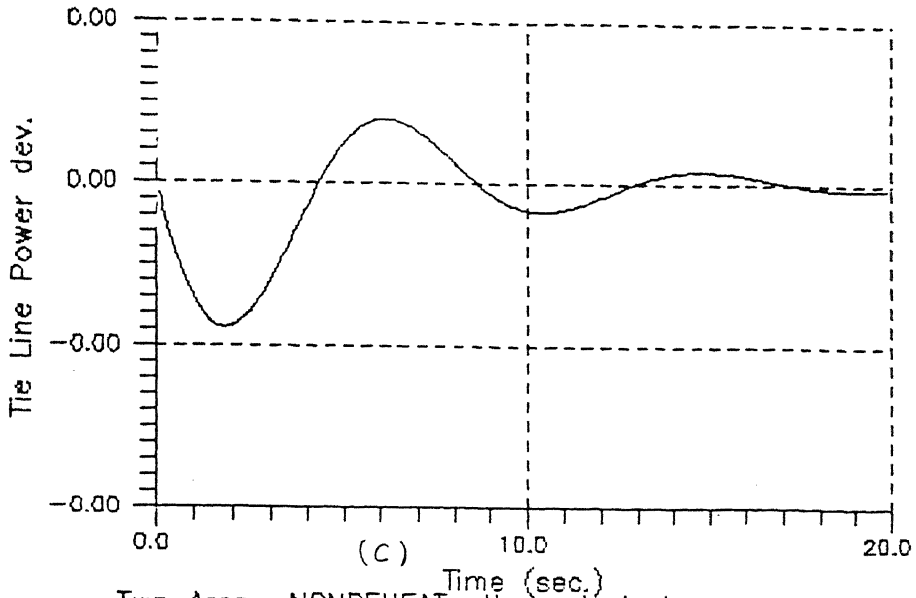

Two Area NONREHEAT thermal plant
Response with P I D CONTROLLER
ki/s in f.path ,kp in R1 f.b.path, 1+a*s*s
in B1 f.b.path kp=2.5 ki=1.5 a=1.5

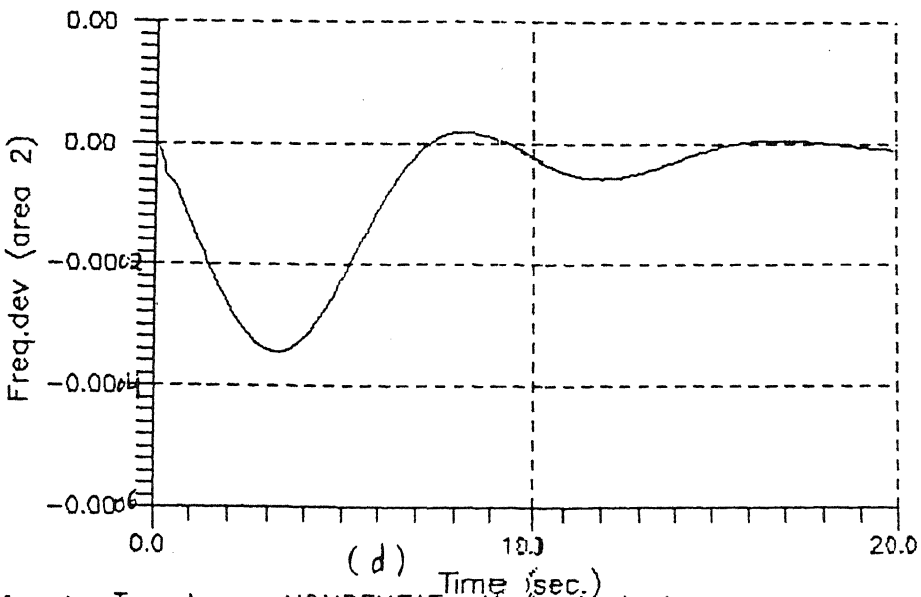

Fig(D.34) Two Area NONREHEAT thermal plant
Freq. Response with P I D CONTROLLER
ki/s in f.path ,kp in R1 f.b.path, 1+a*s*s
in B1 f.b.path kp=2.5 ki=1.5 a=1.5

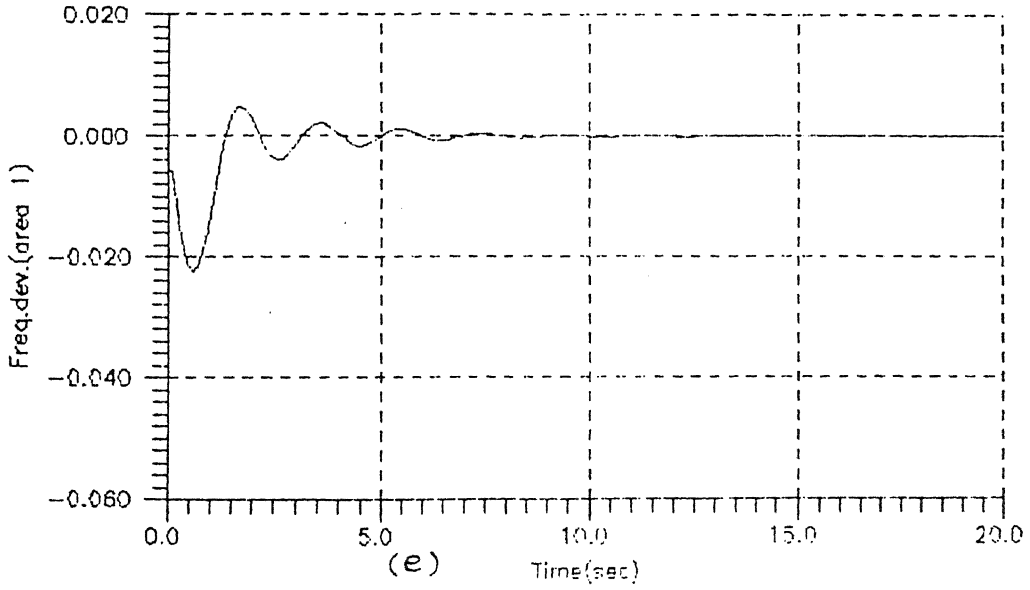

Fig.(D.34)Freq.Responce of two area Nonreheat thermal plant with CONVENTIONAL controller ki=0.67

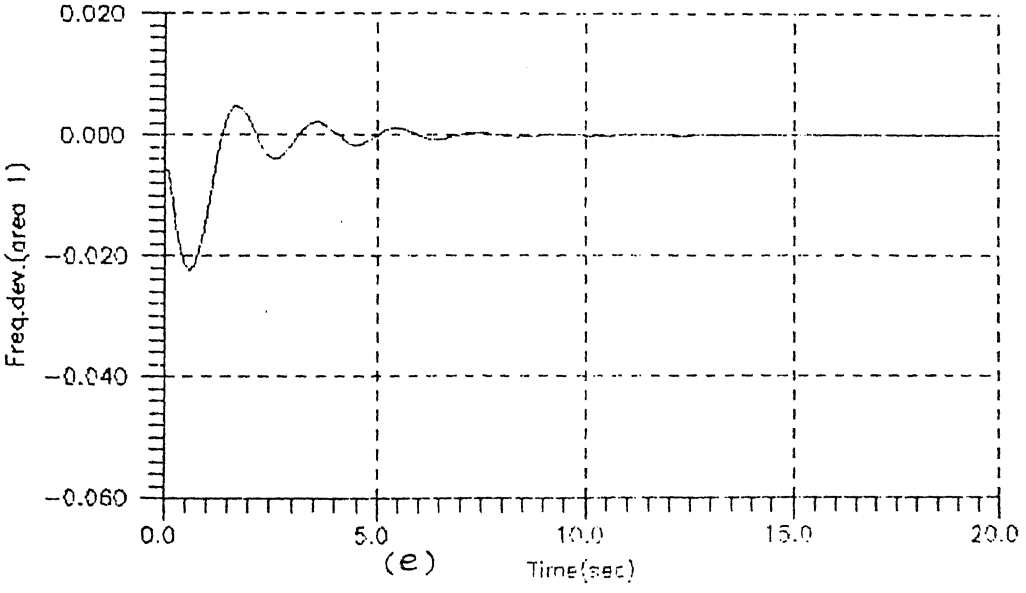

Fig.(D.24)Freq.Responce of two area Nonreheat thermal plant with CONVENTIONAL controller Kie=0.67

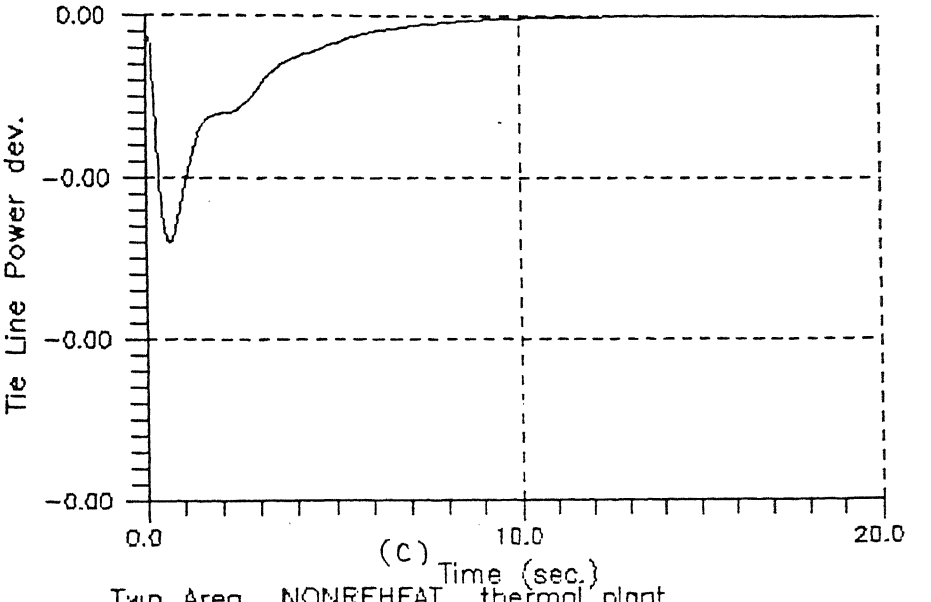

Two Area NONREHEAT thermal plant
system Responce with P I D CONTROLLER
kp in f.path, kds in R1 f.b.path,a1+a2/s
in B1 f.b.path kp=10.0 kd=5.0 a1=5.0 a2=5.0

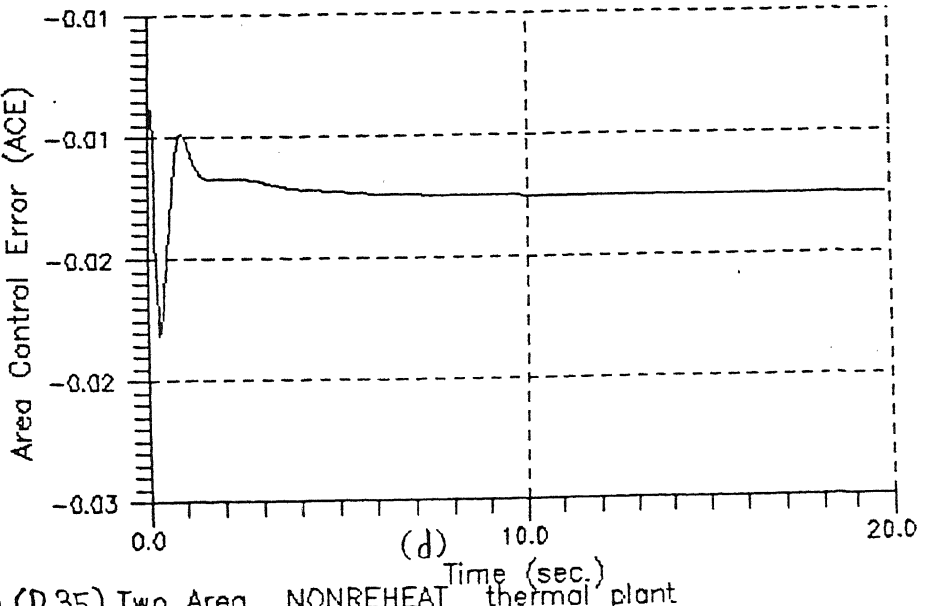

Fig.(D.35) Two Area NONREHEAT thermal plant
system Responce with P I D CONTROLLER
kp in f.path, kds in R1 f.b.path,a1+a2/s
in B1 f.b.path kp=10.0 kd=5.0 a1=5.0 a2=5.0

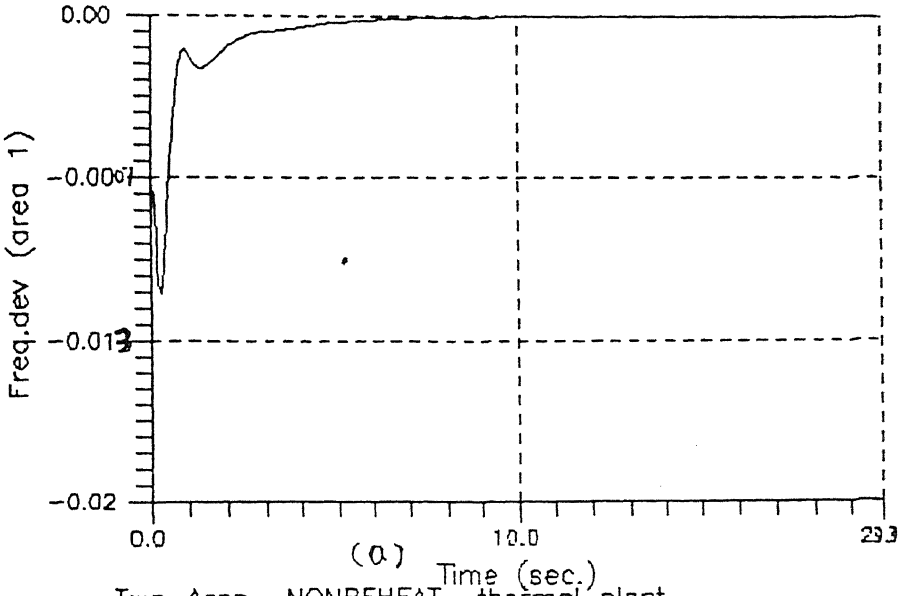

Two Area NONREHEAT thermal plant
system Responce with P I D CONTROLLER
kp in f.path, kds in R1 f.b.path,a1+a2/s
in B1 f.b.path kp=10.0 kd=5.0 a1=5.0 a2=5.0

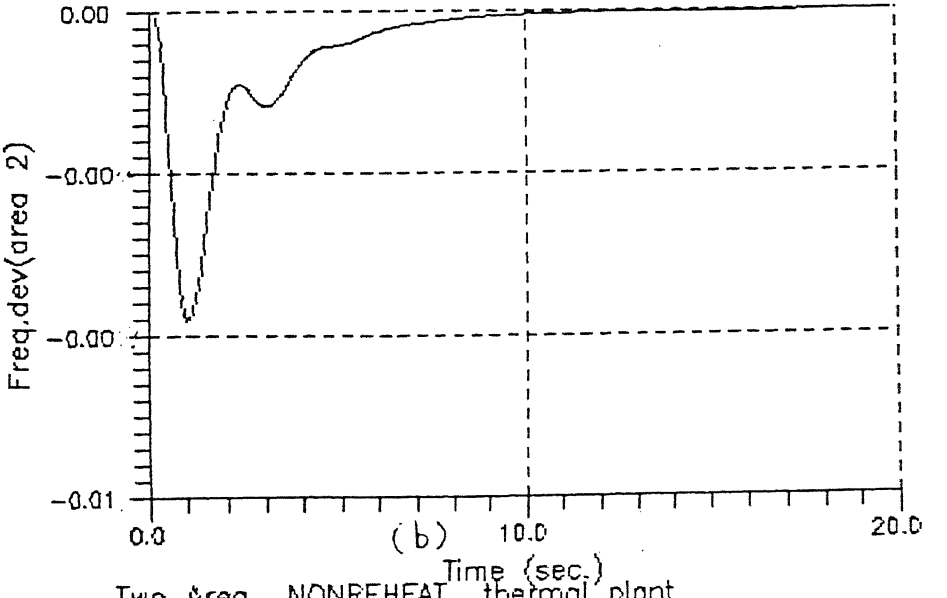

Two Area NONREHEAT thermal plant
system Responce with P I D CONTROLLER
kp in f.path, kds in R1 f.b.path,a1+a2/s
in B1 f.b.path kp=10.0 kd=5.0 a1=5.0 a2=5.0

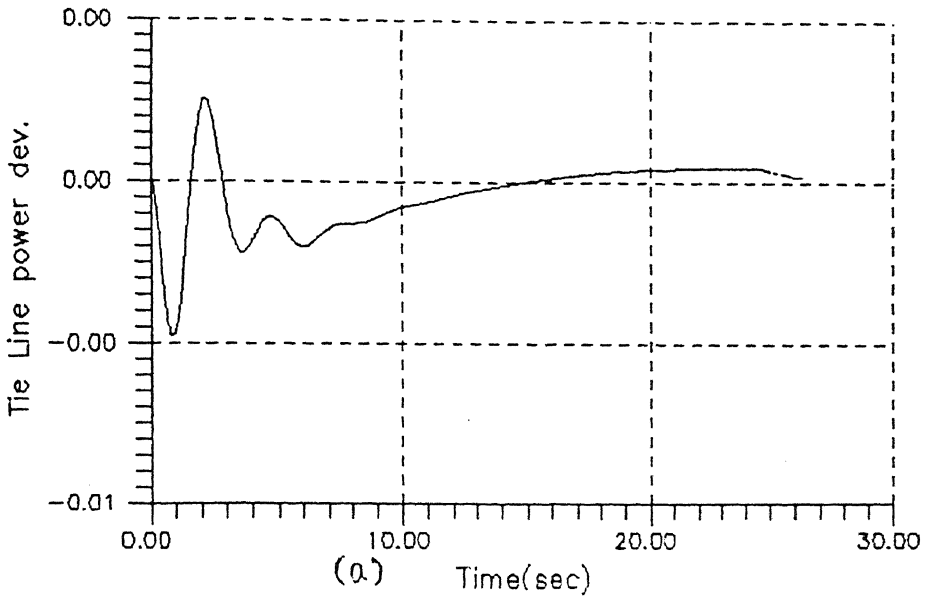

LFC response of TWO area Hydro-thermal plant with P.I.D controller (kp+ki/s+kds) in forward path.→kp=0.8 ki=0.9 kd=0.7

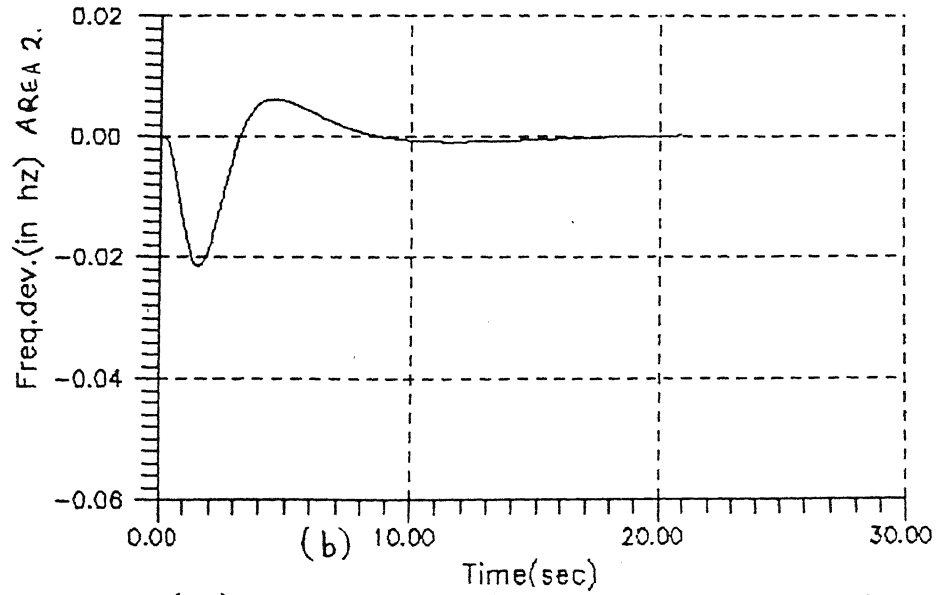

Fig.(D.36)→LFC response of Twc area Hydro-thermal plant with P.I.D controller (kp+ki/s+kds) in forward path.→kp=0.8 ki=0.9 kd=0.7

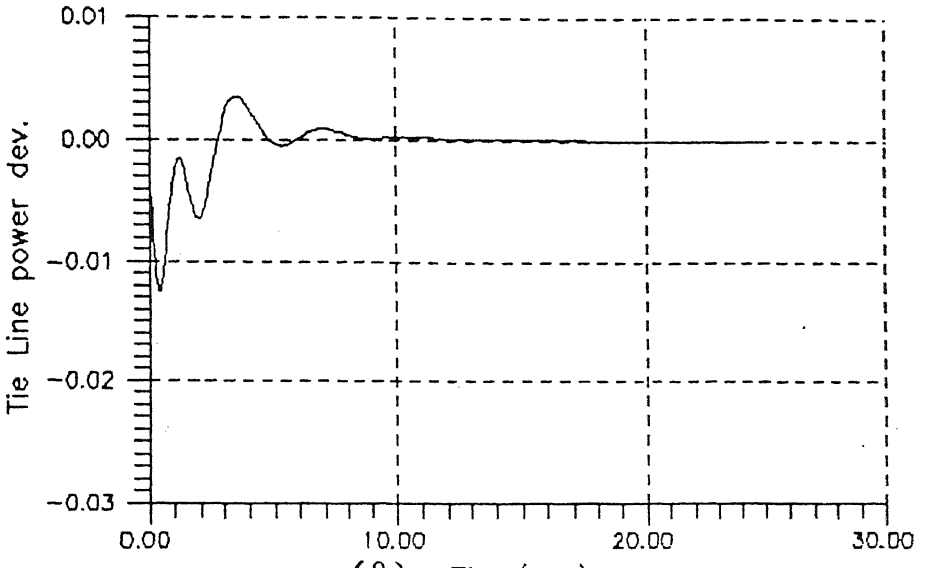

→LFC response of two area Hydro-thermal plant with P.I.D controller (kp in forward path) (kds in R1 f.b.path) (a1+a2/s in B1 f.b. path)
kp=0.8 a1=4.0 kd=0.3 a_2=4.0

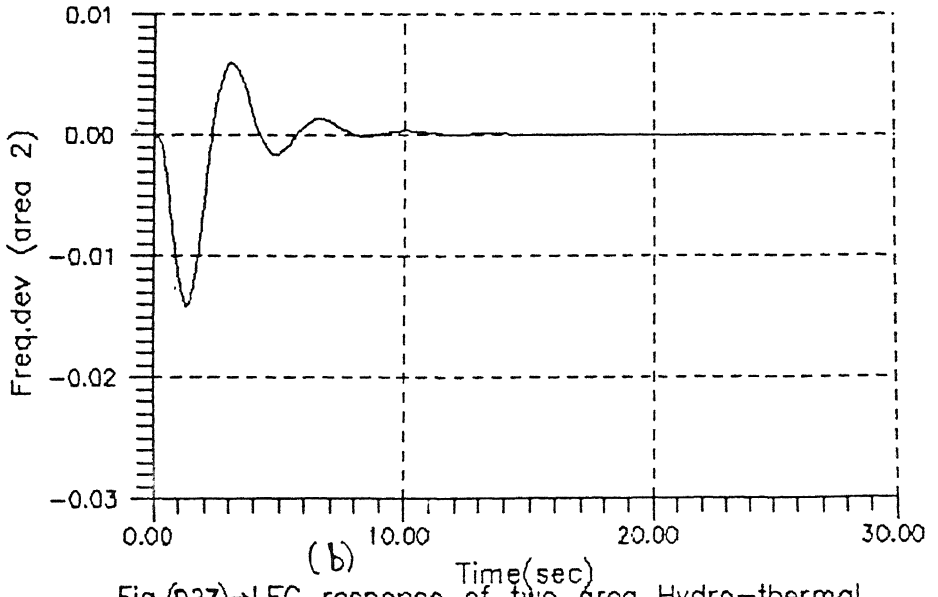

Fig.(D.37)→LFC response of two area Hydro-thermal plant with P.I.D controller (kp in forward path) (kds in R1 f.b.path) (a1+a2/s in B1 f.b. path)
kp= 0.8 a1=4.0 kd=0.3 a_2=4.0

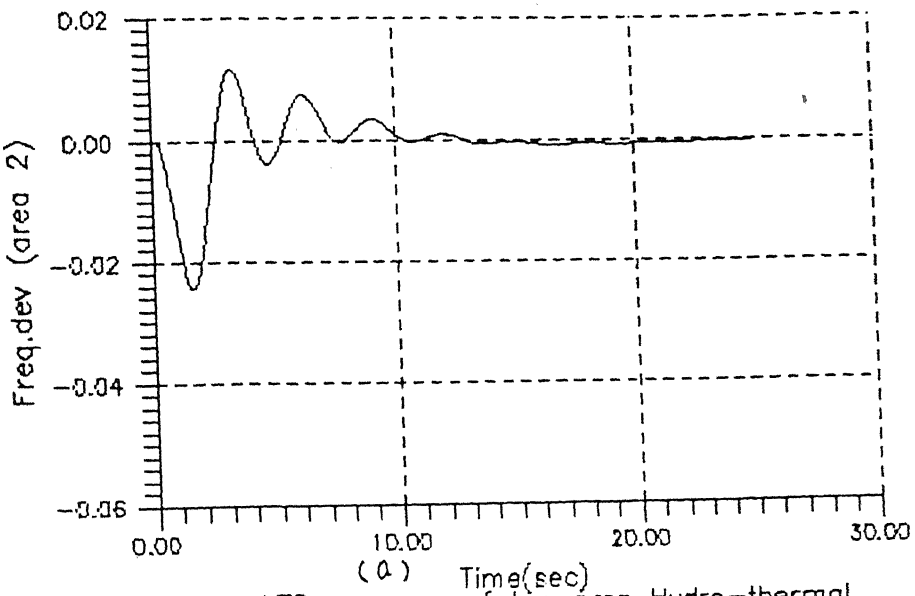

LFC response of two area Hydro-thermal plant with P.I.D controller (ki/sinforward path) (kds in R1 f.b.path) (1+a*s in B1 f.b. path) ki=1.0 a=-1.5 kd=0.25

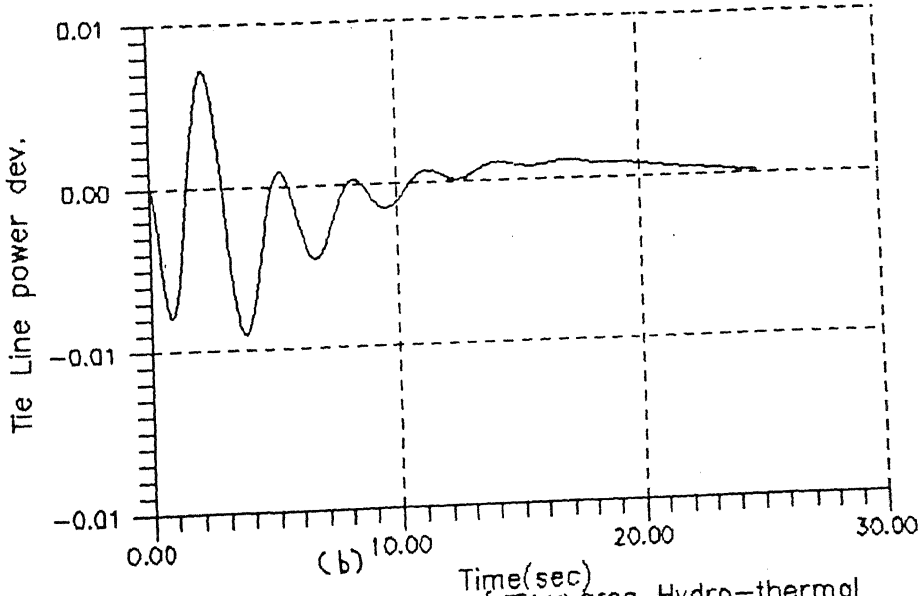

Fig.(3.38)→LFC response of Two area Hydro-thermal plant with P.I.D controller (ki in forward path) (kds in R1 f.b.path) (1+a*s in B1 f.b.path) →→→→→→→→→→→→→→ki=1.0 a=-1.5 kd=0.25

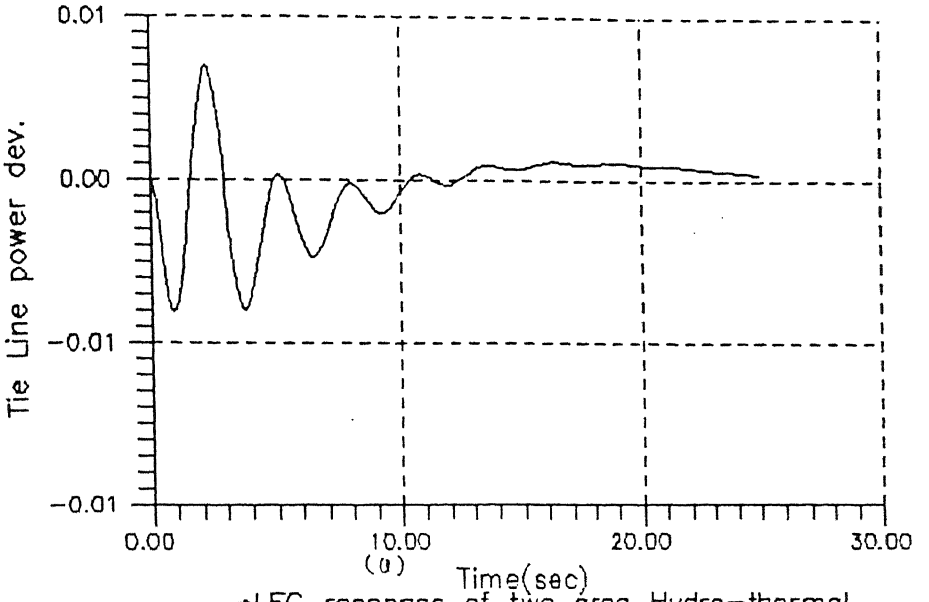

→LFC response of two area Hydro-thermal plant with P.I.D controller (ki/sin forward path) (kp in R1 f.b.path) (1+a*s*s in B1 f.b. path)
→→→→→→→→→→→→→→→→ki=0.9 a=0.7 kp=0.5

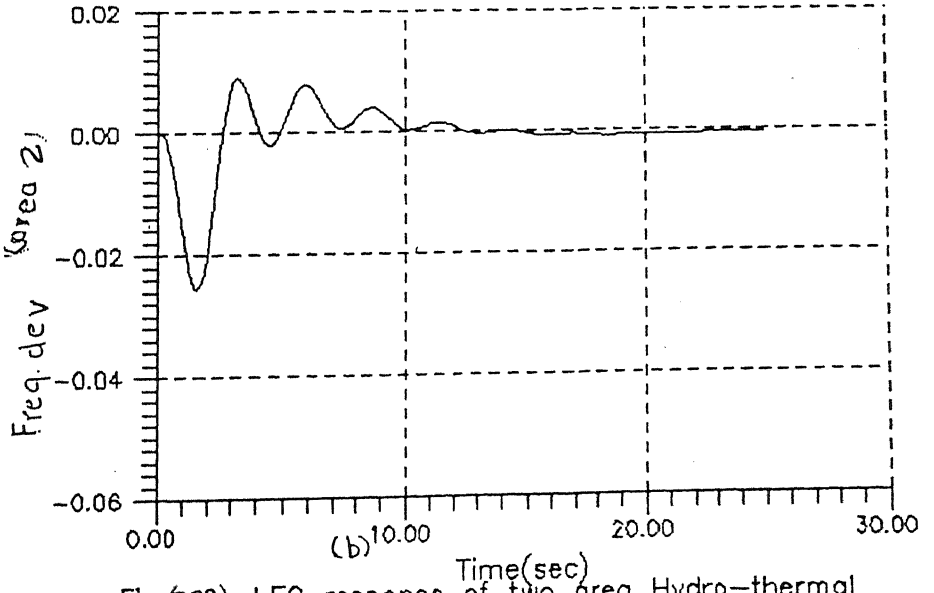

Fig.(b39)→LFC response of two area Hydro-thermal plant with P.I.D controller (ki/sinforward path) (kp in R1 f.b.path) (1+a*s*sin B1 f.b. path)
kp=0.5 a=0.7 ki=0.9